

Identifying Uncertainty Shocks Using the Price of Gold

APPENDICES

Michele Piffer and Maximilian Podstawska^{*}

August 3, 2017

A The Market of Gold

Since gold is traded on several marketplaces around the world, there is no such thing as a single gold market with a single price. Nevertheless, most of the trade occurs in London and in New York. London is the main hub for the trade of physical gold, which occurs through spot transactions over the counter. New York is an exchange and trades mainly paper gold, i.e. futures and several derivatives based on gold.

We use data from the London spot market of physical gold, formally known as the London Bullion Market. We rely on the London spot price of physical gold rather than the New York price on futures contracts on gold for two reasons. Firstly, Bloomberg provides intradaily data on the futures market for only 18 months, while the data on the London market dates back to the 1970s. Secondly, the London market is larger in terms of trade volume.¹ A comparison of the prices on the London spot market and

*Corresponding author: Michele Piffer, Department of Macroeconomics, DIW Berlin, Mohrenstrasse 58, 10117, Berlin, Germany. Email: m.b.piffer@gmail.com.

¹Following O'Connor *et al.* (2015), in 2013 the net transactions in London had a daily turnover of 21bn US dollars. This equals 60% and 350% of the daily turnover on the New York Stock Exchange and on the London Stock Exchange, respectively. These figures underestimate the size of the London Bullion Market, as they only include net transactions. Information on gross transactions is not publicly available due to the confidentiality guaranteed by over-the-counter trading. According

on the New York futures market at daily frequency yields a correlation close to unity.

Since transactions on the London Bullion Market are over-the-counter, market participants are not required to disclose the price of their bilateral agreements. Nevertheless, in order to inform market participants about the tightness of the market, the London Bullion Market Association organises two auctions per day. The price of such auctions is publicly available. This is the price of gold that we use for the analysis. Auctions take place at 10:30 and 15:00, London time. Shortly before 10:30 and 15:00, banks with access to the London Bullion Market vaulting facilities post their orders. It then typically takes 30 seconds to assess if a round of orders can be reconciled with a clearing price, and 3 rounds of orders to find an equilibrium price. Transactions are denominated in US dollars and are settled two days after the transaction.

B Comparing Proxies for the Uncertainty Shock

The selection of the price of gold as the variable to inform our proxy for the uncertainty shock is supported by the results from several regressions, as discussed here.

We depart from daily data on six candidate variables: the price of gold, the price of silver, the price of platinum, the price of the 3-month US treasury bonds, the price of the 30-year US treasury bonds, and the VXX. While intradaily data are available for the price of gold and are used in the analysis, we use daily data for all the series included in this preliminary assessment to ensure a level playing field in the comparison of the candidate assets, as it is the highest frequency available for all candidates. Following the methodology outlined in [Section 2](#) of the paper, for each of the six variables above

to a survey conducted in 2011, gross figures might be between 5 and 10 times higher than net figures (http://www.lbma.org.uk/assets/Loco_London_Liquidity_Surveyrv.pdf). When also considering gross transactions, London is estimated to account for around 90% of the sum of the global gold spot, futures and options trading volumes. New York, instead, accounts for around 9%. The other markets (Shanghai, Tokyo, Mumbai, Dubai and Istanbul) account for the remaining 1% ([Lucey et al., 2013](#)).

we compute the percentage variation Δp^j around each event e_j , with $j = 1, \dots, K$ and K the total number of baseline events. We then compute a candidate proxy for each of these six variables as a time series that equals zero on the days in which no event became known to the market, and that equals Δp^j when event e_j became known to the market. Following this procedure, we obtain six candidate proxies for the uncertainty shock at a daily frequency.

We then add three daily dummy variables. We add a dummy variable taking the value of 1 when a baseline event occurred and zero otherwise, a dummy variable taking the value of 1 when the VXO reached the peaks used by [Bloom \(2009\)](#) and zero otherwise, and a dummy variable taking the value of 1 or -1 when the event was judged to imply an increase or a decrease in uncertainty, and 0 when the variation in uncertainty could not be *a priori* assessed or when no event occurred. For completeness, we also add the two instruments for the uncertainty shock used by [Stock and Watson \(2012\)](#), which are computed as the residual of an AR(2) on the VIX and as the common component of the policy uncertainty index by [Baker *et al.* \(2016\)](#) on media references. These two instruments are available at a monthly frequency. Overall, the collection of candidate proxies delivers a total of eleven candidate proxies for the uncertainty shock, nine of which at a daily frequency and the remaining two at a monthly frequency.

To assess which candidate proxies for the uncertainty shock are more suitable for the analysis of the paper we assess the relevance and strength of each candidate proxy. Firstly, we require that the selected proxy Granger-causes prominent measures of uncertainty available from the literature. This requirement indirectly assesses whether the relevance condition stated in equation (4) in the paper holds with regard to the candidate proxies, under the maintained hypothesis that uncertainty shocks are important drivers of the measures of uncertainty used. Secondly, we require that the

candidate proxy is strongly correlated with the reduced form innovation of the VAR model in correspondence to the equation that features the VXO as the dependent variable. This requirement was discussed in Section 5.1 of the paper and refers to the fact that it is from the VAR innovations that we aim to identify the uncertainty shock. We focus on the residual of the equation of the VXO, under the maintained hypothesis that uncertainty shocks are relatively important drivers of VXO residuals. Section 5.1 assesses the strength of the final proxy, which is based on the intradaily price of gold, and reports the results for the residuals on all equations of the model.

To test for the relevance of the candidate instrument, we estimate the models

$$x_{it} = \gamma + \sum_{l=1}^L \delta_l \cdot m_{t-l} + \eta_{it}, \quad (\text{B.1})$$

where m_t is one of the above candidate proxies for the uncertainty shock and x_{it} indicates a measure of uncertainty. For x_{it} we use five widely used measures of uncertainty, which are the measure by Jurado *et al.* (2015), the measure by Bachmann *et al.* (2013), the VIX, the VXO and a measure of realised volatility of the S&P500.² Rejecting the null hypothesis of no Granger-causality ($\delta_1 = \delta_2 = \dots = \delta_L = 0$) suggests that the proxy correctly reflects variations in uncertainty. For the tests on the strength of the

²The measure of the realized volatility of the S&P500 index is taken from the Oxford-Man Institute of Quantitative Finance. Regarding the VXO and the VIX, both the VIX and the VXO measure market perceived volatility based on option prices and are computed by the Chicago Board Options Exchange (CBOE). The VIX refers to the implied volatility on the S&P500 index, while the VXO refers to the implied volatility on the S&P100 index. Historically, the VIX was introduced first. It was launched in 1993 and it referred originally to the volatility of the S&P100 index rather than the S&P500 index. In 2003 the formula used to compute the volatility index was partly changed. What had been computed as VIX between 1993 and 2003 with the old formula and on the S&P100 index was relabelled as the “original VIX” and became the VXO. The VXO was then computed from 2003 onwards on the S&P100 index using the formula of the “original VIX”, and was reconstructed historically back to 1986. The name “VIX” was, instead, attached to the index computed with the new formula, applied to the S&P500 index rather than to the S&P100 index. The new VIX (nowadays simply referred to as VIX) was computed retroactively back to 1990. Both the VXO and the (new) VIX are widely used measures of implied volatility.

candidate proxy, instead, we use equation (10) from [Section 5.1](#), replicated here in equation (B.2) for convenience. For this equation, we take as dependent variable the residuals in the second equation of the VAR model, which is the equation that features the VXO as dependent variable.

$$\hat{u}_{2t} = \alpha + \beta \cdot m_t + \eta_t. \quad (\text{B.2})$$

A high F statistic for the null hypothesis $\beta = 0$ suggests that the candidate proxy indeed reflects variations in uncertainty in a sufficiently strong way to label the candidate proxy as a strong instrument. Both equation (B.1) and equation (B.2) are estimated using monthly data, after converting the nine daily candidate proxies into monthly frequency. The use of the monthly frequency in equation (B.1) is due to the fact that this is the highest frequency for which all five measure of uncertainty are available. The use of a monthly frequency in equation (B.2) is dictated by the frequency of the data in the VAR model.

The results of the tests are shown in [Table B1](#). Bold values report values supporting the candidate proxy. The Granger-causality tests are displayed in the top part of the table. We report the p -value on the F statistic for the hypothesis $\delta_1 = \delta_2 = \dots = \delta_L = 0$ in equation (B.1), where the regressor in equation (B.1) is indicated in the column of [Table B1](#) and the dependent variable in equation (B.1) is the variable indicated on the row of [Table B1](#). The tests on the strength of the candidate instruments are shown in the lower part of the table. For this test we report the F statistic on the hypothesis $\beta_i = 0$ in equation (B.2), where the regressor in equation (B.2) is indicated in the column of [Table B1](#) and the dependent variable is the estimated VAR innovations of the equation featuring the VXO as a dependent variable. We use the threshold value of 10 to assess if the candidate proxies are sufficiently strong (see [Stock and Yogo](#),

Table B1: Preliminary tests on candidate proxies for the uncertainty shock

| | % variation around events using: | | | | | | Dummies: | | | SW: | |
|---|----------------------------------|-------------|-------------|-------------|-------------|-------------|---------------------|------------------|------------------------|-------------|-------------|
| | Gold | Silver | Platinum | 3m Tbill | 30y Bond | VXO | $D_{0/1}$ events | $D_{0/1}$ VXO | $D_{0/-1/1}$ events | U_{VIX} | U_{BBD} |
| <i>Granger-causality from candidate proxy to measure of uncertainty</i> | | | | | | | | | | | |
| (p-values) | | | | | | | | | | | |
| JLN | 0.00 | 0.00 | 0.75 | 0.21 | 0.40 | 0.86 | 0.77 | 0.18 | 0.75 | 0.07 | 0.04 |
| BES | 0.75 | 0.94 | 0.04 | 0.31 | 0.82 | 0.72 | 0.46 | 0.03 | 0.09 | 0.84 | 0.00 |
| VIX | 0.00 | 0.61 | 0.00 | 0.00 | 0.02 | 0.01 | 0.01 | 0.69 | 0.26 | 0.75 | 0.18 |
| VXO | 0.00 | 0.35 | 0.00 | 0.01 | 0.01 | 0.19 | 0.00 | 0.37 | 0.40 | 0.89 | 0.08 |
| R. Vol. | 0.00 | 0.93 | 0.00 | 0.00 | 0.00 | 0.00 | 0.00 | 0.07 | 0.91 | 0.00 | 0.00 |
| <i>Strength of the candidate instrument</i> | | | | | | | | | | | |
| (F-statistic) | | | | | | | | | | | |
| | 11.60 | 4.50 | 4.51 | 1.63 | 0.01 | 4.99 | 15.48 | 58.61 | 2.89 | 3141 | 21 |

Notes: “JLN” indicates the measure of uncertainty computed by [Jurado et al. \(2015\)](#). “BES” indicates the measure of uncertainty computed by [Bachmann et al. \(2013\)](#). “R. Vol” indicates a measure of real volatility on the S&P500 (see [footnote 2](#)). The candidate proxies labelled U_{VIX} and U_{BBD} are computed on a monthly frequency and refer to the instruments used by [Stock and Watson \(2012\)](#). All the remaining candidate proxies are first computed at a daily frequency and then aggregated to monthly frequency. The models are then estimated on a monthly frequency. Granger-causality tests are run using bivariate VAR models, where the number of lags is chosen using Akaike’s Information Criterion.

2005).

Consider first the candidate proxies constructed around the events, which are the first six proxies in [Table B1](#). Overall, the regressions support the price of gold as a measure to inform the proxy for the uncertainty shock. The proxy variable constructed on the price of gold Granger-causes almost all measures of uncertainty and has an F statistic for the strength of the instrument above 10. While the proxies based on other assets such as platinum and the US treasury bills also somewhat pass the Granger-causality tests, they are less supported by the test on the strength of the instrument. We interpret the lack of Granger-causality from the instruments based on the VXO to the VXO as the by-product of the aggregation of the instruments from daily to monthly frequency.

Two of the three dummy variables perform well in terms of the strength and relevance of the instrument. These are the 0/1 dummy variable on the baseline events and the 0/1 dummy variable on the peaks of the VXO. We do not make use of these proxies as the baseline proxies in the analysis because they are less likely to satisfy the exogeneity condition discussed in [Section 1](#) of the paper. In fact, a variable constrained to 0/1 cannot by construction disentangle the uncertainty-related component of an underlying event from the news-related component of the same event. The use of the price of a safe haven asset around events further isolates the first-moment effect associated with the event. Similarly, the dummy variable on the VXO can reflect other structural shocks that endogenously lead the VXO to spike, given that uncertainty shocks are not the only shocks that can lead to a hike in uncertainty. We also note that the very high F statistic on the strength test for the dummy on the VXO variable is driven by the same variable being indirectly used both as the dependent and the independent variable of equation [\(B.2\)](#). Last, as discussed in [Section 5.1](#), when moving from daily to intradaily data the F statistic on the strength of the proxy constructed on the price of gold increases from 11 to 19, hence above the F statistic on the event based dummy variable.

Last, we compare the results from our candidate proxies for the uncertainty shock to the results when using the instruments used by [Stock and Watson \(2012\)](#). As for the dummy variable on the VXO, the high F statistic on the strength of the instrument constructed on the VIX is driven by the VIX being highly correlated with the dependent variable used in the regression of equation [\(B.2\)](#). While both instruments used by [Stock and Watson \(2012\)](#) Granger-cause several measures of uncertainty, they are not constructed on a clear identification strategy but on reduced form analysis, and hence are unlikely to satisfy the exogeneity condition from equation [\(5\)](#). This is

partly noted also by [Stock and Watson \(2012\)](#), page 116.

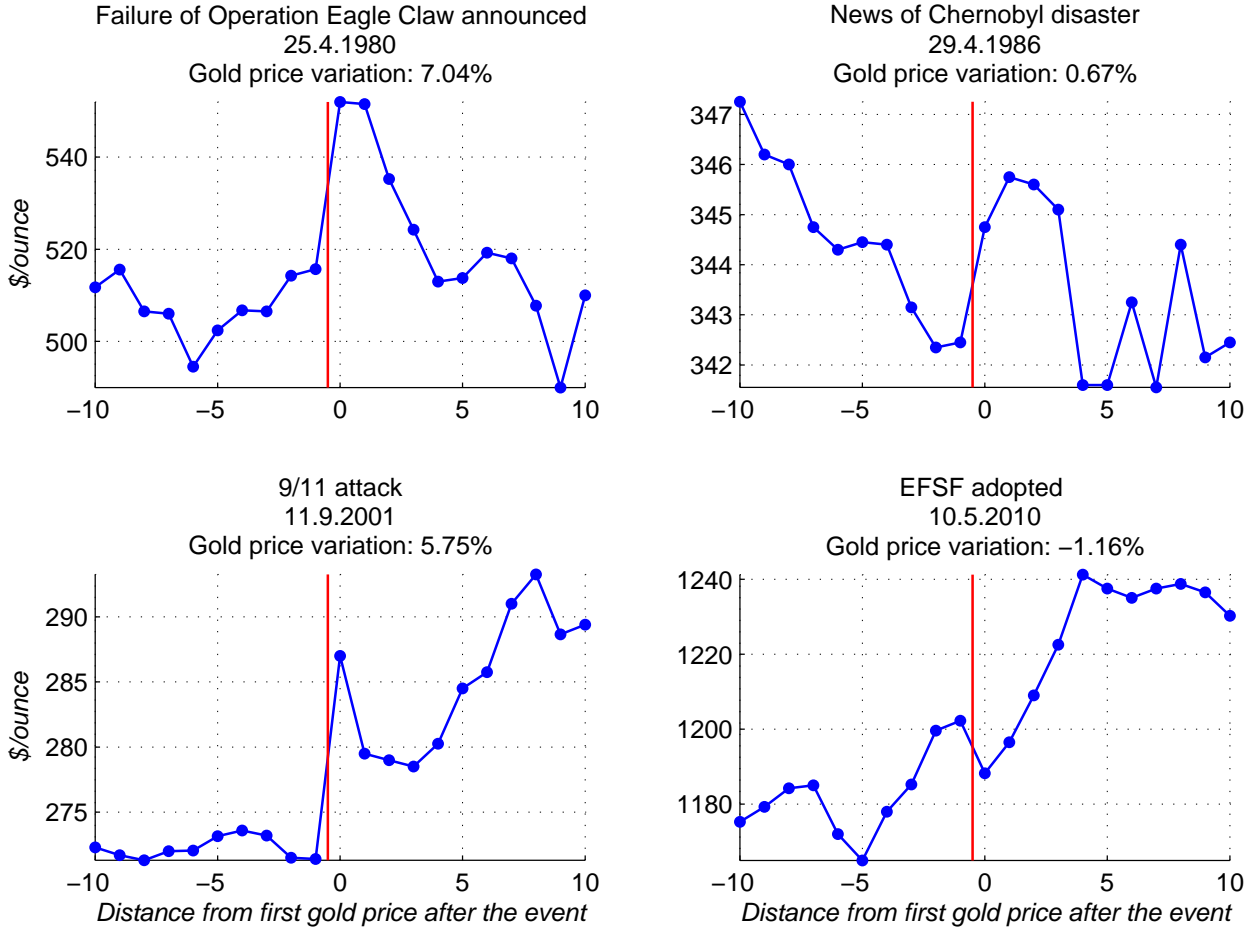
Further support for the use of gold to inform our proxy for uncertainty shocks is provided by [Baur and McDermott \(2010\)](#) and [Baur and Lucey \(2010\)](#), who find evidence supporting the view of gold as a safe haven asset. In [Section G](#) we discuss the robustness of the results using all candidate proxies, as long as they allow for the identifying restrictions to be satisfied.

C A Few Examples

In this section we discuss in detail the behaviour of the price of gold around selected events in order to provide additional intuition for the methodology used. [Figure C1](#) plots the variation in the intradaily gold price (morning and afternoon prices) around four selected illustrative events:

1. On 24 October 1980 President Carter authorised a secret military operation to free the *hostages in the US embassy* in Tehran. The operation had been kept secret to anyone outside of the inner circle of the President, and its failure was announced by Carter at 1:00 on the day after, Washington time. The announcement triggered an increase in uncertainty due to the heightened tension in the region, and London priced gold in its morning auction 7.04% above the afternoon price of the day before, likely pricing in the increased uncertainty that was soon to unfold between the US and Iran;
2. In the morning of 25 April 1986, technicians at the *Chernobyl nuclear station* turned off the emergency cooling system and started a test, which was mishandled, resulting in the explosion of the reactor at 01:23 the following morning. The Russian authorities neither informed the neighbouring villages nor other countries, with the West finding out initially through ordinary tests of radioactivity

Figure C1: Gold price around four events



Notes: The figure shows 10 quotes of the price of gold before and 10 quotes of the price of gold after four different events, whose occurrence is indicated by the vertical line. The figures corresponding to all 117 events collected in the analysis are reported in the on-line appendix. The percentage variations are winsorised at 0.5% on each side of the tail before aggregating them into the proxy. Compared to this figure, the winsorisation is responsible for the lower values in Figure 1 in correspondence to the Failure of Operation Eagle Claw and to the 9/11 attack.

in Sweden, and then through a US satellite picture of the site. The news of winds coming from the East then spread on the day of 29 April, and London priced an increase in the first auction of 30 April, although of only 0.67%;

3. On September 11 2001, at 08:46 New York time, 13:46 London time, the first plane of the 9/11 terrorist attack hit the *World Trade Center*. The event occur-

red between the morning and the afternoon auctions in London. The news of the event travelled around the world immediately and London priced a 5.75% increase in the price of gold in its afternoon auction;

4. During the height of the European sovereign debt crisis the European Council agreed in an overnight meeting upon the establishment of the *European Financial Stabilization Facility* (EFSF). The press release communicating the positive outcome of the meeting is dated on the night of May 9, 2010, with Bloomberg reporting the news in the early hours of May 10. The price of gold in the morning auction drops 1.2% as compared to the afternoon auction the day before.

D Identification of the Structural VAR

This section outlines how external instruments are used to achieve the identification of the structural VAR models. To build the intuition behind the set-identification proposed in the paper, we first outline the case of a single instrument correlated with only one structural shock, as in [Olea et al. \(2012\)](#) and [Stock and Watson \(2012\)](#). We then extend the analysis to the set-identification of more than one structural shock using instruments correlated with more than one shock, building on the analysis by [Mertens and Ravn \(2013\)](#).

The model is given by

$$\mathbf{y}_t = \boldsymbol{\delta} + \mathbf{A}(L)\mathbf{y}_{t-1} + \mathbf{u}_t, \quad (\text{D.3})$$

$$\mathbf{u}_t = \mathbf{B}\boldsymbol{\epsilon}_t, \quad (\text{D.4})$$

$$\boldsymbol{\epsilon}_t = \mathbf{A}\mathbf{u}_t. \quad (\text{D.5})$$

\mathbf{y}_t is a $k \times 1$ vector including the endogenous variables, $\boldsymbol{\delta}$ includes constant terms and

$\mathbf{A}(L)$ is a lag matrix polynomial for the autoregressive form of the model. \mathbf{u}_t is a $k \times 1$ vector of reduced form shocks with covariance matrix Σ and $\boldsymbol{\epsilon}_t$ is a $k \times 1$ vector of serially uncorrelated, normally distributed structural shocks, with covariance matrix normalized to the identity matrix. Matrix \mathbf{B} maps structural shocks into reduced form shocks, while matrix $\mathbf{A} = \mathbf{B}^{-1}$ allows the use of reduced form shocks to recover structural shocks. Covariance restrictions imply $\Sigma = \mathbf{B}\mathbf{B}' = \mathbf{A}^{-1}\mathbf{A}'^{-1}$.

Using one instrument correlated with only one shock

Consider first the case in which the researcher aims to identify only one shock and has one instrument to identify such shock. The shock can be ordered without loss of generality as the first shock in $\boldsymbol{\epsilon}_t$, hence we refer to it here as ϵ_{1t} . Equation (D.4) then rewrites as

$$\mathbf{u}_t = \mathbf{b}_1\epsilon_{1t} + \mathbf{B}^*\boldsymbol{\epsilon}_t^*, \quad (\text{D.6})$$

with $\mathbf{B} = [\mathbf{b}_1, \mathbf{B}^*]$, where \mathbf{b}_1 is the $k \times 1$ impulse vector corresponding to ϵ_{1t} and \mathbf{B}^* contains the impulse vectors of the remaining $k - 1$ shocks. The identification of ϵ_{1t} requires \mathbf{b}_1 for the computation of impulse responses and \mathbf{a}_1 for the estimation of the shocks, with \mathbf{a}_1 the first row of matrix $\mathbf{A} = \mathbf{B}^{-1}$, written as a column vector.

When an instrument m_{1t} is available satisfying conditions

$$E(\epsilon_{1t}m_{1t}) = \phi, \quad E(\boldsymbol{\epsilon}_t^*m_{1t}) = \mathbf{0}, \quad (\text{D.7})$$

then the identification of ϵ_{1t} can be constructed by substituting equation (D.6) into $E(\mathbf{u}_tm_{1t})$, obtaining $E(\mathbf{u}_tm_{1t}) = \mathbf{b}_1\phi$. Since $E(\mathbf{u}_tm_{1t})$ can be estimated, one learns about \mathbf{b}_1 up to an unknown scalar ϕ . This new information can be used to complement the covariance restrictions $\Sigma = \mathbf{B}\mathbf{B}'$ and obtain an estimate for \mathbf{b}_1 . Last, an estimate

for \mathbf{a}_1 can be computed using results from the inverse of partitioned matrices.

More precisely, the identification of ϵ_{1t} can be implemented as follows:

1. Estimate the reduced form model (D.3) and obtain estimates $\hat{\mathbf{u}}_t$ and $\hat{\Sigma}$;
2. Use $\hat{\mathbf{u}}_t$ to estimate $E(\mathbf{u}_t m_{1t})$ and define $\hat{\boldsymbol{\lambda}} = \left(\frac{\hat{E}(\hat{u}_{2t} m_{1t})}{\hat{E}(\hat{u}_{1t} m_{1t})}, \dots, \frac{\hat{E}(\hat{u}_{kt} m_{1t})}{\hat{E}(\hat{u}_{1t} m_{1t})} \right)'$, where $\hat{E}(\cdot)$ indicates the sample mean. Since $E(u_{it} m_{1t}) = b_{i1} E(\epsilon_{1t} m_{1t})$ and since $\hat{E}(\hat{u}_{it} m_{1t})$ is a consistent estimator for $E(u_{it} m_{1t})$, $\hat{\boldsymbol{\lambda}}$ is a consistent estimator for the $(k-1) \times 1$ vector $\boldsymbol{\lambda} = \left(\frac{b_{21}}{b_{11}}, \dots, \frac{b_{k1}}{b_{11}} \right)'$;³
3. Partition matrices \mathbf{B} and Σ as

$$\mathbf{B} = \begin{pmatrix} b_{11} & \mathbf{b}'_{12} \\ \mathbf{b}_{21} & \mathbf{B}_{22} \end{pmatrix}, \quad \Sigma = \begin{pmatrix} \sigma_{11} & \boldsymbol{\sigma}'_{12} \\ \boldsymbol{\sigma}_{21} & \Sigma_{22} \end{pmatrix}, \quad (\text{D.8})$$

with b_{11} and σ_{11} of dimension 1×1 , \mathbf{b}_{21} and $\boldsymbol{\sigma}_{21}$ of dimension $(k-1) \times 1$, \mathbf{b}'_{12} and $\boldsymbol{\sigma}'_{12}$ of dimension $1 \times (k-1)$ and \mathbf{B}_{22} and Σ_{22} of dimension $(k-1) \times (k-1)$.

Estimate $\mathbf{b}_1 = (b_{11}, \mathbf{b}'_{21})'$ with the estimator $\hat{\mathbf{b}}_1 = \hat{b}_{11} \cdot (1, \hat{\boldsymbol{\lambda}}')'$, where the scaling

³ $\boldsymbol{\lambda}$ can also be estimated using the instrumental variable approach outlined in Mertens and Ravn (2013). The estimates are by construction identical even in a finite sample.

factor is obtained as $\hat{b}_{11} = \pm \sqrt{\hat{\sigma}_{11} - \widehat{\mathbf{b}'_{12}\mathbf{b}_{12}}}$ with⁴

$$\widehat{\mathbf{b}'_{12}\mathbf{b}_{12}} = (\hat{\boldsymbol{\sigma}}_{21} - \hat{\sigma}_{11}\hat{\boldsymbol{\lambda}})' \hat{\boldsymbol{\Gamma}}^{-1} (\hat{\boldsymbol{\sigma}}_{21} - \hat{\sigma}_{11}\hat{\boldsymbol{\lambda}}), \quad (\text{D.12})$$

$$\hat{\boldsymbol{\Gamma}} = \hat{\boldsymbol{\Sigma}}_{22} + \hat{\sigma}_{11}\hat{\boldsymbol{\lambda}}\hat{\boldsymbol{\lambda}}' - \hat{\boldsymbol{\sigma}}_{21}\hat{\boldsymbol{\lambda}}' - \hat{\boldsymbol{\lambda}}\hat{\boldsymbol{\sigma}}'_{21}. \quad (\text{D.13})$$

Whether the positive or the negative solution for \hat{b}_{11} is used depends on the sign convention adopted for the interpretation of the shock, for example whether a shock of positive sign is interpreted as expansionary or contractionary. Use $\hat{\mathbf{b}}_1$ to compute impulse responses to a shock of one standard deviation, or use $(1, \hat{\boldsymbol{\lambda}}')' \cdot \frac{\psi}{\hat{\lambda}_{i-1}}$ to compute impulse responses to a shock that increases variable $i = 1, \dots, k$ by ψ , with $\hat{\lambda}_{i-1}$ the element $i-1$ of $\hat{\boldsymbol{\lambda}}$ and $\hat{\lambda}_0 = 1$;

⁴As derived in De Wind *et al.* (2014), combining equation $\boldsymbol{\lambda} = \mathbf{b}_{21}/b_{11}$ with the equations of the system implied by the covariance restrictions delivers

$$b_{11}^2 + \mathbf{b}'_{12}\mathbf{b}_{12} = \sigma_{11}, \quad (\text{D.9})$$

$$b_{11}^2 \boldsymbol{\lambda} + \mathbf{B}_{22}\mathbf{b}_{12} = \boldsymbol{\sigma}_{21}, \quad (\text{D.10})$$

$$b_{11}^2 \boldsymbol{\lambda} \boldsymbol{\lambda}' + \mathbf{B}_{22}\mathbf{B}'_{22} = \boldsymbol{\Sigma}_{22}. \quad (\text{D.11})$$

From equation (D.9) one obtains the initial expression for b_{11} . To solve for $\mathbf{b}'_{12}\mathbf{b}_{12}$, subtract equation (D.9) multiplied by $\boldsymbol{\lambda}$ from (D.10), obtain the expression $\mathbf{b}_{12} = (\mathbf{B}_{22} - \boldsymbol{\lambda}\mathbf{b}'_{12})^{-1}(\boldsymbol{\sigma}_{21} - \sigma_{11}\boldsymbol{\lambda})$ and premultiply it by its transpose, obtaining (D.12) under the expression $\boldsymbol{\Gamma} = (\mathbf{B}_{22} - \boldsymbol{\lambda}\mathbf{b}'_{12})(\mathbf{B}_{22} - \boldsymbol{\lambda}\mathbf{b}'_{12})' = \mathbf{B}_{22}\mathbf{B}'_{22} - \mathbf{B}_{22}\mathbf{b}_{12}\boldsymbol{\lambda}' - \boldsymbol{\lambda}\mathbf{b}'_{12}\mathbf{B}'_{22} + \boldsymbol{\lambda}\mathbf{b}'_{12}\mathbf{b}_{12}\boldsymbol{\lambda}'$. To compute $\boldsymbol{\Gamma}$, subtract equation (D.10) postmultiplied by $\boldsymbol{\lambda}'$ from equation (D.11), obtain an expression for $\mathbf{B}_{22}\mathbf{b}_{12}\boldsymbol{\lambda}'$ and substitute this and its transpose in $\boldsymbol{\Gamma}$. Then start from equation (D.11), subtract equation (D.9) having premultiplied it by $\boldsymbol{\lambda}$ and having postmultiplied it by its transpose, obtaining an expression for $\mathbf{B}'_{22}\mathbf{B}_{22} - \boldsymbol{\lambda}\mathbf{b}'_{12}\mathbf{b}_{12}\boldsymbol{\lambda}'$. Substitute this in $\boldsymbol{\Gamma}$ and obtain equation (D.13).

4. Estimate \mathbf{a}_1 with the estimator $\hat{\mathbf{a}}_1 = (\hat{b}_{11} - \mathbf{b}'_{12} \widehat{\mathbf{B}}_{22}^{-1} \hat{\mathbf{b}}_{21})^{-1} \begin{pmatrix} 1 \\ -\widehat{\mathbf{B}}_{22}^{'-1} \mathbf{b}_{12} \end{pmatrix}$ with⁵

$$\hat{\mathbf{b}}_{21} = \hat{\boldsymbol{\lambda}} \hat{b}_{11} \quad (\text{D.17})$$

$$\mathbf{b}'_{12} \widehat{\mathbf{B}}_{22}^{-1} = (\hat{\boldsymbol{\sigma}}_{21} - \hat{b}_{11} \hat{\mathbf{b}}_{21})' (\hat{\Sigma}_{22} - \hat{\mathbf{b}}_{21} \hat{\mathbf{b}}'_{21})^{-1}. \quad (\text{D.18})$$

Use $\hat{\mathbf{a}}_1$ to obtain estimates $\hat{\epsilon}_{1t} = \mathbf{a}'_1 \mathbf{u}_t$.

Using two instruments both correlated with two shocks

The identification strategy described above aims for the identification of one shock using one instrument, assumed to be correlated only with the shock of interest. We now describe how the approach can be generalised to a case in which the researcher aims for the identification of $l \ll k$ shocks and has l instruments, potentially correlated with more than one shock.

The analysis departs from the decomposition of equation (D.4) into

$$\mathbf{u}_t = \tilde{\mathbf{B}} \tilde{\boldsymbol{\epsilon}}_t + \tilde{\mathbf{B}}^* \tilde{\boldsymbol{\epsilon}}_t^*, \quad (\text{D.19})$$

⁵For a general matrix $\mathbf{B} = \begin{pmatrix} \mathbf{B}_{11} & \mathbf{B}_{12} \\ \mathbf{B}_{21} & \mathbf{B}_{22} \end{pmatrix}$, the formula for the inverse of partitioned matrices is $\mathbf{B}^{-1} = \begin{pmatrix} (\mathbf{B}_{11} - \mathbf{B}_{12} \mathbf{B}_{22}^{-1} \mathbf{B}_{21})^{-1} & -(\mathbf{B}_{11} - \mathbf{B}_{12} \mathbf{B}_{22}^{-1} \mathbf{B}_{21})^{-1} \mathbf{B}_{12} \mathbf{B}_{22}^{-1} \\ -(\mathbf{B}_{22} - \mathbf{B}_{21} \mathbf{B}_{11}^{-1} \mathbf{B}_{12})^{-1} \mathbf{B}_{21} \mathbf{B}_{11}^{-1} & (\mathbf{B}_{22} - \mathbf{B}_{21} \mathbf{B}_{11}^{-1} \mathbf{B}_{12})^{-1} \end{pmatrix}$. Given the partition used for \mathbf{B} , we obtain $\mathbf{a} = (b_{11} - \mathbf{b}'_{12} \mathbf{B}_{22}^{-1} \mathbf{b}_{21})^{-1} \begin{pmatrix} 1 \\ -\mathbf{B}_{22}^{'-1} \mathbf{b}_{12} \end{pmatrix}$. To obtain an expression for $\mathbf{b}'_{12} \mathbf{B}_{22}^{-1}$, rearrange the equations of the system implied by the covariance restrictions, obtaining

$$\mathbf{b}'_{12} \mathbf{b}_{12} = \sigma_{11} - \hat{b}_{11}^2, \quad (\text{D.14})$$

$$\mathbf{B}_{22} \mathbf{b}_{12} = \boldsymbol{\sigma}_{21} - \hat{b}_{11} \hat{\mathbf{b}}_{21}, \quad (\text{D.15})$$

$$\mathbf{B}_{22} \mathbf{B}'_{22} = \Sigma_{22} - \hat{\mathbf{b}}_{21} \hat{\mathbf{b}}'_{21}. \quad (\text{D.16})$$

Equation (D.15) can be rearranged into $\mathbf{B}'_{22}^{-1} \mathbf{b}_{12} = \mathbf{B}'_{22}^{-1} \mathbf{B}_{22}^{-1} (\boldsymbol{\sigma}_{21} - \hat{b}_{11} \hat{\mathbf{b}}_{21})$. An expression for $\mathbf{B}'_{22}^{-1} \mathbf{B}_{22}^{-1}$ can be derived by inverting equation (D.16). Combining these results gives equation (D.18).

with $\mathbf{B} = [\tilde{\mathbf{B}}, \tilde{\mathbf{B}}^*]$. The $k \times l$ matrix $\tilde{\mathbf{B}}$ contains the impulse vectors of the l structural shocks of interest, the $l \times 1$ vector $\tilde{\epsilon}_t$ contains such shocks, and $\tilde{\mathbf{B}}^*$ contains the impulse vectors of the remaining $k - l$ structural shocks. The identification of $\tilde{\epsilon}_t$ requires $\tilde{\mathbf{B}}$ for the computation of impulse responses and $\tilde{\mathbf{A}}$ for the estimation of the shocks, with $\tilde{\mathbf{A}}$, of dimensions $k \times l$, defined as the first l rows of matrix $\mathbf{A} = \mathbf{B}^{-1}$ written as column vectors.

When l instruments $\mathbf{m}_t = (m_{1t}, \dots, m_{lt})'$ are available satisfying conditions

$$E(\tilde{\epsilon}_t \mathbf{m}'_t) = \Phi \quad , \quad E(\epsilon_t^* m_{jt}) = \mathbf{0} \quad , \quad \forall j = 1, \dots, l, \quad (\text{D.20})$$

the identification of each shock in $\tilde{\epsilon}_t$ cannot be achieved using one instrument at the time. In fact, considering for simplicity the case of two shocks and two instruments correlated with both shocks, it now holds that $E(u_{it} m_{1t}) = b_{i1} E(\epsilon_{1t} m_{1t}) + b_{i2} E(\epsilon_{2t} m_{1t})$. This implies that $\hat{\lambda} = \left(\frac{\hat{E}(\hat{u}_{2t} m_{1t})}{\hat{E}(\hat{u}_{1t} m_{1t})}, \dots, \frac{\hat{E}(\hat{u}_{kt} m_{1t})}{\hat{E}(\hat{u}_{1t} m_{1t})} \right)'$ is now a consistent estimator of

$$\left(\frac{b_{21} E(\epsilon_{1t} m_{1t}) + b_{22} E(\epsilon_{2t} m_{1t})}{b_{11} E(\epsilon_{1t} m_{1t}) + b_{12} E(\epsilon_{2t} m_{1t})} \quad \frac{b_{31} E(\epsilon_{1t} m_{1t}) + b_{32} E(\epsilon_{2t} m_{1t})}{b_{11} E(\epsilon_{1t} m_{1t}) + b_{12} E(\epsilon_{2t} m_{1t})} \quad \dots \quad \frac{b_{k1} E(\epsilon_{1t} m_{1t}) + b_{k2} E(\epsilon_{2t} m_{1t})}{b_{11} E(\epsilon_{1t} m_{1t}) + b_{12} E(\epsilon_{2t} m_{1t})} \right)' . \quad (\text{D.21})$$

Hence, $\hat{\lambda}$ does not deliver a consistent estimate of the relative impulse vector $\lambda = (\frac{b_{21}}{b_{11}}, \dots, \frac{b_{k1}}{b_{11}})'$ corresponding to ϵ_{1t} , but an estimate of a nonlinear combination of the impulse vectors corresponding to ϵ_{1t} and ϵ_{2t} . Note that if m_{1t} is only correlated with ϵ_{1t} , $E(\epsilon_{2t} m_{1t}) = 0$ and expression (D.21) simplifies to λ , i.e., $\hat{\lambda}$ converges to λ .

In light of these considerations, the identification of $\tilde{\epsilon}_t$ can be constructed by substituting equation (D.19) into $E(\mathbf{u}_t \mathbf{m}'_t)$, obtaining $E(\mathbf{u}_t \mathbf{m}'_t) = \tilde{\mathbf{B}} \cdot \Phi$. Since $E(\mathbf{u}_t \mathbf{m}'_t)$ can be estimated, one learns about linear combinations of the columns of $\tilde{\mathbf{B}}$ according to unknown weights Φ . This new information can be used to complement the covariance restrictions $\Sigma = \mathbf{B} \mathbf{B}'$ and obtain a set of estimates for $\tilde{\mathbf{B}}$. Last, the corresponding set

of the estimates for $\tilde{\mathbf{A}}$ can be obtained by using results from the inverse of partitioned matrices.

More precisely, the identification of $\tilde{\boldsymbol{\epsilon}}_t$ can be implemented as follows:

1. Estimate the reduced form model (D.3) and obtain estimates $\hat{\mathbf{u}}_t$ and $\hat{\Sigma}$;
2. Define $\hat{\Lambda} = \hat{\mathbf{E}}_{21}\hat{\mathbf{E}}_{11}^{-1}$ given $\hat{\mathbf{E}} = \hat{E}(\hat{\mathbf{u}}_t\mathbf{m}'_t)$ of dimension $k \times l$ and $\hat{\mathbf{E}}_{11}$ and $\hat{\mathbf{E}}_{21}$ its partition into the $l \times l$ upper component and the remaining $(k-l) \times l$ lower component. Define \mathbf{E}_{11} and \mathbf{E}_{21} the equivalent decomposition of $E(\mathbf{u}_t\mathbf{m}'_t)$ and \mathbf{B}_{11} and \mathbf{B}_{12} the equivalent decomposition of $\tilde{\mathbf{B}}$. Since $\mathbf{E}_{11} = \mathbf{B}_{11}\Phi$ and $\mathbf{E}_{21} = \mathbf{B}_{21}\Phi$, it holds that $\mathbf{E}_{21}\mathbf{E}_{11}^{-1} = \mathbf{B}_{21}\mathbf{B}_{11}^{-1}$. Hence $\hat{\Lambda}$ is a consistent estimator for the $(k-l) \times l$ matrix $\Lambda = \mathbf{B}_{21}\mathbf{B}_{11}^{-1}$;
3. Partition matrices \mathbf{B} and Σ as

$$\mathbf{B} = \begin{pmatrix} \mathbf{B}_{11} & \mathbf{B}_{12} \\ \mathbf{B}_{21} & \mathbf{B}_{22} \end{pmatrix}, \quad \Sigma = \begin{pmatrix} \Sigma_{11} & \Sigma_{12} \\ \Sigma_{21} & \Sigma_{22} \end{pmatrix}, \quad (\text{D.22})$$

with \mathbf{B}_{11} and Σ_{11} of dimension $l \times l$, \mathbf{B}_{21} and Σ_{21} of dimension $(k-l) \times l$, \mathbf{B}_{12} and Σ_{12} of dimension $l \times (k-l)$ and \mathbf{B}_{22} and Σ_{22} of dimension $(k-l) \times (k-l)$. Estimate $\tilde{\mathbf{B}}$ with the estimator $\hat{\tilde{\mathbf{B}}} = \begin{pmatrix} \hat{\mathbf{B}}_{11} \\ \hat{\Lambda}\hat{\mathbf{B}}_{11} \end{pmatrix}$ using $\hat{\mathbf{B}}_{11} = \hat{\mathbf{B}}_{11}^c \mathbf{Q}$, given \mathbf{Q} any $l \times l$ orthogonal matrix and $\hat{\mathbf{B}}_{11}^c$ the lower Choleski decomposition of $\hat{\Sigma}_{11} - \widehat{\mathbf{B}_{12}\mathbf{B}_{12}'}$, with⁶

$$\widehat{\mathbf{B}_{12}\mathbf{B}_{12}'} = (\hat{\Sigma}_{21} - \hat{\Lambda}\hat{\Sigma}_{11})'\hat{\Gamma}^{-1}(\hat{\Sigma}_{21} - \hat{\Lambda}\hat{\Sigma}_{11}), \quad (\text{D.23})$$

$$\hat{\Gamma} = \hat{\Sigma}_{22} + \hat{\Lambda}\hat{\Sigma}_{11}\hat{\Lambda}' - \hat{\Sigma}_{21}\hat{\Lambda}' - \hat{\Lambda}\hat{\Sigma}_{21}'. \quad (\text{D.24})$$

⁶The derivations follow from footnote 4, after taking account the new dimensions of the parameters.

Drawing orthogonal matrices generates a set of candidate estimates for $\tilde{\mathbf{B}}$. Identifying restrictions on this set can then be imposed, for example, on the estimated moments $\hat{\Phi} = \hat{\mathbf{B}}_{11}^{-1} \hat{\mathbf{E}}_{11}$, as in the paper. Use $\hat{\tilde{\mathbf{B}}}$ to compute impulse responses to shocks of one standard deviation;⁷

4. For each candidate $\tilde{\mathbf{B}}$, estimate $\tilde{\mathbf{A}}$ with the estimator

$$\hat{\tilde{\mathbf{A}}} = (\hat{\mathbf{B}}_{11} - \mathbf{B}_{12} \widehat{\mathbf{B}}_{22}^{-1} \hat{\mathbf{B}}_{21})^{-1} \begin{pmatrix} \mathbf{I}_2 & -\mathbf{B}_{12} \widehat{\mathbf{B}}_{22}'^{-1} \end{pmatrix} \quad (\text{D.25})$$

with⁸

$$\widehat{\mathbf{B}}_{12}' \widehat{\mathbf{B}}_{22}^{-1} = (\hat{\Sigma}_{21} - \hat{\mathbf{B}}_{11} \hat{\mathbf{B}}_{21}') (\hat{\Sigma}_{22} - \hat{\mathbf{B}}_{21} \hat{\mathbf{B}}_{21}')^{-1} : \quad (\text{D.26})$$

Use $\hat{\tilde{\mathbf{A}}}$ to estimate the shocks $\tilde{\epsilon}_t = \tilde{\mathbf{A}}' \mathbf{u}_t$.

This approach builds on [Mertens and Ravn \(2013\)](#), who identify two shocks using two instruments and then impose a recursive order between these two shocks. They discuss a special case of the methodology outlined above, after imposing $\mathbf{Q} = \mathbf{I}$. Identifying restrictions other than the recursive ordering ([Mertens and Ravn, 2013](#)) and the restrictions on the correlation structure (this paper) can be imposed, for example zero restrictions and sign restrictions, extending the algorithms by [Binning \(2013\)](#) and [Arias et al. \(2014\)](#).

In our paper, $m_{1t} = m_t^g$ is the proxy for the uncertainty shock, $m_{2t} = m_t^n$ is the proxy for the news shock, $\epsilon_{1t} = \epsilon_t^u$ represents the uncertainty shock and $\epsilon_{2t} = \epsilon_t^n$ represents the news shock. The nature of m_t^g discussed in [Section 2](#) of the paper implies that an increase in the proxy is associated with an increase in uncertainty.

⁷In the case of one instrument and one shock of interest, b_{11} is a scalar, it must satisfy $b_{11}^2 = \sigma_{11} + \mathbf{b}'_{12} \mathbf{b}_{12}$ (see footnote 5), and hence is unique up to its sign. On the contrary, \mathbf{B}_{11} is a matrix and must satisfy condition $\mathbf{B}_{11} \mathbf{B}'_{11} = \Sigma_{11} - \mathbf{B}'_{12} \mathbf{B}_{12}$, hence an identification problem emerges which can be addressed with set-identification. Starting for simplicity from the lower decomposition of the estimate of $\Sigma_{11} - \mathbf{B}'_{12} \mathbf{B}_{12}$, rotations can be computed through matrix orthogonal matrices \mathbf{Q} .

⁸The derivations follow from footnote 5, after taking account the new dimensions of the parameters.

Studying the factor loadings when computing m_t^n from the news shocks estimated in the literature, we ensure that increases in m_t^n imply unfavourable news. Regarding the shocks, we normalize the sign of \mathbf{b}_1 to deliver a positive element on its second entry, and normalize the sign of \mathbf{b}_2 to deliver a negative element on its first entry. Having ordered the VXO as the second variable and the S&P500 as the first variable, this normalization ensures that an uncertainty shock of positive sign is interpreted as an exogenous *increase* in uncertainty, and that a news shock of positive sign is interpreted as an exogenous occurrence of *unfavourable* news. These sign conventions then imply that the restrictions on the covariance matrix discussed in [Section 3](#) of the paper are meaningful restrictions and bear an economic interpretation.

The proxy for the news shock is available on a quarterly frequency. To accommodate for this difference in frequency, we estimate the matrix $\hat{\mathbf{E}} = \hat{E}(\hat{\mathbf{u}}_t \mathbf{m}'_t)$ discussed in step 2 of the procedure above using monthly data for the column that corresponds to the proxy for the uncertainty shock, and using quarterly data for the column that corresponds to the proxy for the news shock. Using simulations, we find that while expected values are affected by the aggregation from monthly to quarterly frequency, the relative moments computed in $\hat{\Lambda} = \hat{\mathbf{E}}_{21}\hat{\mathbf{E}}_{11}^{-1}$ are not notably affected, indicating that the approach is not distorted by the presence of the proxies with different frequencies. Monthly estimates for the news shock can then be computed using the estimated $\hat{\tilde{A}}$ matrix from step 4 above and applying the computation of estimated shocks to the monthly residuals from the VAR model.⁹

⁹To ensure consistency within the bootstrap we construct bootstrapped data by changing the sign of randomly selected quarters, rather than months.

E Simulations on the New Keynesian Model

We use Monte Carlo simulations to study the performance of the identification strategy outlined in [Section D](#). As a data generating process we use a standard New Keynesian model, which we take from [An and Schorfheide \(2007\)](#) and [Komunjer and Ng \(2011\)](#). Following the discussion in [Giacomini \(2013\)](#), the calibration of the deep parameters used in [Komunjer and Ng \(2011\)](#) implies the following VAR representation of the model,

$$\begin{pmatrix} r_t \\ x_t \\ \pi_t \end{pmatrix} = \begin{pmatrix} 0.79 & 0 & 0.25 \\ 0.19 & 0.95 & -0.46 \\ 0.12 & 0 & 0.62 \end{pmatrix} \begin{pmatrix} r_{t-1} \\ x_{t-1} \\ \pi_{t-1} \end{pmatrix} + \begin{pmatrix} 0.61 & 0 & 0.69 \\ 1.49 & 1 & -1.10 \\ 1.49 & 0 & -0.75 \end{pmatrix} \begin{pmatrix} \epsilon_t^z \\ \epsilon_t^g \\ \epsilon_t^r \end{pmatrix}, \quad (\text{E.27})$$

with covariance matrix of the vector $(\epsilon_t^z, \epsilon_t^g, \epsilon_t^r)'$ given by

$$\mathbf{D} = \begin{pmatrix} 0.003^2 & 0 & 0 \\ 0 & 0.006^2 & 0 \\ 0 & 0 & 0.002^2 \end{pmatrix}. \quad (\text{E.28})$$

We use model (E.27) as a data generating process, drawing the shocks from a normal distribution with covariance matrix \mathbf{D} from equation (E.28). In the model, r_t is the interest rate, x_t is output and π_t is inflation. The data are driven by three structural shocks: a TFP shock ϵ_t^z , a government spending shock ϵ_t^g and a monetary shock ϵ_t^r .

We investigate a similar setup as in the paper, jointly identifying two structural shocks. We focus on the impulse responses to the TFP shock and to the monetary shock because, in contrast to the government spending shock, these shocks affect all variables in the model contemporaneously. As such, they display dynamics that are

more general and more similar to the ones outlined in the paper.

Given a pseudo dataset of size T generated from model (E.27), we construct the instruments

$$m_{1t} = \iota_1 \epsilon_t^z + (1 - \iota_1) \epsilon_t^r + \iota_2 \nu_{1t}. \quad (\text{E.29a})$$

$$m_{2t} = (1 - \iota_1) \epsilon_t^z + \iota_1 \epsilon_t^r + \iota_2 \nu_{2t}, \quad (\text{E.29b})$$

with ν_{1t} and ν_{2t} two independent white noise disturbances. It then holds that

$$\begin{aligned} \tilde{\Phi} &= \begin{pmatrix} \text{corr}(\epsilon_t^z, m_{1t}) & \text{corr}(\epsilon_t^z, m_{2t}) \\ \text{corr}(\epsilon_t^r, m_{1t}) & \text{corr}(\epsilon_t^r, m_{2t}) \end{pmatrix} = \\ &= \begin{pmatrix} \iota_1 \frac{\sigma_z}{\sigma_{m_1}} & (1 - \iota_1) \frac{\sigma_z}{\sigma_{m_2}} \\ (1 - \iota_1) \frac{\sigma_r}{\sigma_{m_1}} & \iota_1 \frac{\sigma_r}{\sigma_{m_2}} \end{pmatrix}, \end{aligned} \quad (\text{E.30})$$

with $\sigma_{m_1} = \sqrt{\iota_1^2 \sigma_z^2 + (1 - \iota_1)^2 \sigma_r^2 + \iota_2^2}$ and $\sigma_{m_2} = \sqrt{(1 - \iota_1)^2 \sigma_z^2 + \iota_1^2 \sigma_r^2 + \iota_2^2}$. For $\iota_1 = 1$, m_{1t} and m_{2t} are relevant instruments for the TFP shock and for the monetary shock respectively, and neither instrument is correlated with more than one structural shock. Accordingly, they can be used separately following the procedure by Stock and Watson (2012) and Mertens and Ravn (2013). If, instead, ι_1 is smaller than 1, then m_{1t} is a relevant instrument for the TFP shock, but it also correlates with the monetary shock. Similarly, m_{2t} is a relevant instrument for the monetary shock, but it also correlates with the TFP shock. Accordingly, one can aim to identify both shocks using the methodology discussed in Section D.

We construct the Monte Carlo experiment following Paustian (2007). We generate 1000 dataset of size T . For each dataset, we estimate the reduced form and we draw 500 structural representations that satisfy the restrictions $\text{corr}(\epsilon_t^z, m_{1t}) > 0$ and

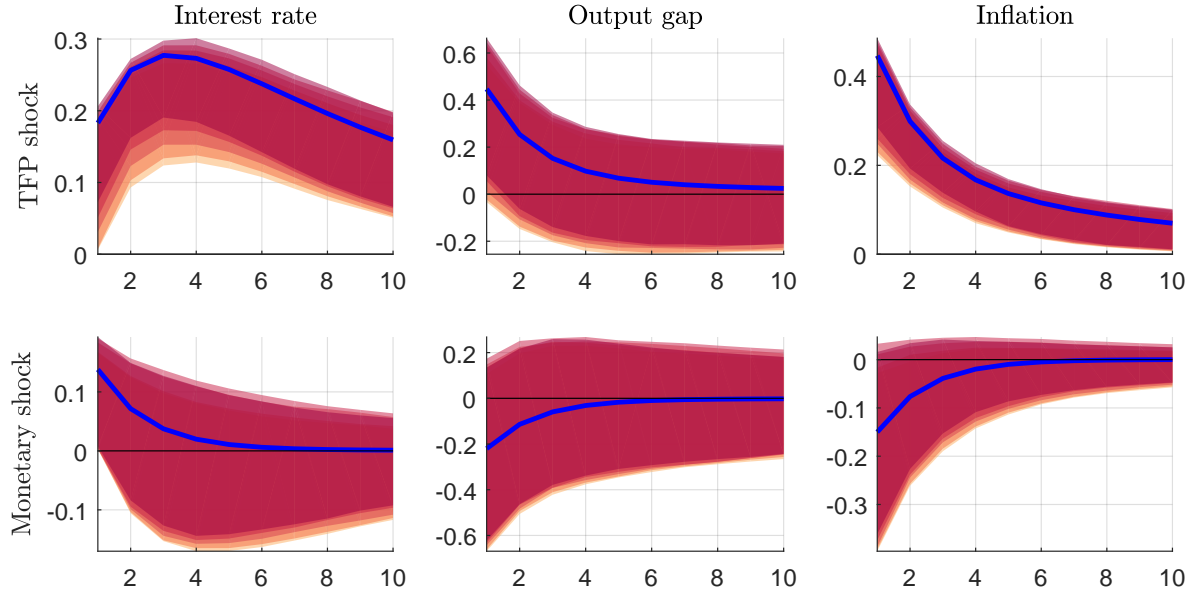
$\text{corr}(\epsilon_t^r, m_{2t}) > 0$, which correspond to restriction (9a) in the paper. Then, following restriction (9b) in the paper, we further narrow down the identified set by imposing that $\text{corr}(\epsilon_t^z, m_{1t}) - \text{corr}(\epsilon_t^z, m_{2t}) > \psi$ and $\text{corr}(\epsilon_t^r, m_{2t}) - \text{corr}(\epsilon_t^r, m_{1t}) > \psi$. This implies an identified set, which we summarize using the 95% pointwise confidence bands. We repeat this procedure for all pseudo datasets and compute the 2.5th-percentile of the 1000 lower bounds and the 97.5th-percentile of the 1000 upper bounds. As a value for ψ we use 0, 0.05, 0.01, 0.15, 0.20. This implies confidence bands that progressively become narrower, the higher the value of ψ .

The results are reported in [Figure E2](#), [Figure E3](#) and [Figure E4](#). In each figure, the thick line indicates the true impulse response to a one standard deviation shock and the bands correspond to the estimated one standard deviation shock, displaying darker shades of red the higher the corresponding value of ψ . Each figure reports the underlying true correlation structure $\tilde{\Phi}$ from equation (E.30). [Figure E2](#) shows the case for $\iota_2 = 0.01$ and $T = 300$, setting ι_1 either to 0.10 or 0.40. The first case implies that each instrument is more strongly correlated with only one shock of interest, while the second case implies a higher correlation of each instrument with the other shock. [Figure E3](#) replicates the analysis by changing the size of the sample, setting $T = 100$ or $T = 500$ and keeping $\iota_1 = 0.10$ and $\iota_2 = 0.10$. Last, [Figure E4](#) increases the noise of the instruments by increasing ι_2 to 0.05 and to 0.10, keeping $\iota_1 = 0.10$ and $T = 300$.

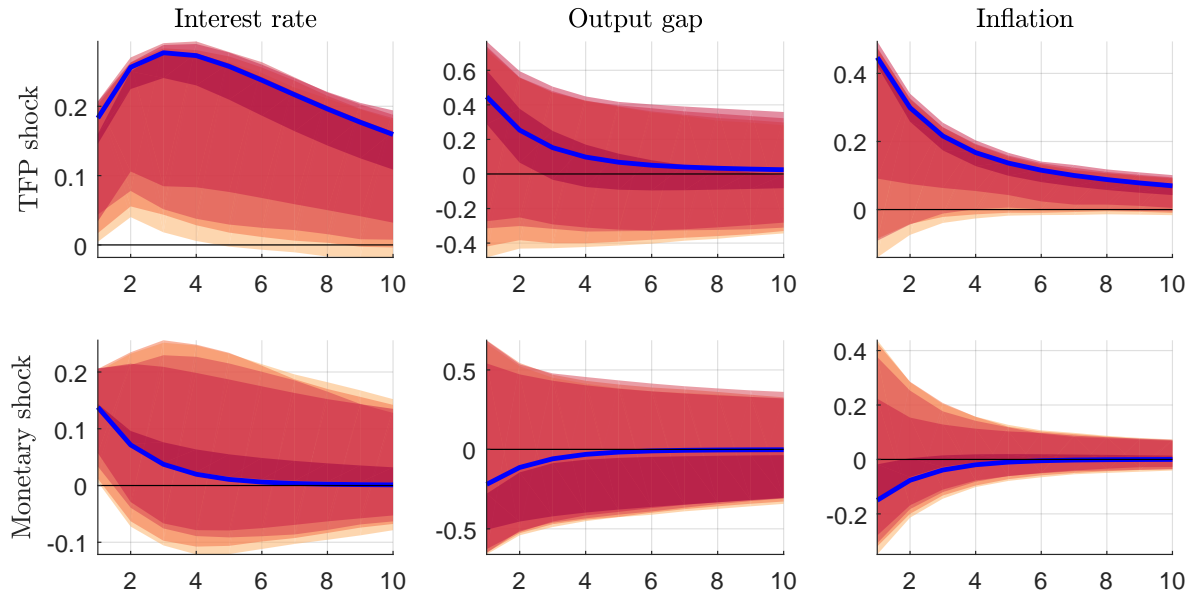
Overall, the results suggest that the set-identification developed in the paper successfully identifies sets of impulse responses that contain the true impulse responses. [Figure E2](#) suggests that the more each instrument correlates also with the other shock, the more helpful it is to use higher values of ψ in order to narrow down the confidence set. In particular, for $\iota_1 = 0.10$, each instrument is mainly correlated with only one shock, and the additional restrictions from ψ are not required for the es-

timated impulse responses to detect the correct sign. By contrast, when $\iota_1 = 0.40$ each instrument is more contaminated by the other shock of interest, and additional restrictions from ψ are required for the estimated shocks to give the correct sign of the impulse responses. A similar result holds with regard to the sample size. [Figure E3](#) shows, as expected, that the higher the sample size and the narrower the estimated bands. Last, [Figure E4](#) shows that when the exogenous noise of the instruments is relatively low ($\iota_2 = 0.05$) the true impulse responses are correctly set-identified. If, instead, it is relatively high ($\iota_2 = \iota_1 = 0.10$), the correct sign of the impulse responses is lost unless the restrictions from $\psi \neq 0$ are imposed.

Figure E2: Monte Carlo simulations (I)



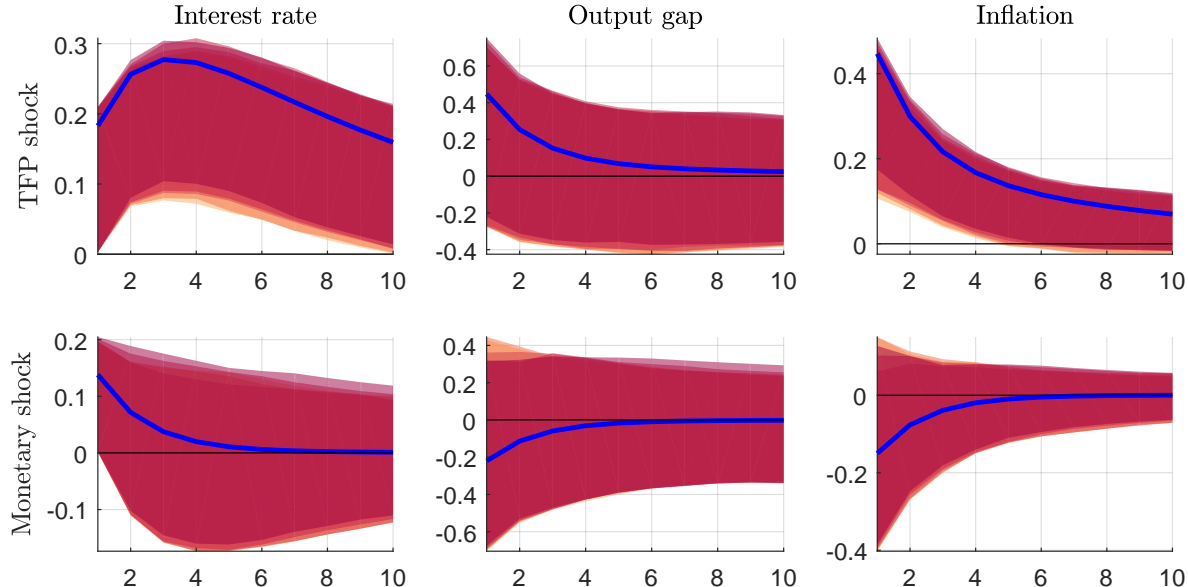
$$\text{Panel a)} \quad \nu_1 = 0.10, \nu_2 = 0.01, T = 300: \tilde{\Phi} = \begin{pmatrix} 0.2606 & 0.0295 \\ 0.0193 & 0.1771 \end{pmatrix}.$$



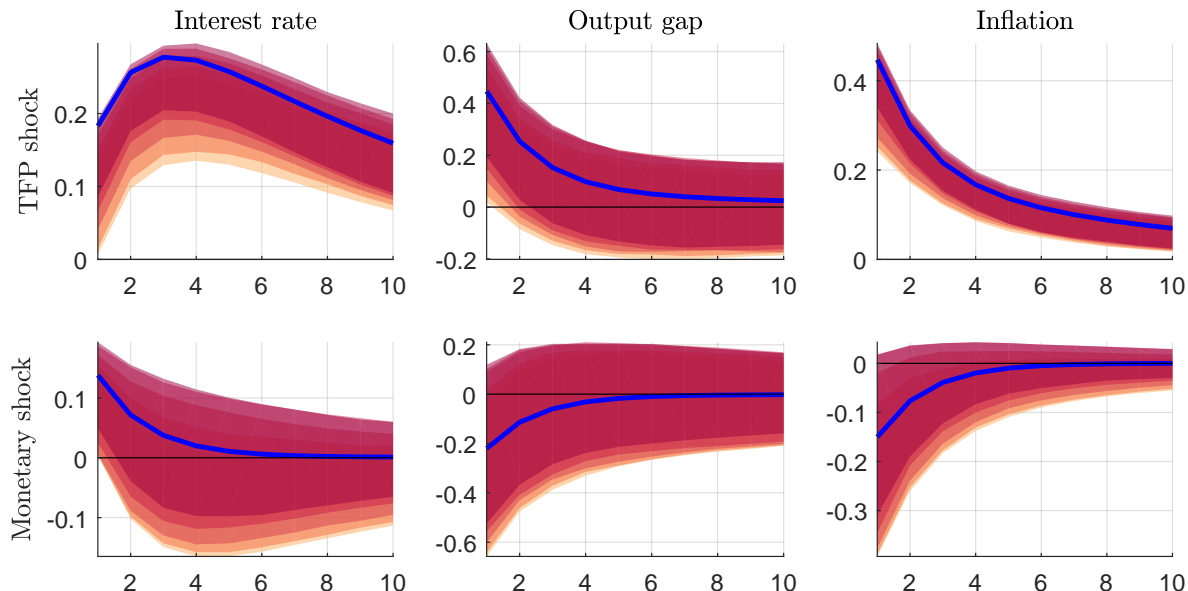
$$\text{Panel b)} \quad \nu_1 = 0.40, \nu_2 = 0.01, T = 300: \tilde{\Phi} = \begin{pmatrix} 0.1766 & 0.1183 \\ 0.0785 & 0.1183 \end{pmatrix}.$$

Note: The figure shows the true impulse responses to a TFP shock and to a monetary shock from the model by [An and Schorfheide \(2007\)](#), and the confidence bands of the estimated impulse responses using the set-identification outlined in the paper. The estimated models satisfy the restrictions $\text{corr}(\epsilon_t^z, m_{1t}) > 0$ and $\text{corr}(\epsilon_t^r, m_{2t}) > 0$. Darker bands imply a higher value of ψ in the additional restrictions $\text{corr}(\epsilon_t^z, m_{1t}) - \text{corr}(\epsilon_t^z, m_{2t}) > \psi$ and $\text{corr}(\epsilon_t^r, m_{2t}) - \text{corr}(\epsilon_t^r, m_{1t}) > \psi$.

Figure E3: Monte Carlo simulations (II)



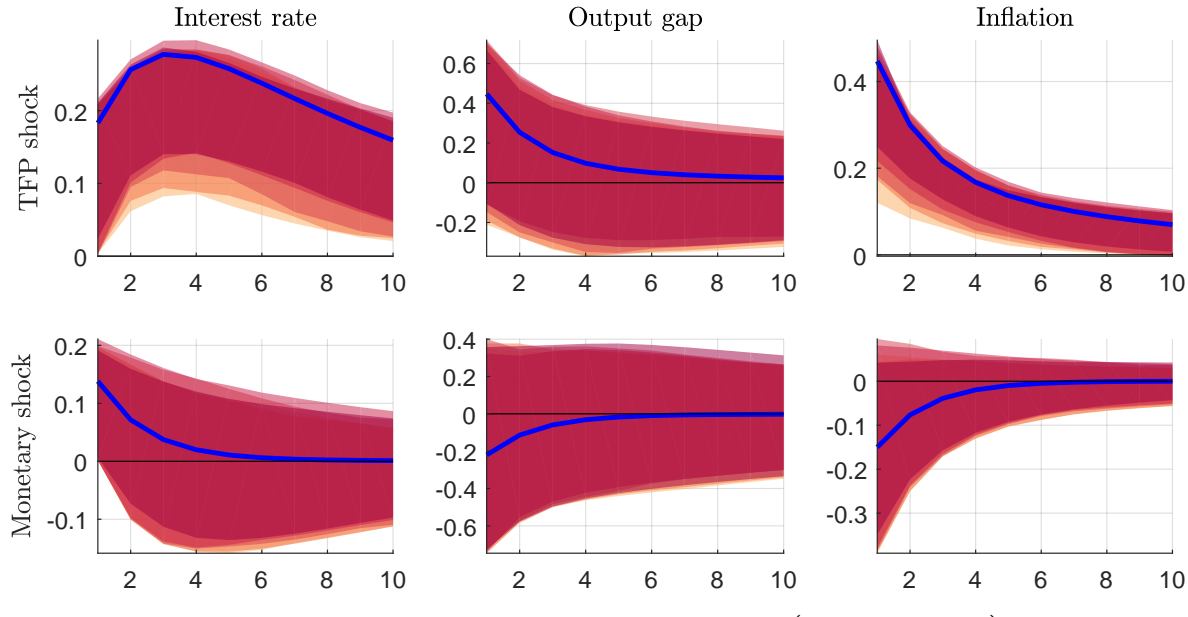
$$\text{Panel a)} \quad \nu_1 = 0.10, \nu_2 = 0.01, T = 100: \tilde{\Phi} = \begin{pmatrix} 0.2606 & 0.0295 \\ 0.0193 & 0.1771 \end{pmatrix}.$$



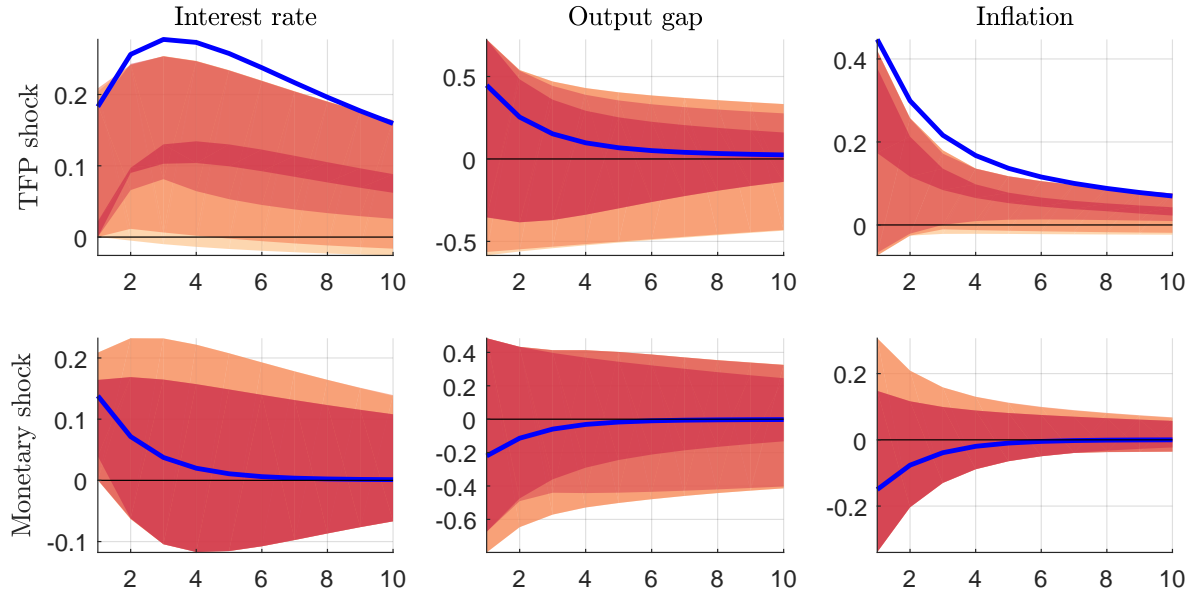
$$\text{Panel b)} \quad \nu_1 = 0.10, \nu_2 = 0.01, T = 500: \tilde{\Phi} = \begin{pmatrix} 0.2606 & 0.0295 \\ 0.0193 & 0.1771 \end{pmatrix}.$$

Note: The figure shows the true impulse responses to a TFP shock and to a monetary shock from the model by [An and Schorfheide \(2007\)](#), and the confidence bands of the estimated impulse responses using the set-identification outlined in the paper. The estimated models satisfy the restrictions $\text{corr}(\epsilon_t^z, m_{1t}) > 0$ and $\text{corr}(\epsilon_t^r, m_{2t}) > 0$. Darker bands imply a higher value of ψ in the additional restrictions $\text{corr}(\epsilon_t^z, m_{1t}) - \text{corr}(\epsilon_t^z, m_{2t}) > \psi$ and $\text{corr}(\epsilon_t^r, m_{2t}) - \text{corr}(\epsilon_t^r, m_{1t}) > \psi$.

Figure E4: Monte Carlo simulations (III)



$$\text{Panel a)} \quad \nu_1 = 0.10, \nu_2 = 0.05, T = 300: \tilde{\Phi} = \begin{pmatrix} 0.0539 & 0.0006 \\ 0.0040 & 0.0360 \end{pmatrix}.$$



$$\text{Panel b)} \quad \nu_1 = 0.10, \nu_2 = 0.10, T = 300: \tilde{\Phi} = \begin{pmatrix} 0.0270 & 0.0030 \\ 0.0020 & 0.0180 \end{pmatrix}.$$

Note: The figure shows the true impulse responses to a TFP shock and to a monetary shock from the model by [An and Schorfheide \(2007\)](#), and the confidence bands of the estimated impulse responses using the set-identification outlined in the paper. The estimated models satisfy the restrictions $\text{corr}(\epsilon_t^z, m_{1t}) > 0$ and $\text{corr}(\epsilon_t^r, m_{2t}) > 0$. Darker bands imply a higher value of ψ in the additional restrictions $\text{corr}(\epsilon_t^z, m_{1t}) - \text{corr}(\epsilon_t^z, m_{2t}) > \psi$ and $\text{corr}(\epsilon_t^r, m_{2t}) - \text{corr}(\epsilon_t^r, m_{1t}) > \psi$.

F Relative Impulse Response Distance

Define $\hat{\psi}_{i,j}$ as a column vector containing the estimated impulse response of variable i , with $j = chol, unc, news$ indicating whether the impulse response corresponds to the uncertainty shock from the recursive approach, to the uncertainty shock from the proxy SVAR, or to the news shock from the proxy SVAR. Define

$$d_{i,j} = (\hat{\psi}_{i,chol} - \hat{\psi}_{i,j})' \mathbf{W}^{-1} (\hat{\psi}_{i,chol} - \hat{\psi}_{i,j}), \quad (\text{F.31})$$

as the distance between the impulse response from the recursive identification and the impulse response to either the uncertainty or the news shock from the proxy SVAR, with \mathbf{W} a weighting matrix discussed below. Last, define $d_i = \frac{d_{i,unc}}{d_{i,news}}$ as the ratio between such measures. $d_i > 1$ indicates that the impulse response of variable i corresponding to the uncertainty shock from the recursive identification is closer to the impulse response that the proxy SVAR attributes to the news shock rather than to the uncertainty shock.

We compute d_i using as weighting matrix the identity matrix, as well as using a diagonal matrix containing the variance of each element of the vector $\hat{\psi}_{i,chol} - \hat{\psi}_{i,j}$ on the diagonal. The first weighting matrix is taken from [Rotemberg and Woodford \(1997\)](#), while the second weighting matrix is taken from [Christiano et al. \(2005\)](#), adjusted for the application of this paper and computed here using the bootstrapped variances. For both weighting schemes, we compute the impulse response distance d_i for the horizons 4, 12 and 24 months after the shock occurred, including the contemporaneous effect of the shock.¹⁰

¹⁰Our bootstrap procedure generates 1000 models, each of which is associated with an uncertainty shock from the recursive model, an uncertainty shock from the proxy SVAR and a news shock from the proxy SVAR. We compute the measures d_i for each bootstrapped model. For the VXO, we drop the observation corresponding to the impact effect of the shock, since within each bootstrap the shock

Table F2: Relative distance among impulse responses to the shocks identified in the recursive model and in the proxy SVAR

| | horizon 1:4 | | horizon 1:12 | | horizon 1:24 | |
|-----------------------|----------------------------|-----------------------------|---------------------------|----------------------------|---------------------------|----------------------------|
| | RW | CEE | RW | CEE | RW | CEE |
| S&P 500 | 0.01 <i>0.00/0.16</i> | 0.01 <i>0.00/0.03</i> | 0.01 <i>0.00/0.16</i> | 0.01 <i>0.01/0.06</i> | 0.01 <i>0.00/0.16</i> | 0.02 <i>0.01/0.13</i> |
| VXO | 0.02 <i>0.00/0.18</i> | 0.26 <i>0.01/2.34</i> | 0.03 <i>0.00/0.53</i> | 0.24 <i>0.04/5.23</i> | 0.10 <i>0.01/1.07</i> | 0.83 <i>0.07/10.68</i> |
| Fed funds rate | 3.51 <i>0.68/83.52</i> | 5.17 <i>1.01/65.49</i> | 6.27 <i>0.63/46.13</i> | 9.60 <i>1.61/63.24</i> | 9.09 <i>0.44/46.50</i> | 12.30 <i>1.37/63.14</i> |
| Wage | 3.24 <i>0.77/13.12</i> | 3.55 <i>0.66/10.26</i> | 2.61 <i>0.58/7.79</i> | 2.37 <i>0.49/5.39</i> | 2.58 <i>0.56/7.44</i> | 2.45 <i>0.29/6.61</i> |
| CPI | 0.13 <i>0.02/0.38</i> | 0.16 <i>0.03/0.38</i> | 0.18 <i>0.05/0.40</i> | 0.35 <i>0.09/0.87</i> | 0.22 <i>0.06/0.44</i> | 0.69 <i>0.11/1.73</i> |
| Hours | 10.27 <i>1.96/31.95</i> | 45.62 <i>7.20/113.98</i> | 2.16 <i>0.54/17.58</i> | 10.43 <i>2.76/56.84</i> | 1.64 <i>0.36/13.66</i> | 7.68 <i>1.65/43.41</i> |
| Employment | 15.63 <i>2.22/70.28</i> | 53.84 <i>6.09/163.42</i> | 4.18 <i>0.72/18.31</i> | 13.07 <i>1.77/48.85</i> | 4.10 <i>0.71/14.72</i> | 11.16 <i>1.66/41.16</i> |
| Industrial production | 13.54 <i>2.83/54.68</i> | 12.91 <i>4.60/65.54</i> | 9.33 <i>1.76/14.30</i> | 9.84 <i>1.89/17.90</i> | 8.10 <i>1.68/13.84</i> | 6.30 <i>1.76/22.00</i> |

Notes: The table shows the measure of relative impulse response distance $\frac{d_{i,unc}}{d_{i,new}}$, with $d_{i,j}$ defined in equation (F.31). A value greater than 1 indicates that the impulse response of the uncertainty shock identified recursively resembles more the impulse response of the news shock rather than of the uncertainty shock from the proxy SVAR.

Table F2 shows the results of the analysis by reporting the measure corresponding to the median target model and the 95% confidence band. The table shows that the impulse responses to the uncertainty shock from the recursive approach share several features of the responses to both the uncertainty shock and the news shock from the proxy SVAR. The impulse responses to the uncertainty shock from the recursive approach and to the uncertainty shock from the proxy SVAR behave very similarly for three variables, namely the stock market index, the VXO and CPI, especially at the shorter horizon. The opposite is true for the remaining five variables. For these variables, which include the real variables as well as the monetary policy rate, the impulse response to the recursively identified uncertainty shock is more similar to the in the recursive identification is calibrated to generate the same increase in the VXO as in response to the uncertainty shock in the proxy SVAR.

news shock response.

G Robustness of the Results in the Paper

We assess the robustness of the results of the paper along three main dimensions. First, we consider alternative specifications of the reduced form models, adding variables in levels or HP-filtered as in Bloom (2009), replacing the VXO with other measures of uncertainty, adding a measure of financial frictions, and changing the number of lags in the autoregression. Second, we consider variations in the identification approach, studying exact-identification rather than set-identification, changing the order of the variables for the recursive identification and changing the threshold value used for the restriction from equation (9b). Last, we use modifications of the baseline proxies by considering alternative computations of both proxies.

The robustness analysis, reported for simplicity only for the impulse responses, shows that the results discussed in Section 5 of the paper are largely robust to the alternative dimensions considered. We find that the results hold when using HP-filtered data as in Bloom (2009) (Figure H12). Adding the Excess Bond Premium by Gilchrist and Zakrajšek (2012) as a measure of financial frictions (Figure H14) only mildly attenuates the impact response of the real economy to the uncertainty shock. Replacing the VXO with the measure by Jurado *et al.* (2015) (Figure H15) does not change the results, while the use of the measure by Bachmann *et al.* (2013) made the results more pronounced (Figure H16).

When changing the order of the variables and allowing for the uncertainty shock to affect all variables under the recursive identification (Figure H17), we find that the recursive approach still falls short of detecting an impact response of the variables capturing real economic activity, and still delivers the hump-shaped responses displayed

also by the news shock. When identifying the model using the instruments in isolation under the additional assumption that each proxy is orthogonal to all structural shocks except the shock that it aims to proxy (equivalently, setting $\phi_{12} = \phi_{21} = 0$ in equation (8)), we find that the results are somewhat more pronounced, and qualitatively very similar ([Figure H18](#)).

The results are also robust to alternative specifications of the proxies. In particular, the results are not affected by dropping the events that were associated with decreases in the price of gold ([Figure H20](#)) and, hence, dropping events partly associated with a counterintuitive variation of the price of gold given the nature of the event (see [Table H3](#)). The results are also not affected by randomly dropping 20% of the baseline events multiple times ([Figure H21](#)), nor by aggregating the daily proxy as in [Gertler and Karadi \(2014\)](#) ([Figure H22](#)). Confirming the intuition that identification can be improved using data on safe haven assets, we find that the results hold also when using the price of silver rather than gold in constructing the proxy for the uncertainty shock ([Figure H23](#)). When using the proxy constructed on Treasury bonds we find that the restrictions were never satisfied, possibly reflecting the very limited strength of these candidate proxies, as documented in [Section B](#) of the appendix.

Identification with proxies based on dummy variables fails to detect the difference between uncertainty and news shocks documented by the proxy SVAR and predict a more hump-shaped response to the uncertainty shock ([Figure H26](#) and [Figure H27](#)). This might be due to the more limited ability of a simple dummy to control for first-moment effects associated with the events, relative to the price of a safe haven asset. Turning to the instruments used by [Stock and Watson \(2012\)](#), the result that the uncertainty shock affects the real variables already on impact also broadly hold when using as proxy for the uncertainty shock the component of the policy uncertainty index

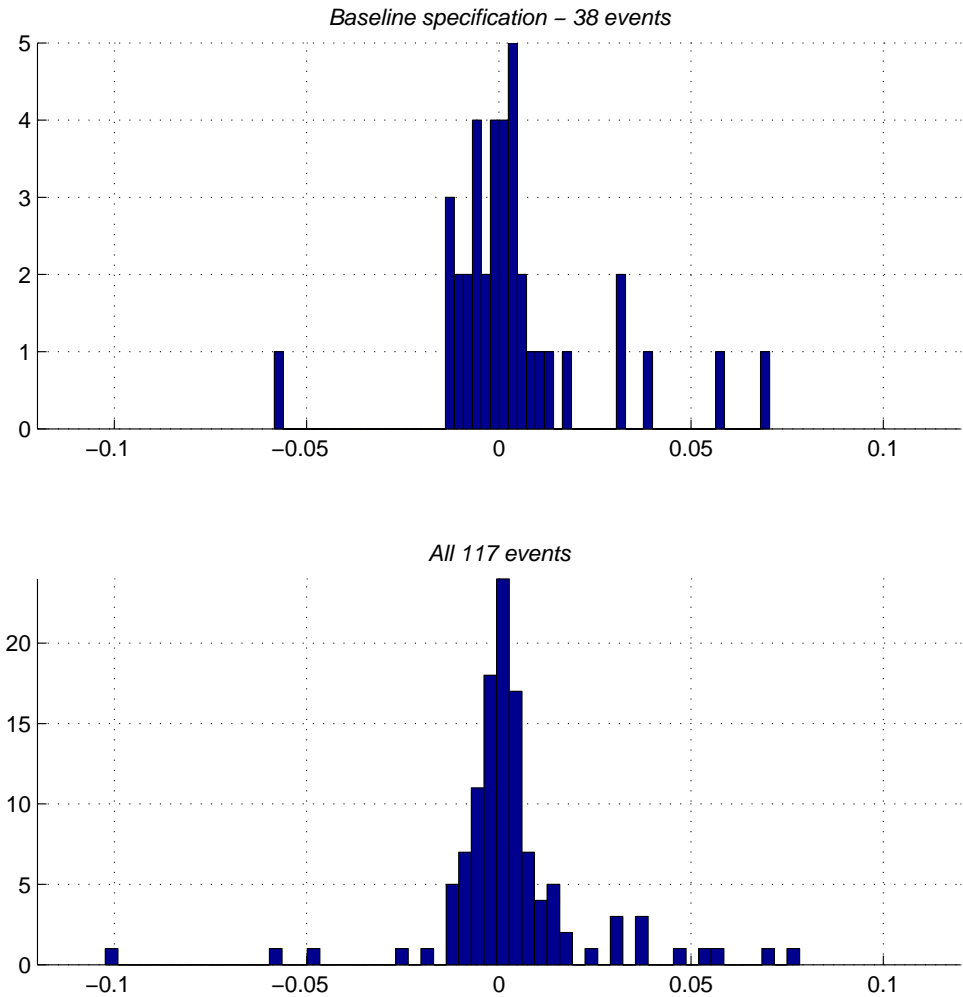
by Baker *et al.* (2016) (Figure H29). On the contrary, using as proxy for the uncertainty shock the residual on the AR(2) on the VIX delivered dynamics of the uncertainty shock that resembled the ones associated with the news shock (Figure H28). The results also hold when the proxy for the news shock is computed as the principal component of only the shocks by Barsky and Sims (2011) and by Kurmann and Otrok (2013) or only the shocks by Beaudry and Portier (2014) (Figure H30).

In Section F we used a measure of relative impulse response distance to compare the difference between the impulse responses from the recursively identified shock and from the two shocks identified in the proxy SVAR. Our baseline result also holds across all the alternative reduced form specifications considered. Table H7 shows that the measure of relative impulse response distance was hardly ever below unity for the variables capturing monetary policy and the real economy. This confirms the results from Table F2.

We conclude the discussion by noticing that the correlation among the estimated uncertainty shocks when using alternative proxies for the uncertainty shock are overall very high (Table H6). In particular, the correlation between the uncertainty shock estimated using the baseline proxy and using alternative proxies like the dummy variables or the instruments by Stock and Watson (2012) is on the order of magnitude of 0.80. This correlation remains high and around 0.65 when using the price of silver, suggesting that the estimated uncertainty shock is overall robust to alternative specifications.

H Additional Figures and Tables

Figure H5: Distribution of the proxy for the uncertainty shock



Note: The histogram is computed on the individual events, not on their monthly aggregation.

Table H3: Events used in the baseline specification, out of the 117 events collected

| # | Date | Δp_{gold} | Event |
|----|-------------|-------------------|---|
| 1 | 25 Apr 1980 | +7.04% | Failure of Operation Eagle Claw in the Iranian crisis announced |
| 2 | 11 Sep 2001 | +5.75% | 9/11 attack |
| 3 | 15 Sep 2008 | +3.87% | AIG asks for lending + Lehman Brothers |
| 4 | 02 Aug 1990 | +3.22% | Iraq invades Kuwait, Gulf War I |
| 5 | 19 Oct 1987 | +3.06% | Black Monday |
| 6 | 03 Jun 1989 | +1.72% | Tienanmen Square |
| 7 | 04 Nov 1979 | +1.39% | Iran: hostages in US embassy |
| 8 | 07 Jul 2005 | +1.03% | London bombing |
| 9 | 19 Aug 1991 | +0.84% | Attempted coup in Moscow |
| 10 | 29 Apr 1986 | +0.67% | News of Chernobyl disaster reaches the West |
| 11 | 23 Sep 1998 | +0.59% | LTCM default |
| 12 | 12 Sep 2012 | +0.35% | German Court approves ESM |
| 13 | 21 Jul 2002 | +0.34% | Worldcom bankruptcy |
| 14 | 14 Sep 2007 | +0.32% | Northern Rock receives liquidity support by the Bank of England |
| 15 | 11 Mar 1985 | +0.26% | Start of Perestroika, Gorbachev's speech in Leningrad |
| 16 | 10 Oct 1980 | +0.26% | Earthquake destroys Algeri |
| 17 | 21 Dec 1988 | +0.23% | Lockerbie bombing, Libyan terrorists crash the Pan Am Flight |
| 18 | 13 Nov 1985 | +0.15% | Volcanic Eruption in Columbia, 30,000 dead |
| 19 | 19 Sep 1985 | +0.13% | Earthquake in Mexico, 15,000 dead |
| 20 | 11 Mar 2011 | +0.12% | Fukushima evacuation order |
| 21 | 10 Jun 2014 | +0.00% | IS seizes Mosul |
| 22 | 02 Dec 2001 | -0.09% | Enron bankruptcy |
| 23 | 01 Apr 1982 | -0.12% | Argentina invades Falkland Islands |
| 24 | 09 Nov 1989 | -0.17% | Fall of Berlin Wall |
| 25 | 07 Gen 2015 | -0.27% | Charlie Hebdo attack |
| 26 | 05 Jul 2015 | -0.32% | Greek referendum supports Tsipras |
| 27 | 07 Aug 1998 | -0.56% | US embassy bombing, Kenia and Tanzania |
| 28 | 07 Dec 1988 | -0.56% | Earthquake in Armenia 25,000 dead |
| 29 | 02 Jul 1997 | -0.67% | Thailand unpegs currency |
| 30 | 21 Nov 2013 | -0.68% | Ukraine rejects EU association agreement |
| 31 | 11 Mar 2004 | -0.71% | Madrid train bombing |
| 32 | 17 Oct 1989 | -0.75% | Loma Prieta earthquake (California) |
| 33 | 24 Mar 1989 | -0.92% | Exxon-Valdes hits ground and leaks 40,000 tons of oil |
| 34 | 09 Nov 2011 | -1.01% | Berlusconi announces resignation |
| 35 | 10 May 2010 | -1.16% | EFSF adopted |
| 36 | 15 Apr 2013 | -1.22% | Boston marathon bombing |
| 37 | 01 Feb 1979 | -1.31% | Khomeini returns to Tehran |
| 38 | 26 Gen 1980 | -5.84% | Israel and Egypt establish diplomatic relations |

Notes: The table lists the events used in the baseline specification of the model. The results are robust to alternative combinations of events used, as discussed in [Section G](#) of the paper.

Table H4: Average absolute correlation among groups of estimated shocks

| | This paper | | Stock and Watson (2012) | | | | | |
|---------------------|--------------------|----------------|-------------------------|---------------|--------------|----------------|----------------|---------------|
| | <i>Uncertainty</i> | <i>News</i> | <i>Oil</i> | <i>Monet.</i> | <i>Prod.</i> | <i>Uncert.</i> | <i>Financ.</i> | <i>Fiscal</i> |
| <i>Uncertainty</i> | 1.00 | | | | | | | |
| <i>News</i> | 0.04 (.01/.12) | 1.00 | | | | | | |
| <i>Oil</i> | 0.18 (.11/.24) | 0.08 (.06/.16) | 0.45 | | | | | |
| <i>Monetary</i> | 0.24 (.17/.32) | 0.10 (.06/.19) | 0.28 | 0.37 | | | | |
| <i>Productivity</i> | 0.12 (.06/.17) | 0.09 (.07/.17) | 0.51 | 0.31 | 0.67 | | | |
| <i>Uncertainty</i> | 0.42 (.32/.55) | 0.44 (.24/.47) | 0.36 | 0.35 | 0.22 | 0.78 | | |
| <i>Financial</i> | 0.37 (.28/.51) | 0.40 (.28/.46) | 0.24 | 0.34 | 0.16 | 0.73 | 0.66 | |
| <i>Fiscal</i> | 0.27 (.17/.32) | 0.13 (.07/.22) | 0.20 | 0.51 | 0.24 | 0.12 | 0.21 | 0.59 |

Notes: The table is a summary of [Table H5](#). [Table H5](#) shows the correlations among each of the shocks estimated in [Stock and Watson \(2012\)](#) and the shocks estimated in our paper. The table here, instead, summarises the individual correlations in [Table H5](#) by averaging the absolute values of correlations among the different groups of shocks. Since the factor model by [Stock and Watson \(2012\)](#) estimates shocks at a quarterly frequency, we first aggregate to this frequency the uncertainty and news shocks estimated in our paper.

Table H5: Correlations among the shocks identified in this paper and the shocks identified in Stock and Watson (2012)

| | ε^{unc} | ε^{news} | ε^{news} | O_H | O_K | O_{RV} | M_{RR} | M_{SW} | M_{GSS} | P_F | P_G | P_{SW} | U_{VIX} | U_{BBDD} | L_{GZ} | L_{TED} | L_{BCDZ} | F_R | F_{FP} | F_{RR} | |
|----------------------|---------------------|----------------------|----------------------|-------|-------|----------|----------|----------|-----------|-------|-------|----------|-----------|------------|----------|-----------|------------|-------|----------|----------|------|
| ε^{unc} | | 1.00 | | | | | | | | | | | | | | | | | | | |
| ε^{news} | 0.05 (.01/.12) | | 1.00 | | | | | | | | | | | | | | | | | | |
| O_H | -0.09 (-.17/.02) | 0.20 | (.17/.29) | | | | | | | | | | | | | | | | | | |
| O_K | -0.22 (-.26/-1.18) | -0.01 | (-.02/.10) | 0.42 | 1.00 | | | | | | | | | | | | | | | | |
| O_{RV} | -0.24 (.31/-1.18) | -0.03 | (-.07/.11) | 0.77 | 0.16 | 1.00 | | | | | | | | | | | | | | | |
| M_{RR} | -0.39 (-.44/-3.1) | -0.00 | (-.07/.16) | 0.37 | 0.65 | 0.25 | 1.00 | | | | | | | | | | | | | | |
| M_{SW} | 0.11 (.06/.17) | 0.06 | (-.02/.08) | 0.09 | 0.11 | -0.36 | 0.09 | 1.00 | | | | | | | | | | | | | |
| M_{SZ} | -0.36 (-.41/-2.7) | 0.02 | (-.04/.18) | 0.33 | 0.35 | 0.27 | 0.93 | 0.16 | 1.00 | | | | | | | | | | | | |
| M_{GSS} | 0.14 (.05/.27) | 0.33 | (.26/.36) | 0.44 | -0.12 | -0.03 | 0.24 | 0.43 | 0.39 | 1.00 | | | | | | | | | | | |
| P_F | -0.09 (-.13/-1.03) | -0.06 | (-.11/-0.9) | -0.64 | 0.30 | -0.53 | 0.20 | -0.09 | 0.06 | -0.57 | 1.00 | | | | | | | | | | |
| P_G | 0.21 (.15/.26) | -0.02 | (-.13/.01) | -0.40 | 0.34 | -0.65 | -0.30 | 0.35 | -0.53 | -0.37 | 0.52 | 1.00 | | | | | | | | | |
| P_{SW} | 0.06 (-.05/.14) | -0.20 | (-.28/-1.18) | -0.91 | -0.03 | -0.78 | -0.24 | -0.07 | -0.36 | -0.59 | 0.82 | 0.68 | 1.00 | | | | | | | | |
| U_{VIX} | 0.44 (.35/.58) | 0.41 | (.21/.47) | -0.37 | -0.37 | -0.69 | -0.39 | 0.30 | -0.29 | 0.37 | 0.19 | 0.34 | 0.27 | 1.00 | | | | | | | |
| U_{BBDD} | 0.39 (.29/.53) | 0.44 | (.26/.49) | 0.10 | 0.11 | -0.50 | -0.17 | 0.45 | -0.22 | 0.57 | -0.06 | 0.45 | -0.01 | 0.78 | 1.00 | | | | | | |
| L_{GZ} | 0.42 (.32/.55) | 0.41 | (.23/.46) | -0.20 | -0.42 | -0.47 | -0.41 | 0.44 | -0.24 | 0.34 | 0.07 | 0.24 | 0.08 | 0.92 | 0.66 | 1.00 | | | | | |
| L_{TED} | 0.28 (.19/.42) | 0.37 | (.23/.41) | -0.09 | 0.01 | -0.57 | 0.03 | 0.73 | 0.10 | 0.48 | 0.21 | 0.37 | 0.09 | 0.80 | 0.76 | 0.84 | 1.00 | | | | |
| L_{BCDZ} | -0.41 (-.55/-3.3) | -0.44 | (-.50/-2.27) | 0.04 | 0.22 | 0.14 | 0.56 | 0.13 | 0.55 | 0.04 | -0.09 | -0.28 | -0.06 | -0.69 | -0.54 | -0.73 | -0.40 | 1.00 | | | |
| F_R | 0.29 (.23/.39) | 0.08 | (-.04/.14) | -0.17 | -0.64 | 0.13 | -0.84 | -0.32 | -0.72 | -0.34 | -0.17 | -0.01 | 0.26 | -0.08 | 0.40 | -0.13 | -0.69 | 1.00 | | | |
| F_{FP} | 0.28 (.17/.33) | -0.11 | (-.23/.-0.05) | 0.04 | -0.21 | -0.09 | -0.72 | 0.20 | -0.78 | -0.03 | -0.49 | 0.40 | -0.02 | 0.03 | 0.25 | 0.03 | -0.12 | -0.14 | 0.38 | 1.00 | |
| F_{RR} | -0.23 (.31/-1.0) | 0.20 | (.15/.31) | 0.20 | 0.15 | 0.19 | 0.77 | -0.10 | 0.88 | 0.37 | 0.18 | -0.59 | -0.28 | 0.01 | -0.10 | 0.02 | 0.19 | 0.17 | -0.45 | -0.93 | 1.00 |

Notes: The table reports the correlation among the shocks estimated in this paper (ε_t^{unc} and ε_t^{news}) and the shocks estimated by Stock and Watson (2012).

Given the use of set-identification, for ε_t^{unc} and ε_t^{news} we report the correlation corresponding to the median target model and the pointwise 90% confidence band. Stock and Watson (2012) estimate the shocks using the instruments listed in Table 1 of the paper, except for the shock labelled here as P_G , which uses the internal restrictions by Galí (1999). Since the shocks estimated by Stock and Watson (2012) have a quarterly frequency we aggregate ε_t^{unc} and ε_t^{news} to such frequency. Note that this implies a small non zero correlation between ε_t^{unc} and ε_t^{news} . On a monthly frequency ε_t^{unc} and ε_t^{news} are uncorrelated by construction. The shocks estimated by Stock and Watson (2012) are:

Oil shocks: Hamilton (2003) (O_H), Kilian (2008) (O_K), Ramey and Vine (2010) (O_{RV});

Monetary policy shocks: Romer and Romer (2004) (M_{RR}), Smets and Wouters (2007) (M_{SW}), Sims and Zha (2006) (M_{SZ}), Gurkaynak *et al.* (2005) (M_{GSS});

Productivity shocks: Basu *et al.* (2006) (P_F), Galí (1999) (P_G); Smets and Wouters (2007) (P_{SW});

Uncertainty shocks: AR(2) residuals of VIX (U_{VIX}), Baker *et al.* (2016) (U_{BBDD});

Financial shocks: Gilchrist and Zakrajšek (2012) (L_{GZ}), TED spread (L_{TED}), Bassett *et al.* (2014) (L_{BCDZ});

Fiscal shocks: Ramey (2011) (F_R), Fisher and Peters (2010) (F_{FP}), Romer and Romer (2010) (F_{RR}).

Table H6: Correlation among uncertainty shocks estimated using alternative proxies for the uncertainty shock

| | Gold | Silver | Platinum | VXO | $D_{0/1}$ events | $D_{0/1}$ VXO | U_{VIX} by SW | U_{BBD} by SW |
|---------------------|-------------------|-----------------|-------------------|-----------------|---------------------|------------------|--------------------|--------------------|
| Gold | 1.00 | | | | | | | |
| Silver | 0.65 .40/.78 | 1.00 | | | | | | |
| Platinum | -0.13 -.20/.26 | 0.33 .05/.61 | 1.00 | | | | | |
| VXO | 0.85 .59/.92 | 0.35 .11/.65 | -0.11 -.25/.29 | 1.00 | | | | |
| $D_{0/1}$ events | 0.79 .61/.88 | 0.55 .27/.71 | 0.27 .16/.56 | 0.88 .63/.92 | 1.00 | | | |
| $D_{0/1}$ VXO | 0.79 .67/.89 | 0.60 .36/.74 | 0.33 .21/.58 | 0.82 .56/.91 | 0.89 .69/.95 | 1.00 | | |
| U_{VIX} by SW | 0.72 .51/.84 | 0.67 .35/.81 | 0.46 .32/.70 | 0.70 .45/.80 | 0.89 .62/.92 | 0.89 .62/.95 | 1.00 | |
| U_{BBD} by SW | 0.70 .45/.79 | 0.50 .25/.74 | -0.02 -.13/.41 | 0.78 .52/.89 | 0.80 .56/.88 | 0.56 .35/.75 | 0.56 .30/.70 | 1.00 |

Notes: The table reports the correlations among the uncertainty shocks estimated using alternative proxies for the uncertainty shock. The frequency of the estimated shocks is monthly. The correlations among the shocks corresponding to the eight proxies considered are reported among the median target models, together with the 90% band computed by first calculating the correlation structure within each bootstrapped model, and then replicating the analysis for all bootstrapped models.

- 1) Gold: proxy constructed on the intradaily price of gold around the baseline events (baseline specification);
 - 2) Silver: proxy constructed on the daily price of silver around the baseline events;
 - 3) Platinum: proxy constructed on the daily price of platinum around the baseline events;
 - 4) VXO: proxy constructed on the VXO around the baseline events;
 - 5) $D_{0/1}$ events: proxy equals dummy taking value of 1 on baseline events;
 - 6) $D_{0/1}$ VXO: proxy equals dummy taking value of 1 when VXO reaches the peaks used by [Bloom \(2009\)](#);
 - 7) U_{VXO} by SW: proxy equals first instrument for the uncertainty shock used by [Stock and Watson \(2012\)](#), which is the residual on an AR(2) process on the VIX;
 - 8) U_{BBD} by SW: proxy equals second instrument for the uncertainty shock used by [Stock and Watson \(2012\)](#), which is the common component of policy uncertainty index;
- The proxies listed in [Table B1](#) and not reported here are proxies for which it was not possible to find representations that satisfied the identifying restrictions.

Table H7: Relative distance among impulse responses using alternative reduced form specifications

| | horizon 1:4 | | horizon 1:12 | | horizon 1:24 | |
|-----------------------|---|---|--|---|---|---|
| | RW | CEE | RW | CEE | RW | CEE |
| S&P 500 | 0.01 [0.67, 0.06, 0.03, 0.06, 0.03, 0.16, 0.40, 0.04] | 0.01 [0.68, 0.01, 0.01, 0.01, 0.01, 0.04, 0.13, 0.01] | 0.01 [5.30, 0.05, 0.04, 0.06, 0.04, 0.17, 0.39, 0.04] | 0.01 [2.43, 0.02, 0.03, 0.03, 0.03, 0.15, 0.21, 0.04] | 0.01 [6.52, 0.05, 0.04, 0.06, 0.04, 0.17, 0.39, 0.04] | 0.02 [2.99, 0.02, 0.04, 0.04, 0.07, 0.23, 0.28, 0.10] |
| Uncertainty | 0.02 [3.73, 0.14, 0.01, 0.00, 0.02, 0.01, 0.01, 0.01] | 0.26 [8.04, 0.51, 0.09, 0.06, 0.13, 0.18, 0.07, 0.10] | 0.03 [5.65, 0.22, 0.02, 0.03, 0.09, 0.06, 0.03, 0.01] | 0.24 [6.50, 1.31, 0.26, 0.20, 0.80, 0.30, 0.11, 0.10] | 0.10 [5.57, 0.22, 0.09, 0.07, 0.11, 0.06, 0.35, 0.01] | 0.83 [5.50, 0.81, 1.70, 0.76, 0.75, 0.30, 1.17, 0.13] |
| Fed funds rate | 3.51 [1.47, 3.03, 3.40, 1.56, 1.91, 348.75, 1.21, 1.85] | 5.17 [2.20, 4.79, 5.39, 2.80, 3.45, 127.80, 2.19, 2.26] | 6.27 [3.11, 4.12, 8.84, 0.37, 7.66, 11.11, 3.58, 1.74] | 9.60 [3.09, 6.52, 8.82, 1.46, 9.50, 40.71, 5.70, 3.13] | 9.09 [4.17, 1.90, 12.36, 0.21, 21.45, 5.90, 2.00, 1.60] | 12.30 [3.48, 2.93, 10.14, 0.97, 17.53, 22.01, 4.02, 3.22] |
| Wage | 3.24 [0.89, 1.13, 1.00, 0.75, 0.73, 1.09, 0.15, 9.86] | 3.55 [0.97, 1.09, 0.79, 0.43, 0.64, 0.98, 0.19, 5.31] | 2.61 [0.49, 0.80, 0.96, 0.49, 0.44, 0.94, 0.12, 4.53] | 2.37 [0.54, 0.91, 0.79, 0.40, 0.43, 1.06, 0.15, 1.82] | 2.58 [0.46, 0.73, 0.97, 0.48, 0.41, 0.96, 0.11, 4.43] | 2.45 [0.43, 0.86, 0.92, 0.40, 0.42, 1.68, 0.11, 1.64] |
| CPI | 0.13 [0.62, 0.63, 0.05, 0.12, 0.39, 0.30, 0.15, 0.07] | 0.16 [1.17, 0.74, 0.02, 0.11, 0.45, 0.61, 0.19, 0.07] | 0.18 [0.14, 1.17, 0.07, 0.13, 0.39, 0.36, 0.12, 0.09] | 0.35 [0.34, 0.99, 0.11, 0.14, 0.70, 1.69, 0.15, 0.14] | 0.22 [0.15, 2.54, 0.09, 0.13, 0.41, 0.40, 0.11, 0.09] | 0.69 [0.21, 1.70, 0.23, 0.15, 1.12, 2.01, 0.11, 0.22] |
| Hours | 10.27 [38.97, 12.31, 7.13, 5.93, 2.67, 2.71, 6.52, 5.65] | 45.62 [88.33, 39.78, 24.65, 21.48, 5.40, 5.28, 33.99, 15.23] | 2.16 [29.08, 1.22, 9.84, 4.66, 0.97, 4.97, 3.78, 4.38] | 10.43 [37.99, 2.32, 32.27, 18.20, 2.31, 8.58, 12.14, 13.36] | 1.64 [5.68, 1.17, 7.62, 1.92, 0.48, 4.25, 2.38, 5.21] | 7.68 [4.95, 2.30, 22.46, 6.49, 1.10, 8.14, 6.24, 15.54] |
| Employment | 15.63 [7.51, 13.35, 45.84, 5.44, 5.25, 2.28, 7.77, 5.59] | 53.84 [15.74, 92.89, 167.54, 11.95, 9.70, 4.16, 22.55, 12.82] | 4.18 [4.90, 0.93, 29.65, 1.81, 1.67, 2.13, 2.49, 5.13] | 13.07 [9.77, 5.09, 96.39, 5.00, 3.38, 4.29, 5.57, 12.88] | 4.10 [1.11, 0.39, 30.21, 1.80, 0.96, 2.15, 2.77, 6.02] | 11.16 [2.58, 1.84, 97.98, 4.92, 1.55, 4.86, 8.47, 22.54] |
| Industrial production | 13.54 [7.63, 12.96, 10.57, 6.68, 10.43, 1.03, 4.30, 9.18] | 12.91 [14.16, 56.77, 14.80, 9.59, 10.20, 1.95, 5.69, 11.29] | 9.33 [14.73, 0.74, 9.43, 4.11, 4.09, 1.10, 2.19, 8.42] | 9.84 [16.36, 3.26, 11.86, 6.42, 3.89, 2.33, 3.10, 12.16] | 8.10 [19.40, 0.44, 9.65, 4.04, 3.90, 1.11, 2.29, 8.48] | 6.30 [17.34, 1.75, 15.26, 6.50, 3.37, 2.87, 4.84, 14.43] |

Notes: The table shows the measure of relative impulse response distance $\frac{d_{i,unc}}{d_{i,newsp}}$, with $d_{i,j}$ defined in equation (F.31) of the paper. A value greater than 1 indicates that the impulse response to the uncertainty shock identified recursively resembles more the impulse response to the news shock rather than to the uncertainty shock from the proxy SVAR. The alternative model specifications for the results reported in brackets correspond (in the following order) to Figure H11, Figure H12, Figure H13, Figure H14, Figure H15, Figure H16 and Figure H17.

Figure H6: Data used in the baseline specification of the VAR model

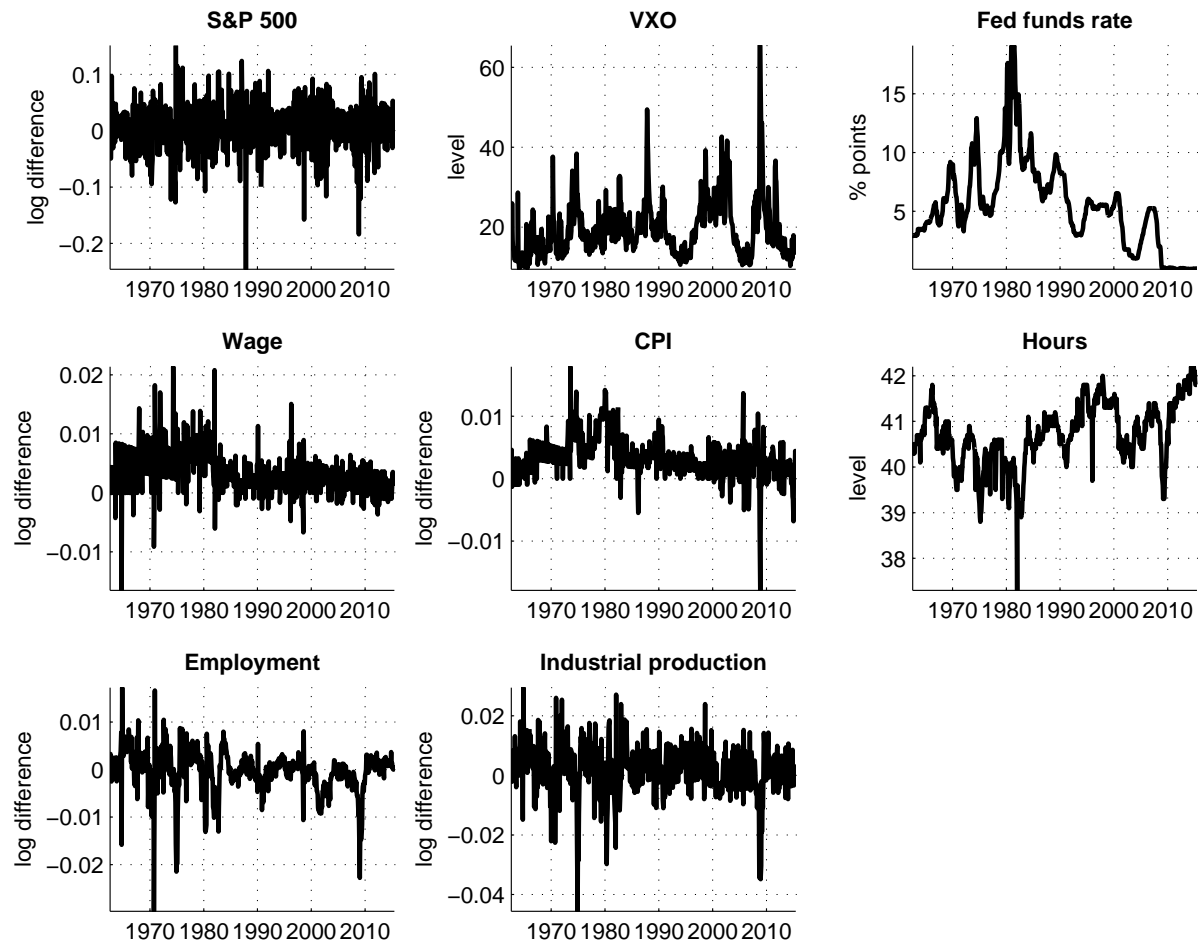
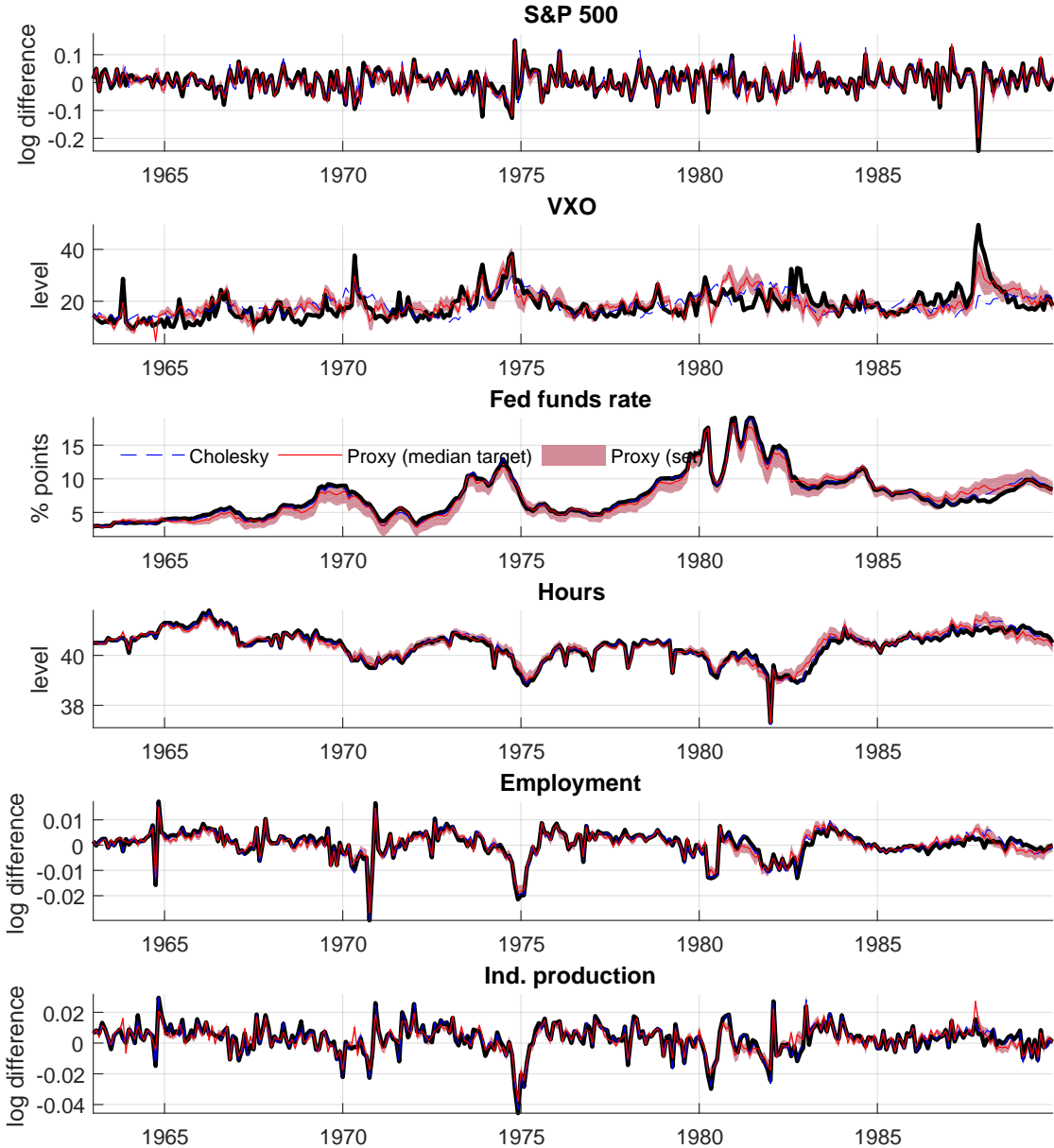
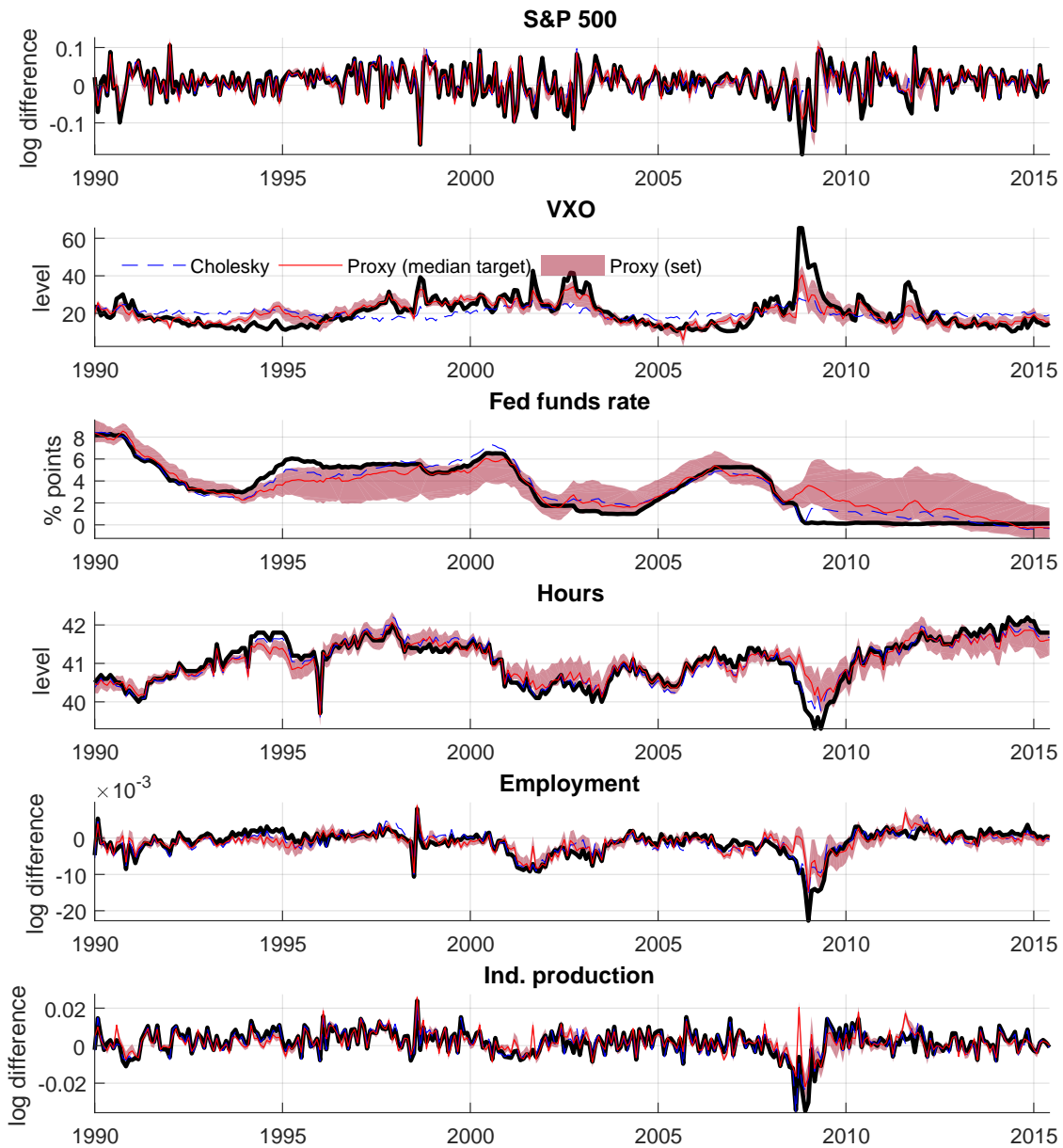


Figure H7: Historical decomposition for uncertainty shocks, subperiod 1963-1989



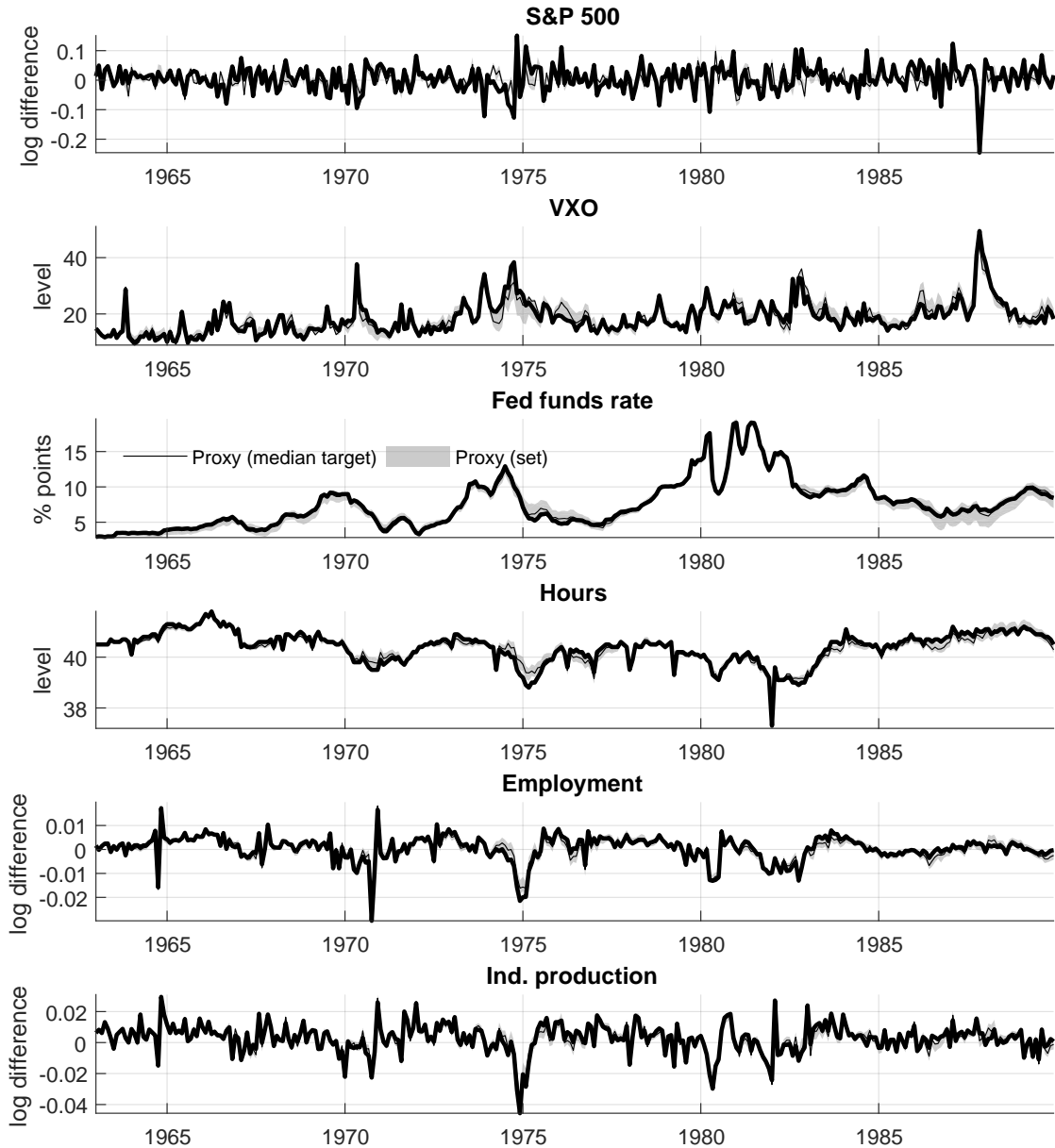
Notes: We report the data as it enters the model (solid black line) and the data after subtracting, at each time t , the cumulative effect of the uncertainty shocks between 1962M8 and time t . To make the figure clearer, we report here the decomposition for the subperiod 1963M1-1989M12. We report decompositions for all variables in the VAR except wages and consumer prices because they are hardly affected by the shock. The decomposition for the period 1990M1-2015M6 is shown in [Figure H8](#).

Figure H8: Historical decomposition for uncertainty shocks, subperiod 1990-2015



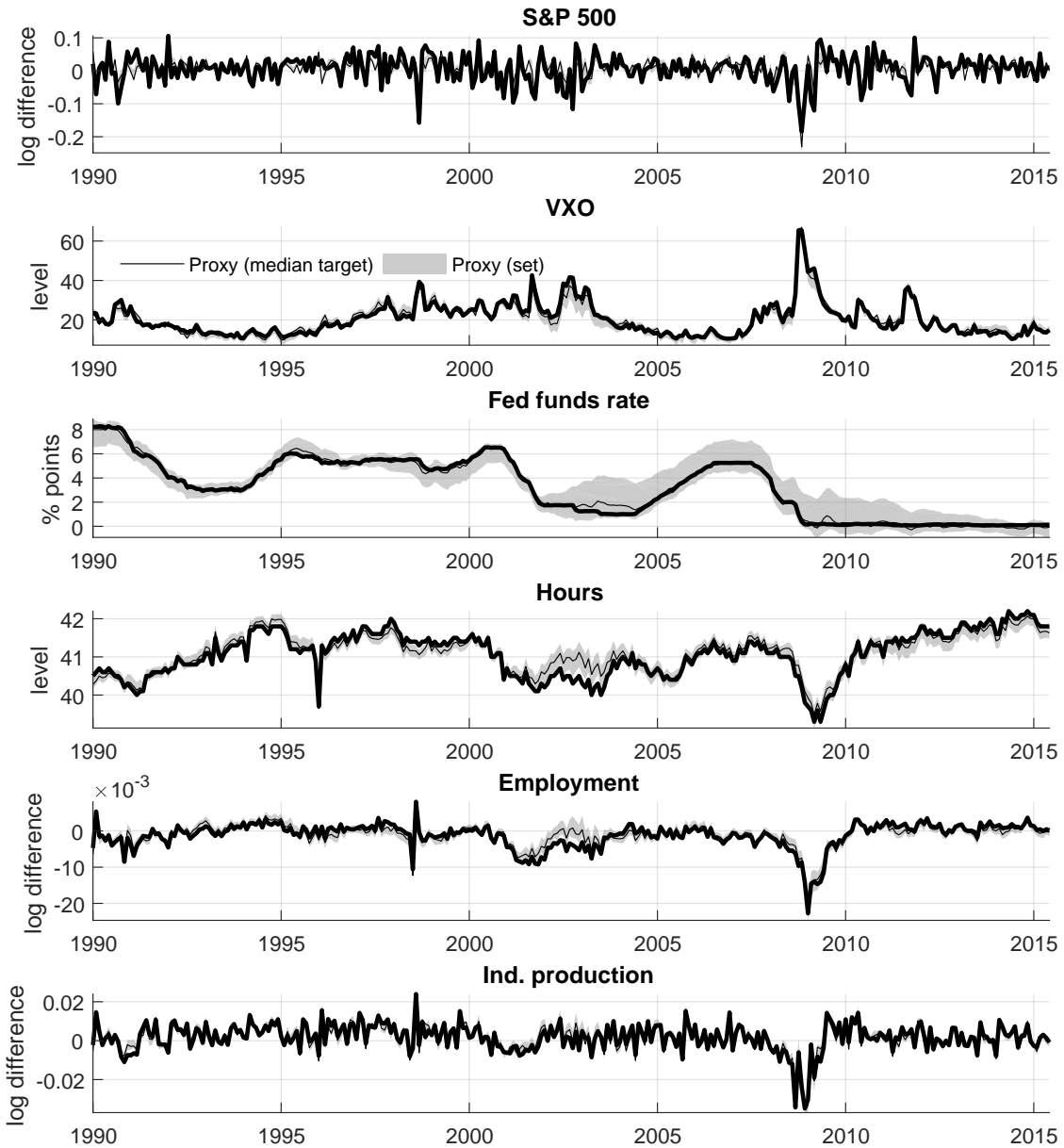
Notes: We report the data as it enters the model (solid black line) and the data after subtracting, at each time t , the cumulative effect of the uncertainty shocks between 1962M8 and time t . To make the figure clearer, we report here the decomposition for the subperiod 1990M1-2015M6. We report decompositions for all variables in the VAR except wages and consumer prices because they are hardly affected by the shock. The decomposition for the period 1963M1-1989M12 is shown in [Figure H7](#).

Figure H9: Historical decomposition for news shocks, subperiod 1963-1989



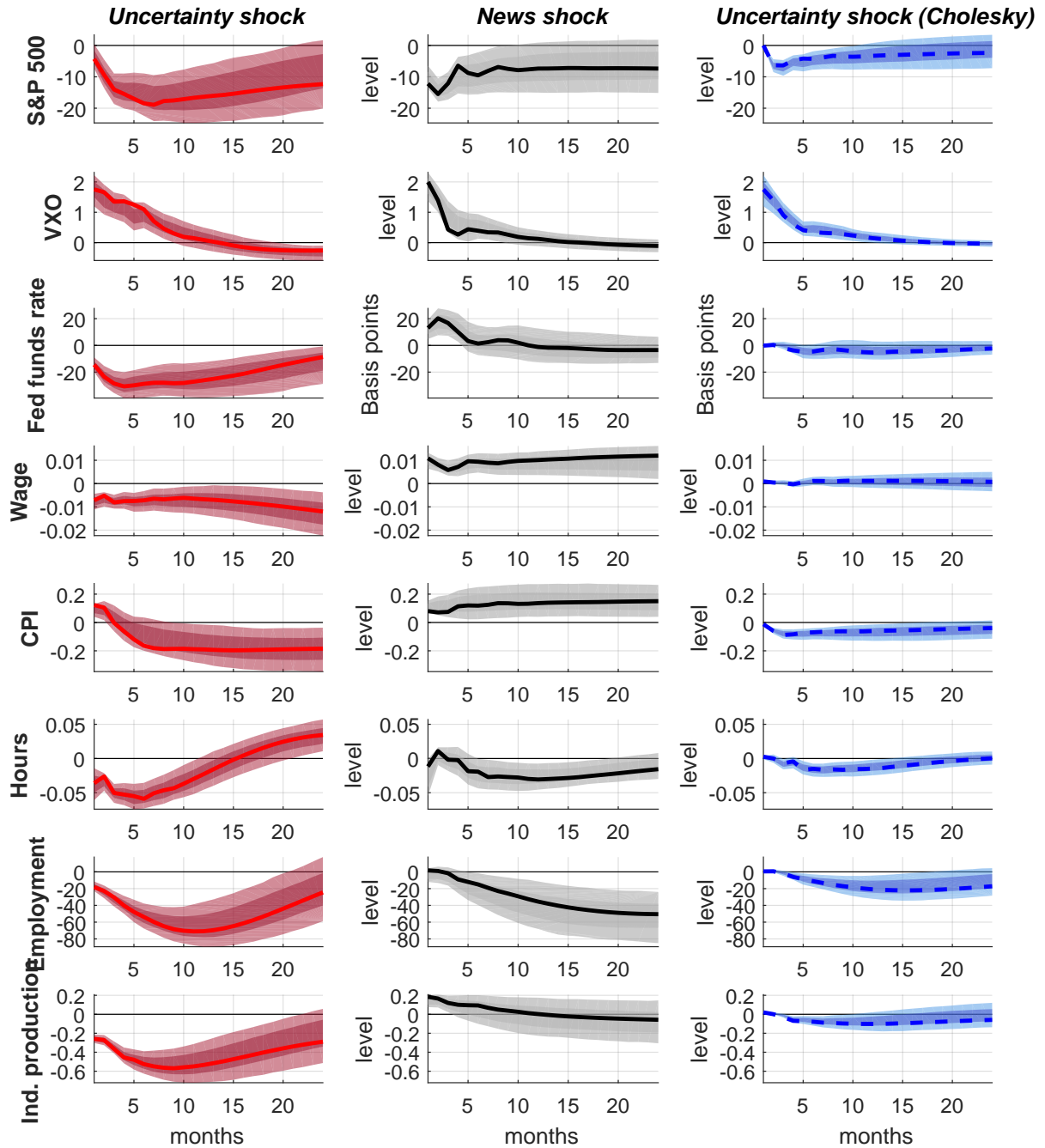
Notes: We report the data as it enters the model (solid black line) and the data after subtracting, at each time t , the cumulative effect of the uncertainty shocks between 1962M8 and time t . To make the figure clearer, we report here the decomposition for the subperiod 1963M1-1989M12. We report decompositions for all variables in the VAR except wages and consumer prices because they are hardly affected by the shock. The decomposition for the period 1990M1-2015M6 is shown in [Figure H10](#).

Figure H10: Historical decomposition for news shocks, subperiod 1990-2015



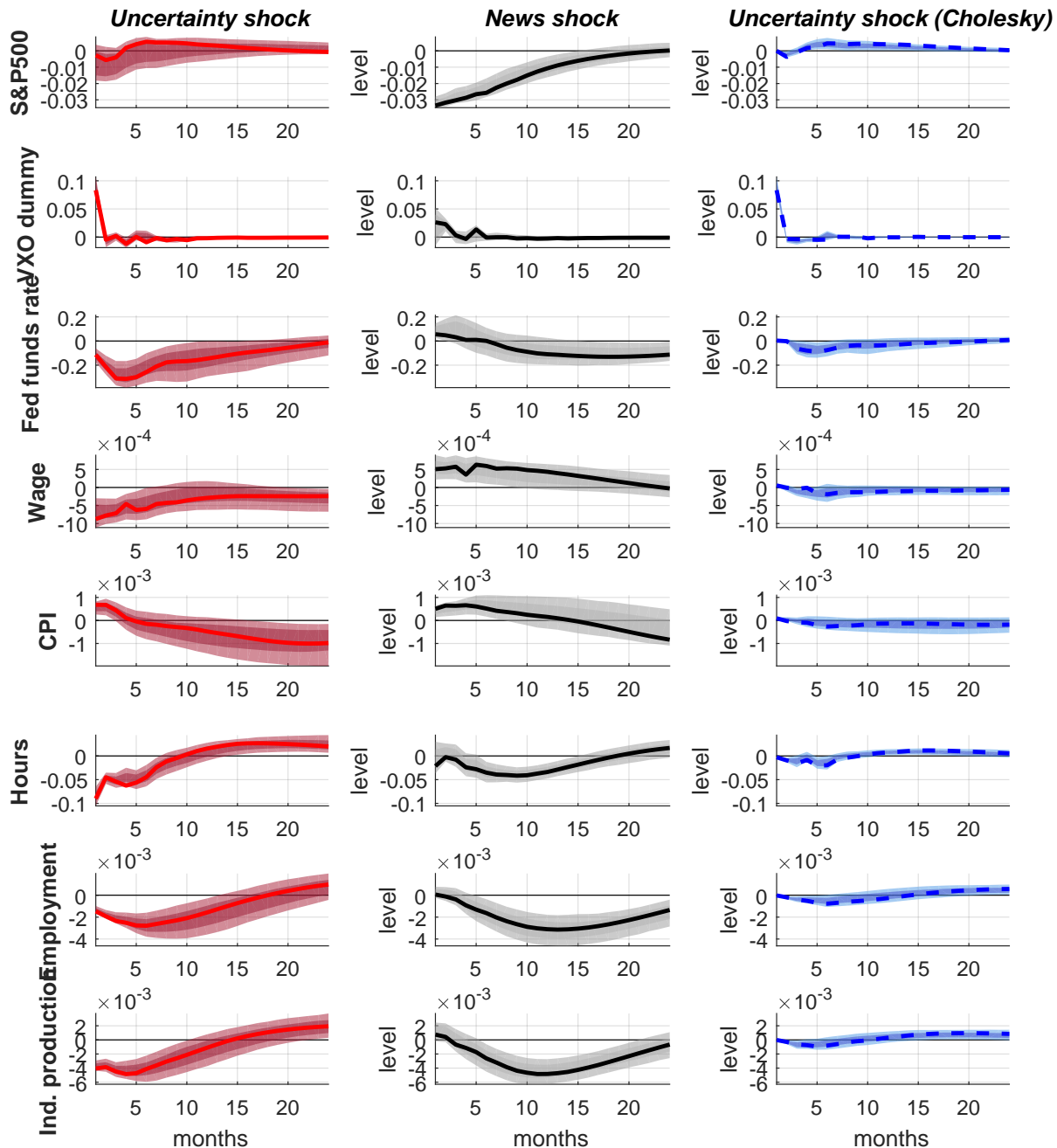
Notes: We report the data as it enters the model (solid black line) and the data after subtracting, at each time t , the cumulative effect of the news shocks between 1962M8 and time t . To make the figure clearer, we report here the decomposition for the subperiod 1990M1-2015M6. We report decompositions for all variables in the VAR except wages and consumer prices because they are hardly affected by the shock. The decomposition for the period 1963M1-1989M12 is shown in Figure H9.

Figure H11: Impulse responses, with all variables entering in levels



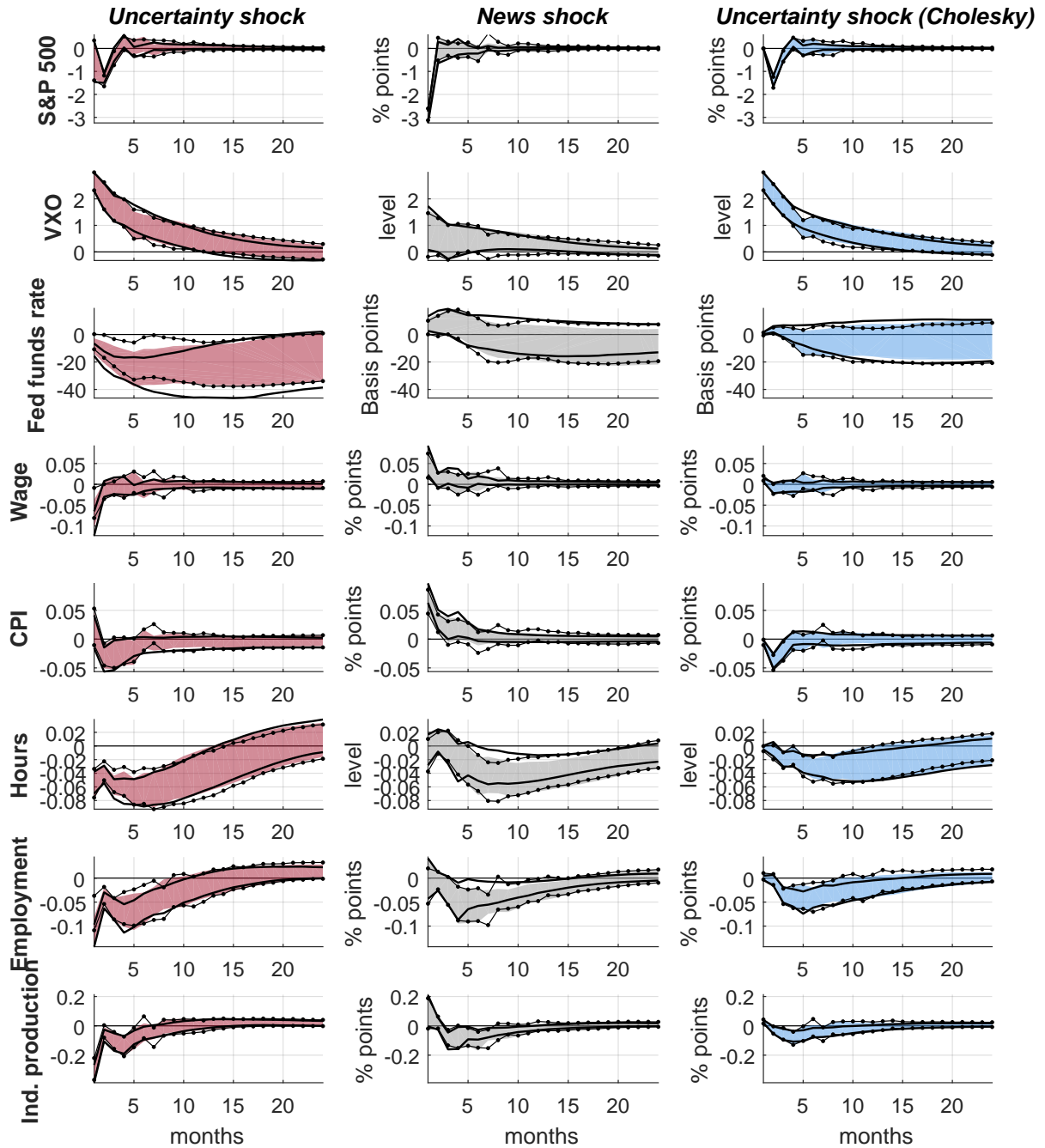
Note: Impulse responses of the median target model, together with the pointwise 95% and 68% bands based on 1000 bootstrap replications.

Figure H12: Impulse responses, with all variables entering the model as in the specification by Bloom (2009)



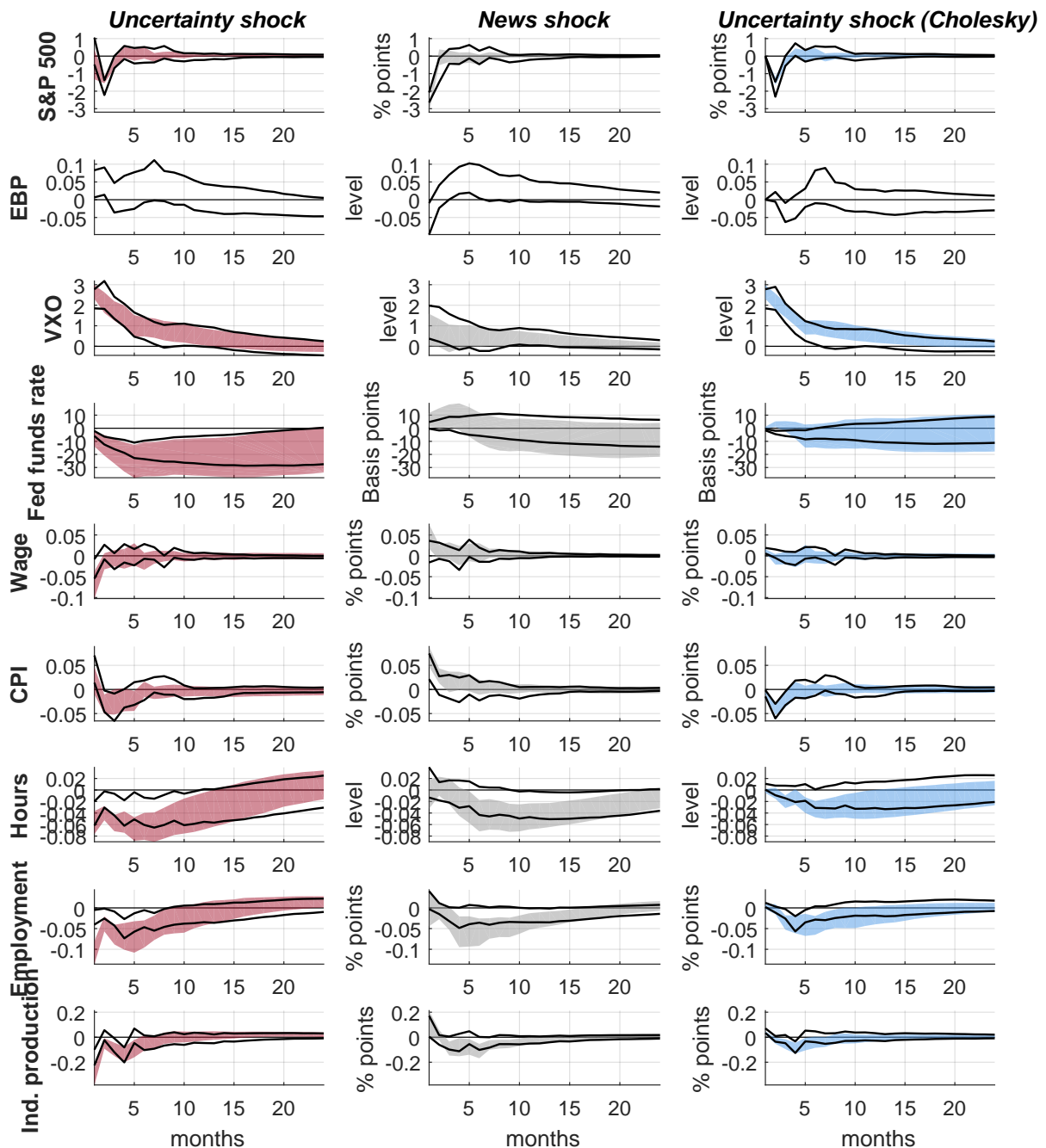
Note: Impulse responses of the median target model, together with the pointwise 95% and 68% bands based on 1000 bootstrap replications.

Figure H13: Impulse responses, using alternative lags for the estimated reduced form



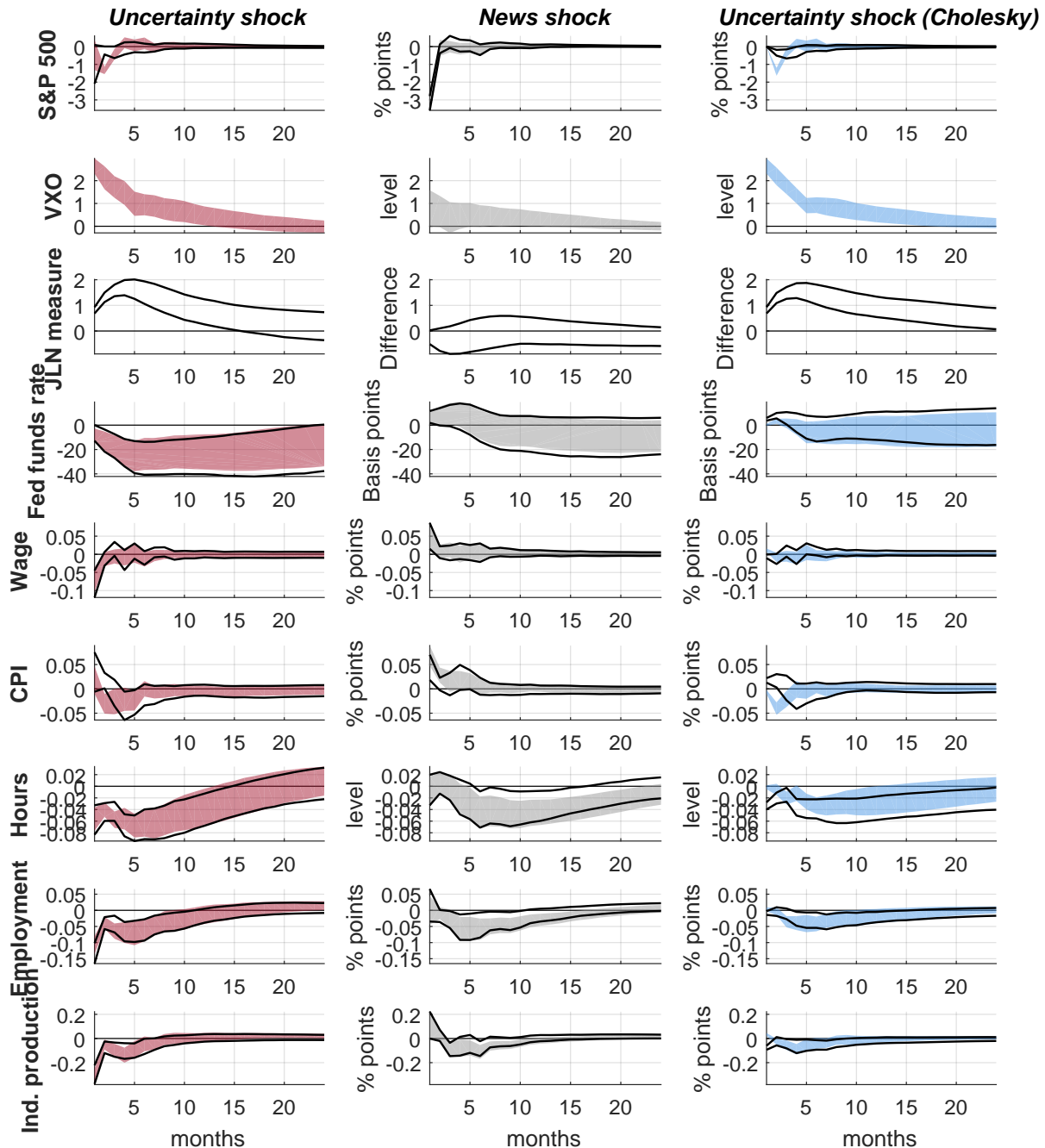
Note: Pointwise 95% bands computed on 1000 bootstrap replications, for a VAR model estimated with 5 lags (baseline specification, shaded area), 3 lags (solid line) and 7 lags (dotted line).

Figure H14: Impulse responses, adding the Excess Bond Premium by Gilchrist and Zakrajšek (2012)



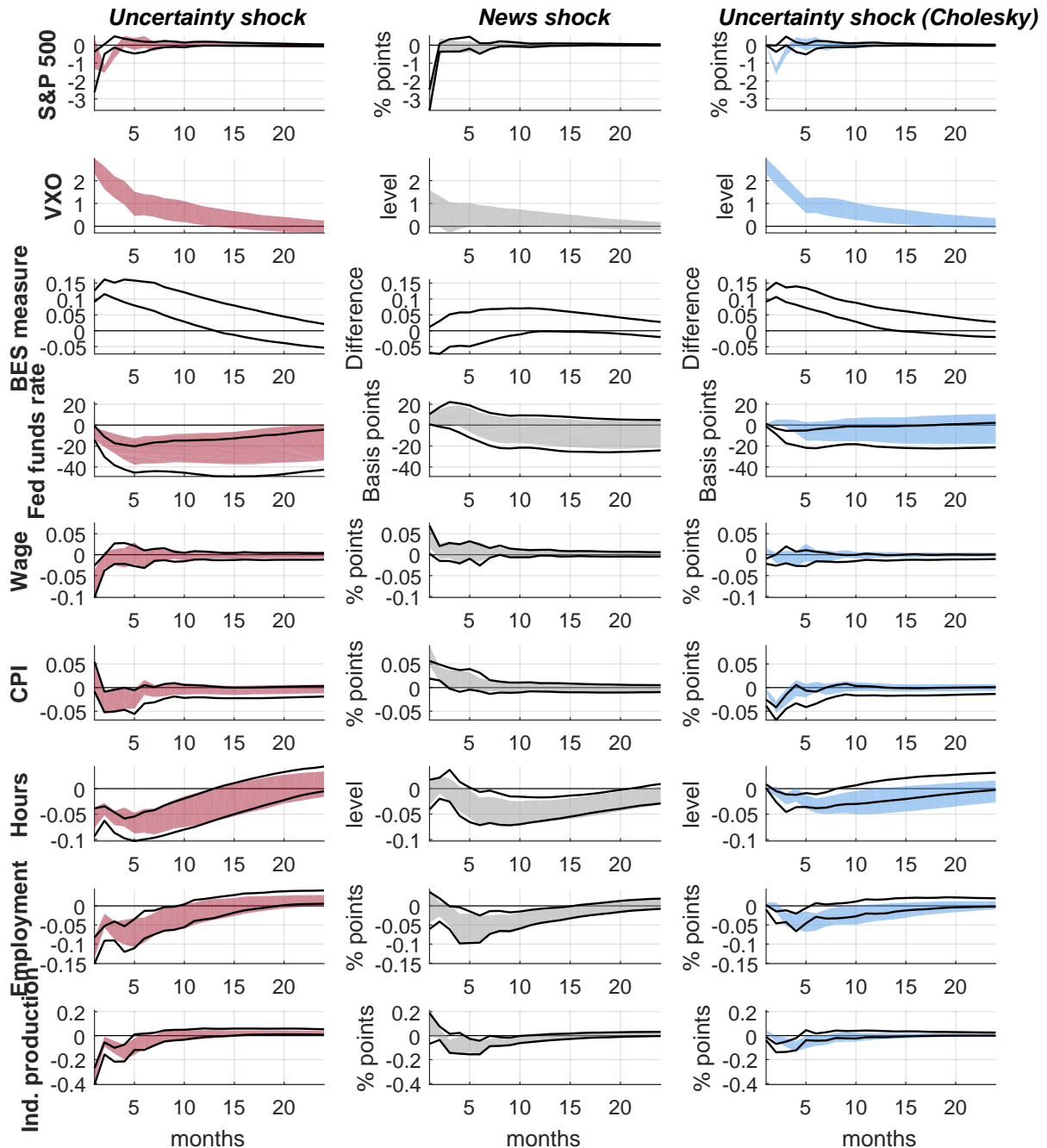
Note: Pointwise 95% bands computed on 1000 bootstrap replications, shown when including the baseline variables (baseline specification, shaded area) or the baseline variables plus the Excess Bond Premium by Gilchrist and Zakrajšek (2012), ordered as the second variable (solid line).

Figure H15: Impulse responses, replacing the VXO with the measure of uncertainty by Jurado *et al.* (2015)



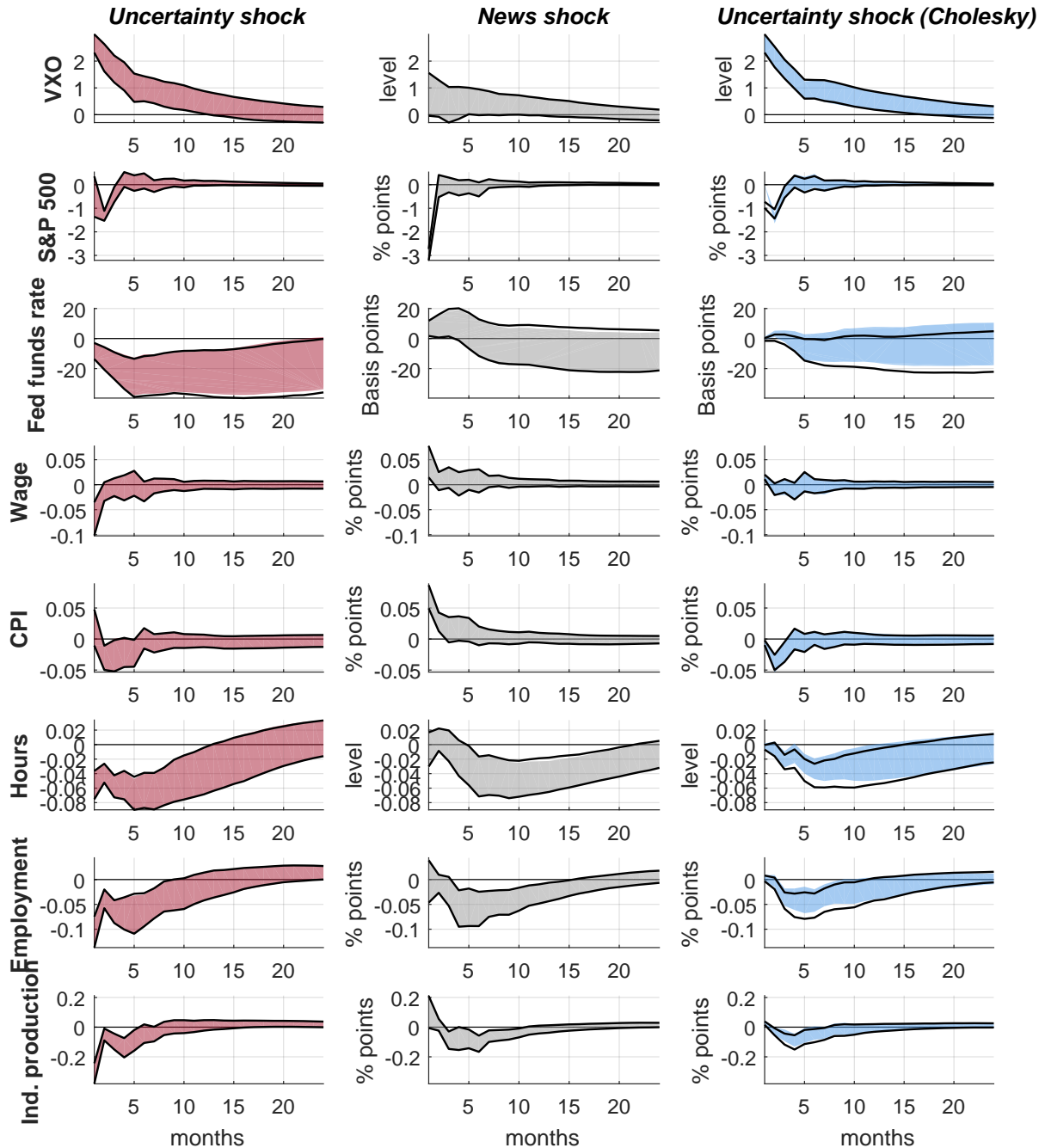
Note: Pointwise 95% bands computed on 1000 bootstrap replications, measuring uncertainty using the VXO (baseline specification, shaded area) or the measure by Jurado *et al.* (2015) (solid line).

Figure H16: Impulse responses, replacing the VXO with the measure of uncertainty by Bachmann *et al.* (2013)



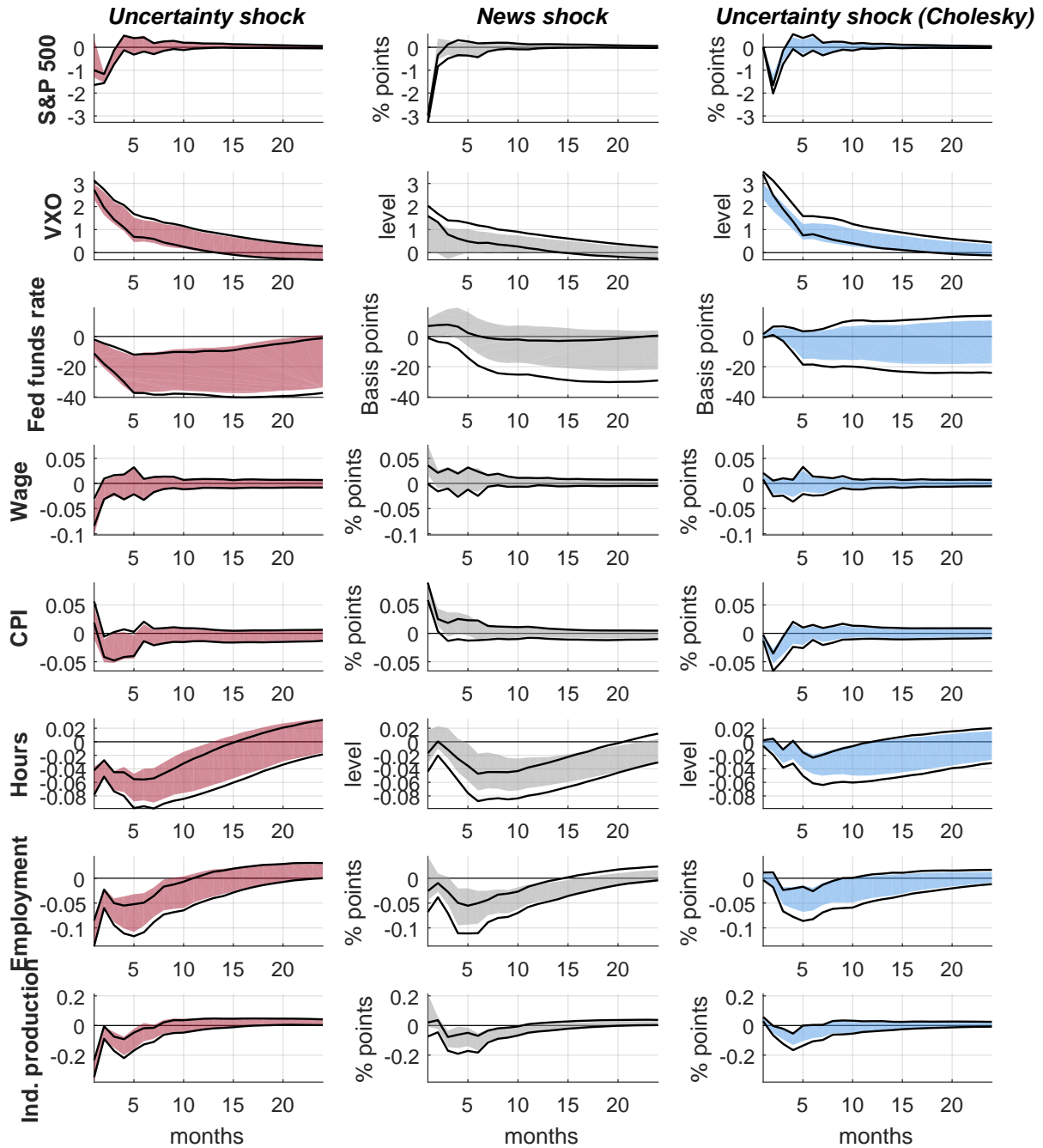
Note: Pointwise 95% bands computed on 1000 bootstrap replications, measuring uncertainty using the VXO (baseline specification, shaded area) or the measure by Bachmann *et al.* (2013).

Figure H17: Impulse responses, ordering the VXO as the first variable rather than the second



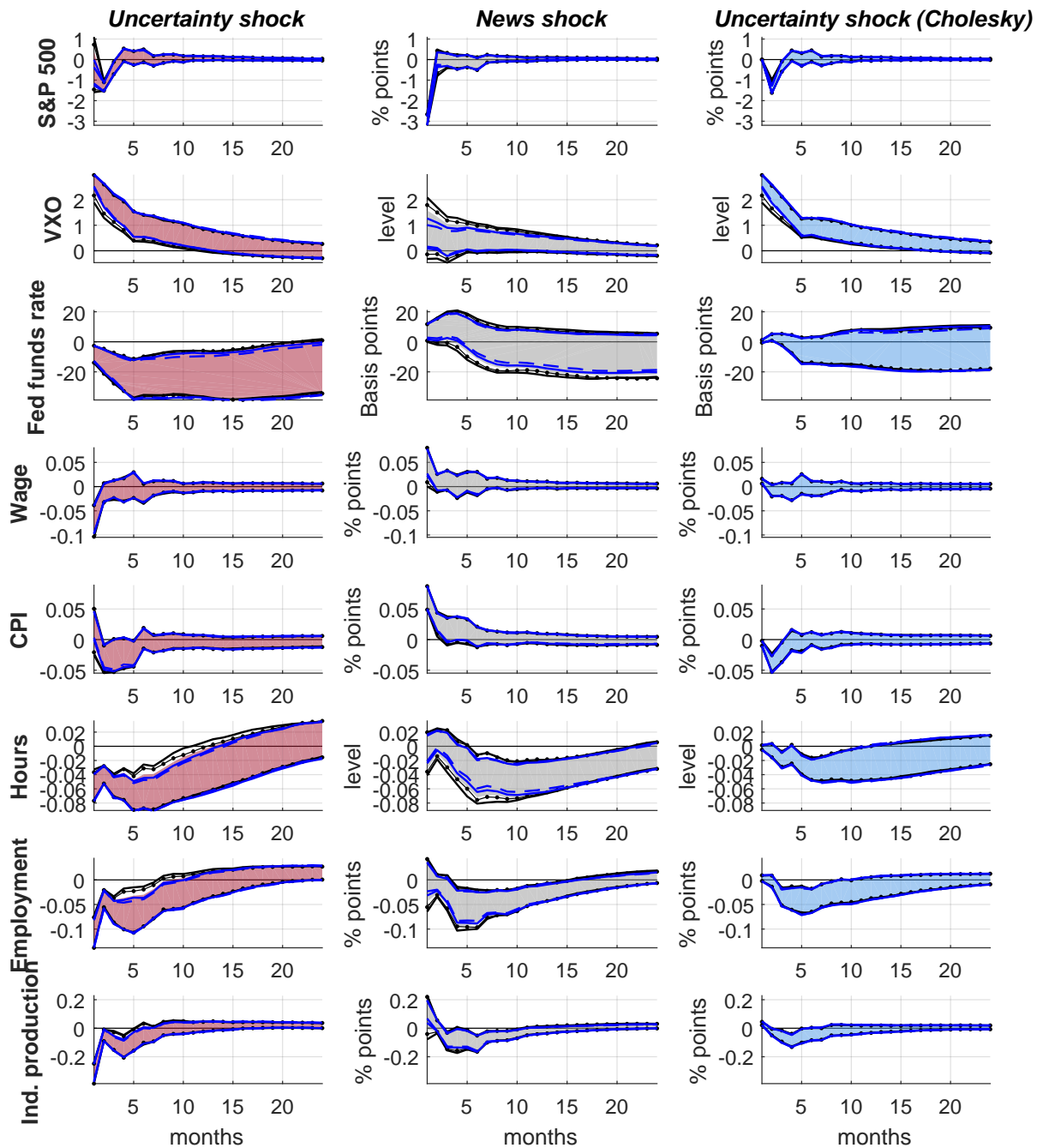
Note: Pointwise 95% bands computed on 1000 bootstrap replications, shown using the baseline ordering of the variables (shaded area) or switching the ordering of the first two variables and allowing the recursive identified uncertainty shock to affect on impact also the financial variable (solid black line).

Figure H18: Impulse responses, using exact- rather than set-identification



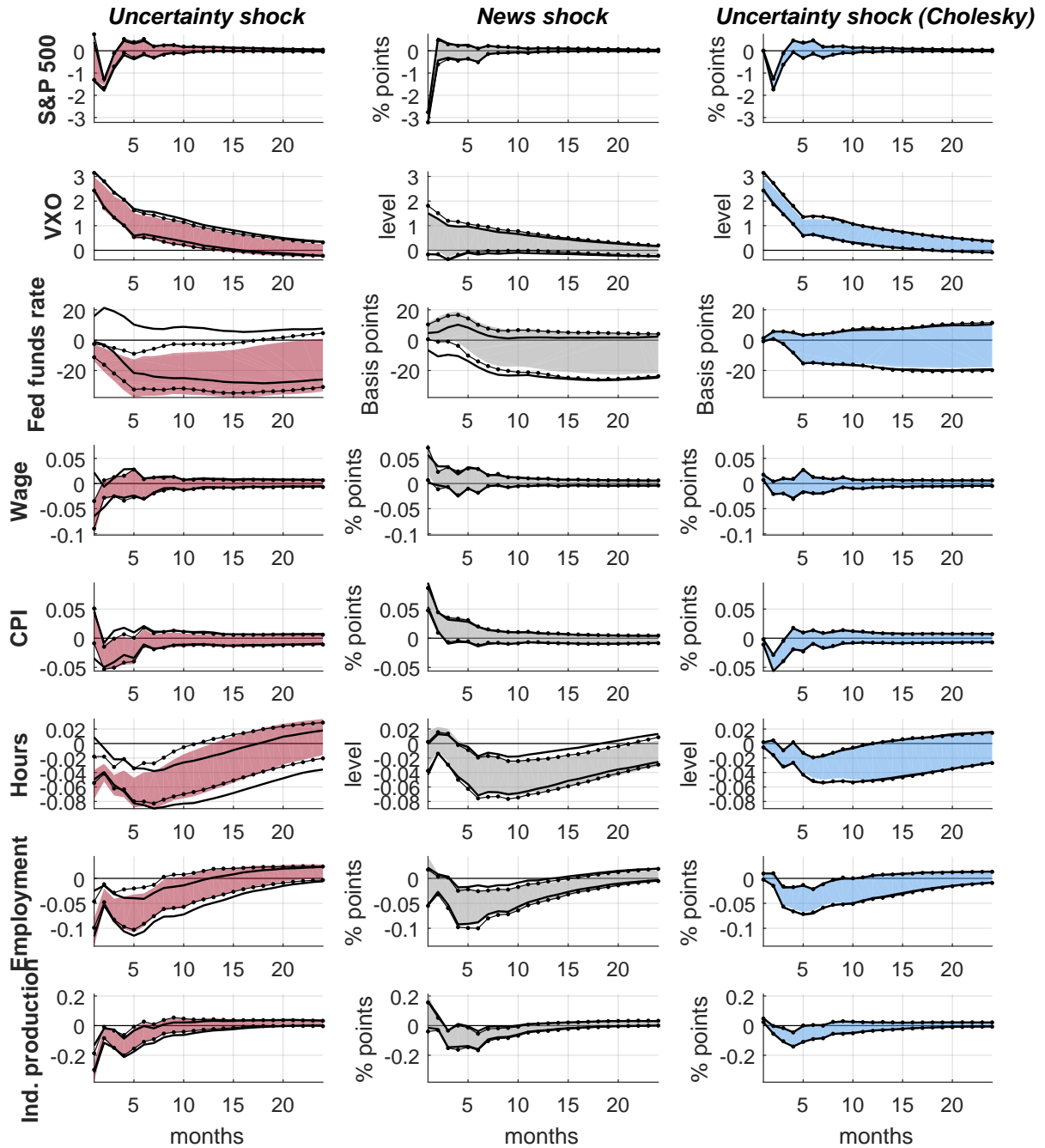
Note: Pointwise 95% bands computed on 1000 bootstrap replications, using the set-identification (baseline specification, shaded area) or using exact identification for the uncertainty shock and for the news shock separately (solid line). In the third column, we show the response to a shock of one standard deviation (solid line) and to a shock normalized as discussed in Section 5.3 of the paper (baseline specification, shaded area).

Figure H19: Impulse responses, using different values of ψ in equation (9b)



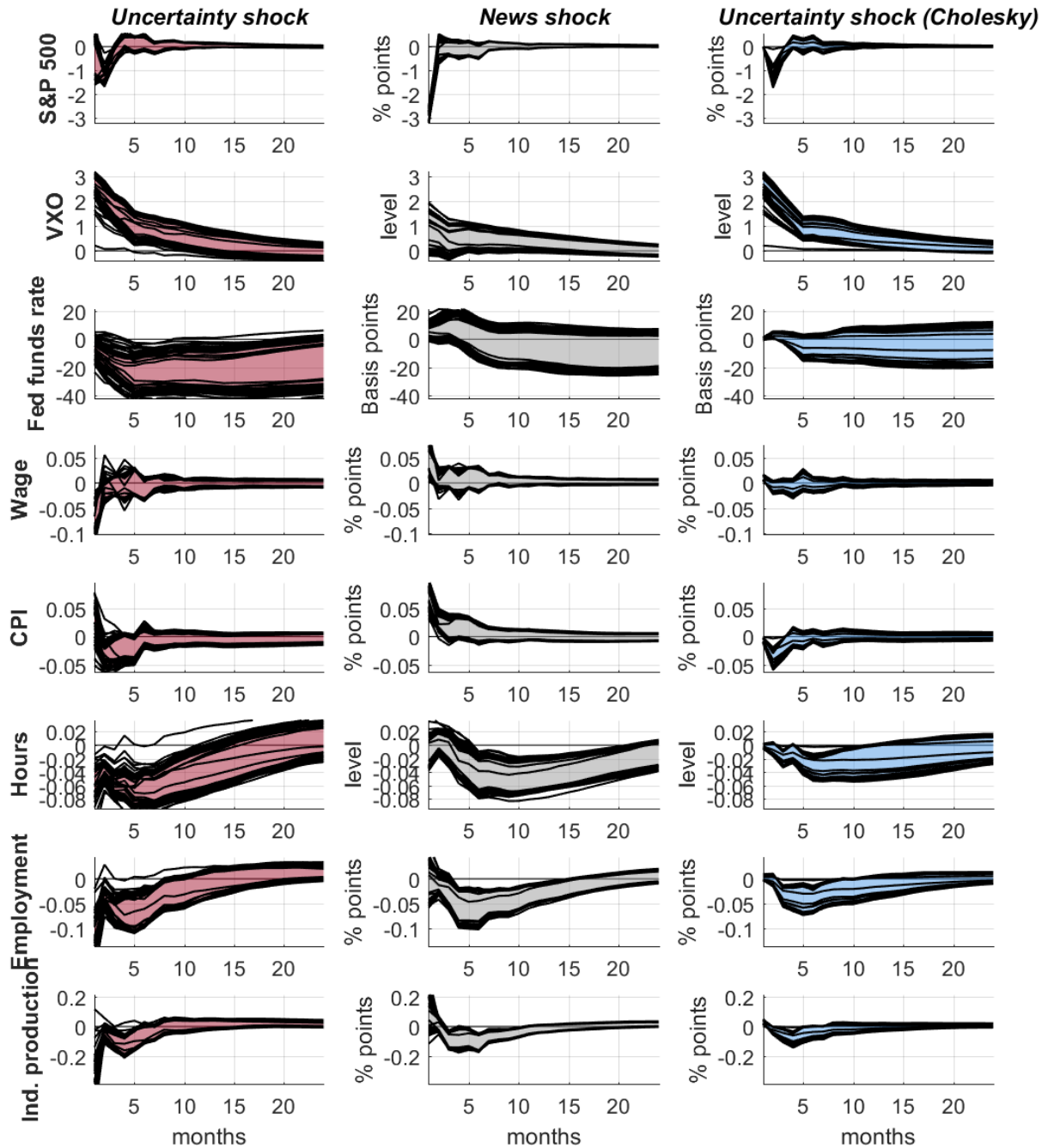
Note: Pointwise 95% bands computed on 1000 bootstrap replications, using for the identifying restrictions from (9b) $\psi = 0.10$ (baseline specification, shaded area), $\psi = 0$ (solid black line), $\psi = 0.05$ (dotted black line), $\psi = 0.15$ (solid blue line) and $\psi = 0.20$ (dashed blue line).

Figure H20: Impulse responses, using alternative selections of events in the construction of the proxy for the uncertainty shock



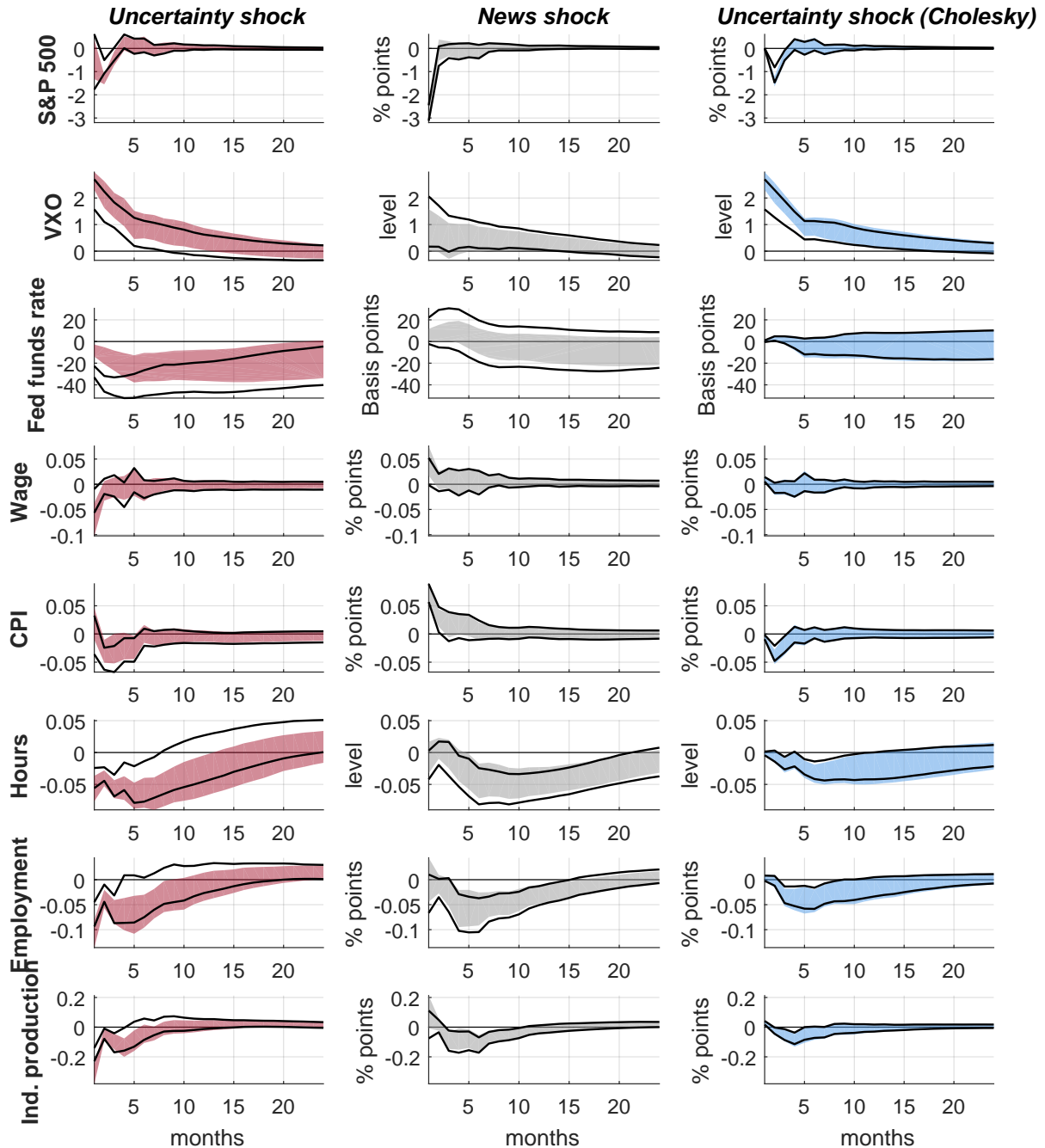
Note: Pointwise 95% bands computed on 1000 bootstrap replications, shown when constructing the proxy for the uncertainty shock on the baseline events (baseline specification, shaded area), on all 117 events (solid black line) or on the baseline events under the condition that they were associated with an increase in the price of gold (dotted black line).

Figure H21: Impulse responses, using alternative selections of events in the construction of the proxy for the uncertainty shock



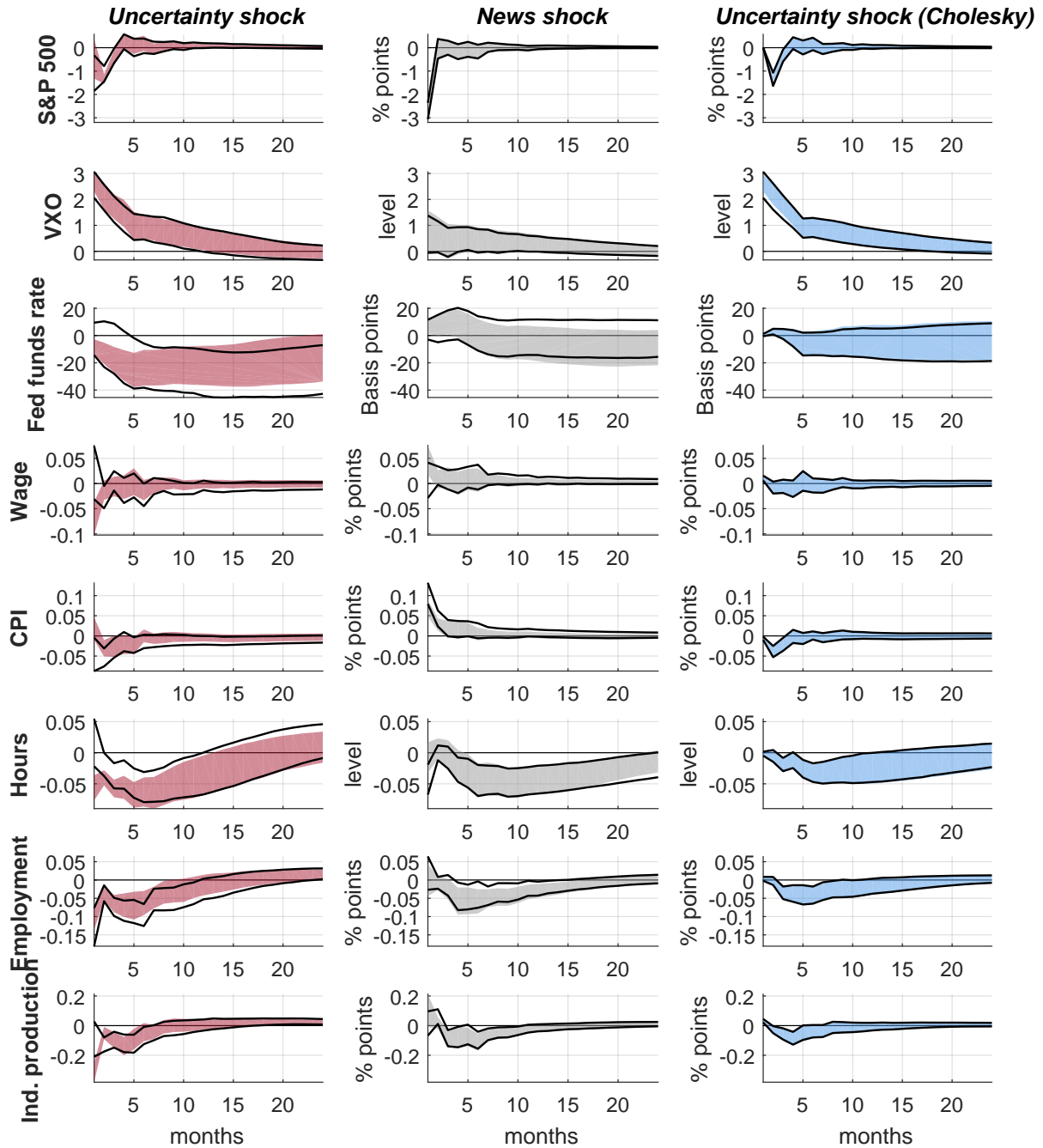
Note: Pointwise 95% bands computed on 1000 bootstrap replications, shown when constructing the proxy for the uncertainty shock on the baseline events (baseline specification, shaded area) or on the baseline events after dropping 20% of randomly selected events, and repeating 20 times (solid black lines).

Figure H22: Impulse responses, aggregating the uncertainty shock as in Gertler and Karadi (2014)



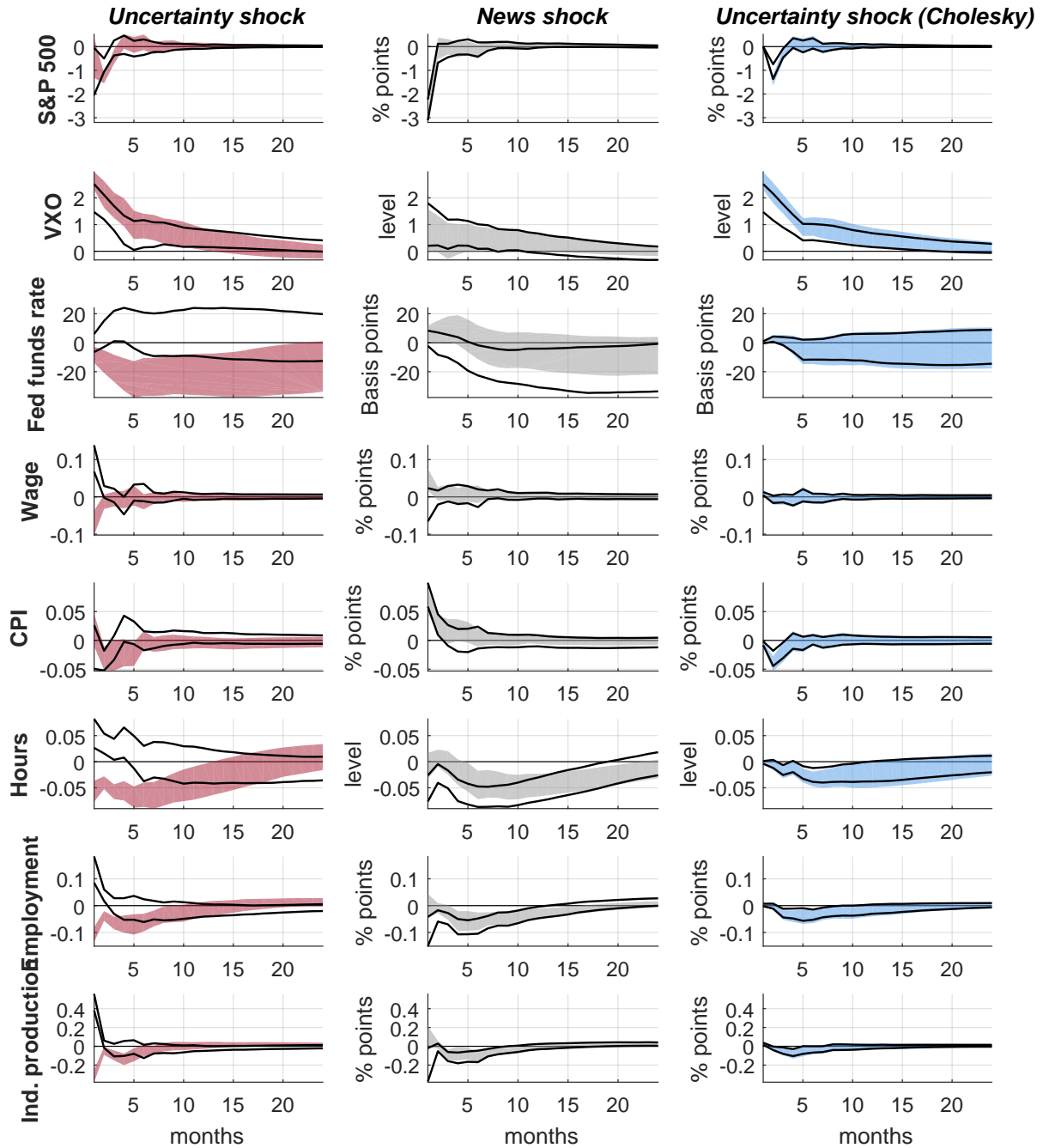
Note: Pointwise 95% bands computed on 1000 bootstrap replications, shown after aggregating the daily proxy to a monthly frequency using the sum within month (baseline specification, shaded area) or using the aggregation by Gertler and Karadi (2014) (solid line).

Figure H23: Impulse responses, constructing the proxy for the uncertainty shock from the variations of the price of silver



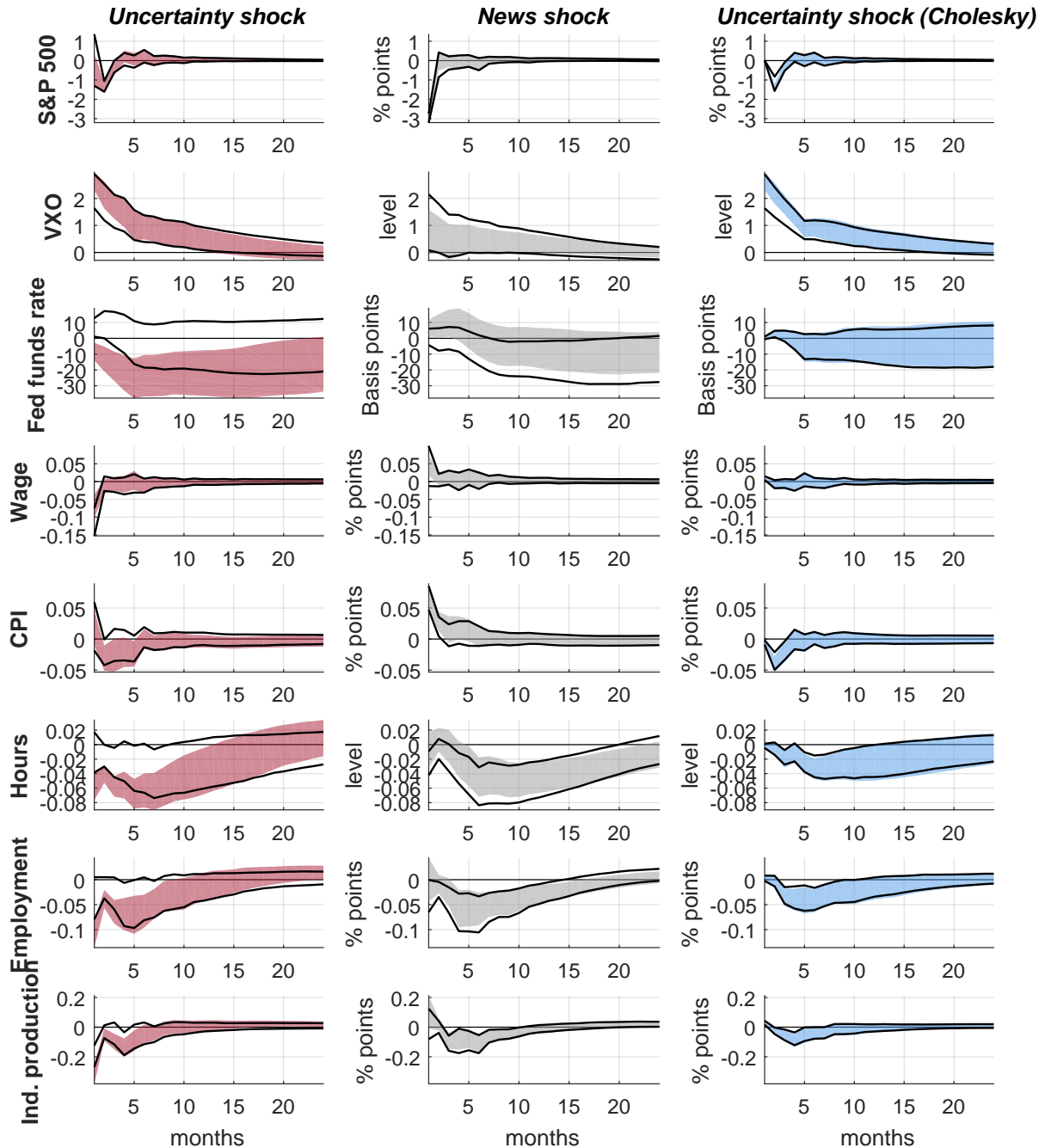
Note: Pointwise 95% bands computed on 1000 bootstrap replications, computing the proxy for the uncertainty shock from the price of gold (baseline specification, shaded area) or from the price of silver (solid line).

Figure H24: Impulse responses, constructing the proxy for the uncertainty shock from the variations of the price of platinum



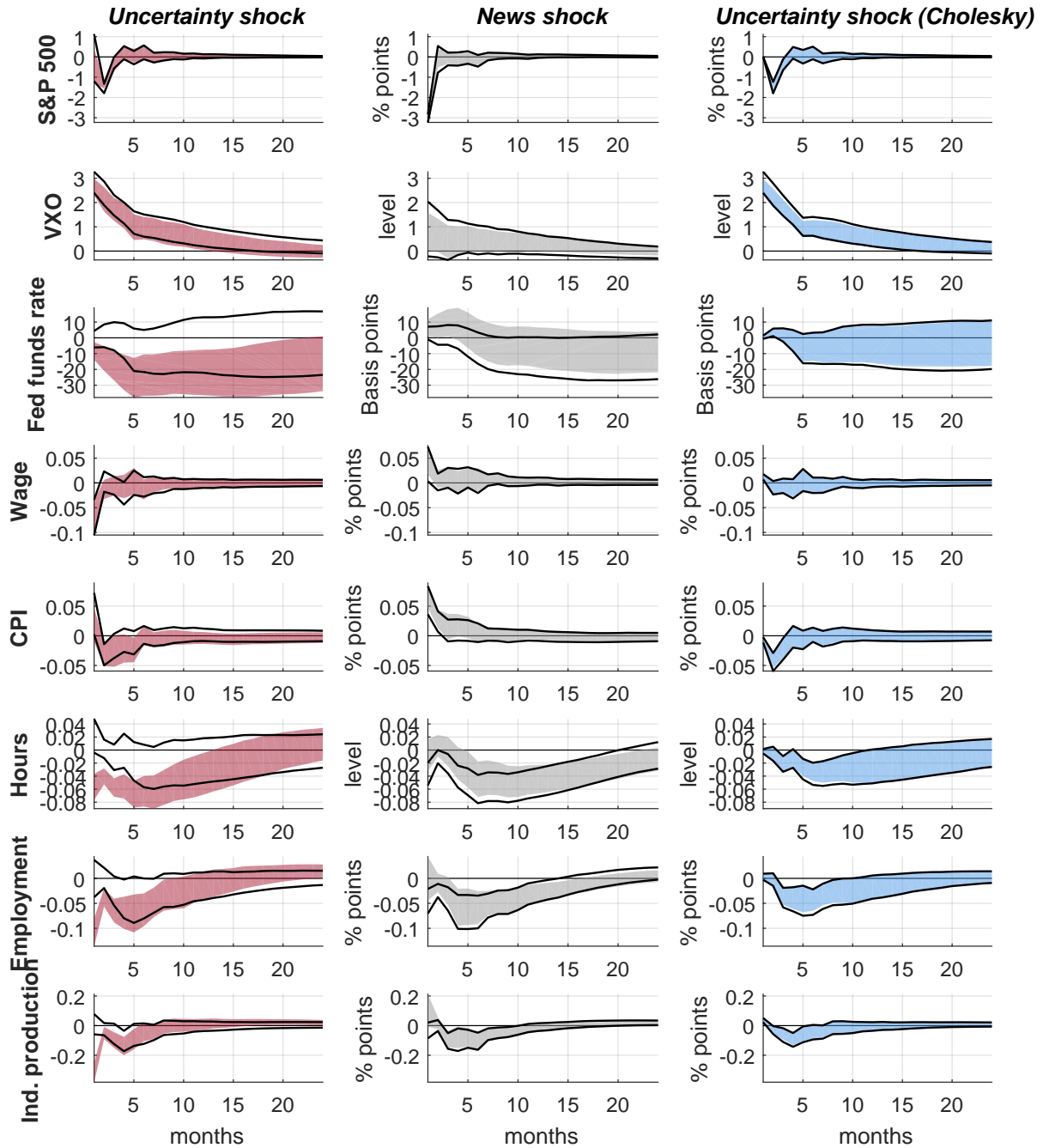
Note: Pointwise 95% bands computed on 1000 bootstrap replications, computing the proxy for the uncertainty shock from the price of gold (baseline specification, shaded area) or from the price of platinum (solid line).

Figure H25: Impulse responses, constructing the proxy for the uncertainty shock from the variations of the VXO around the baseline events



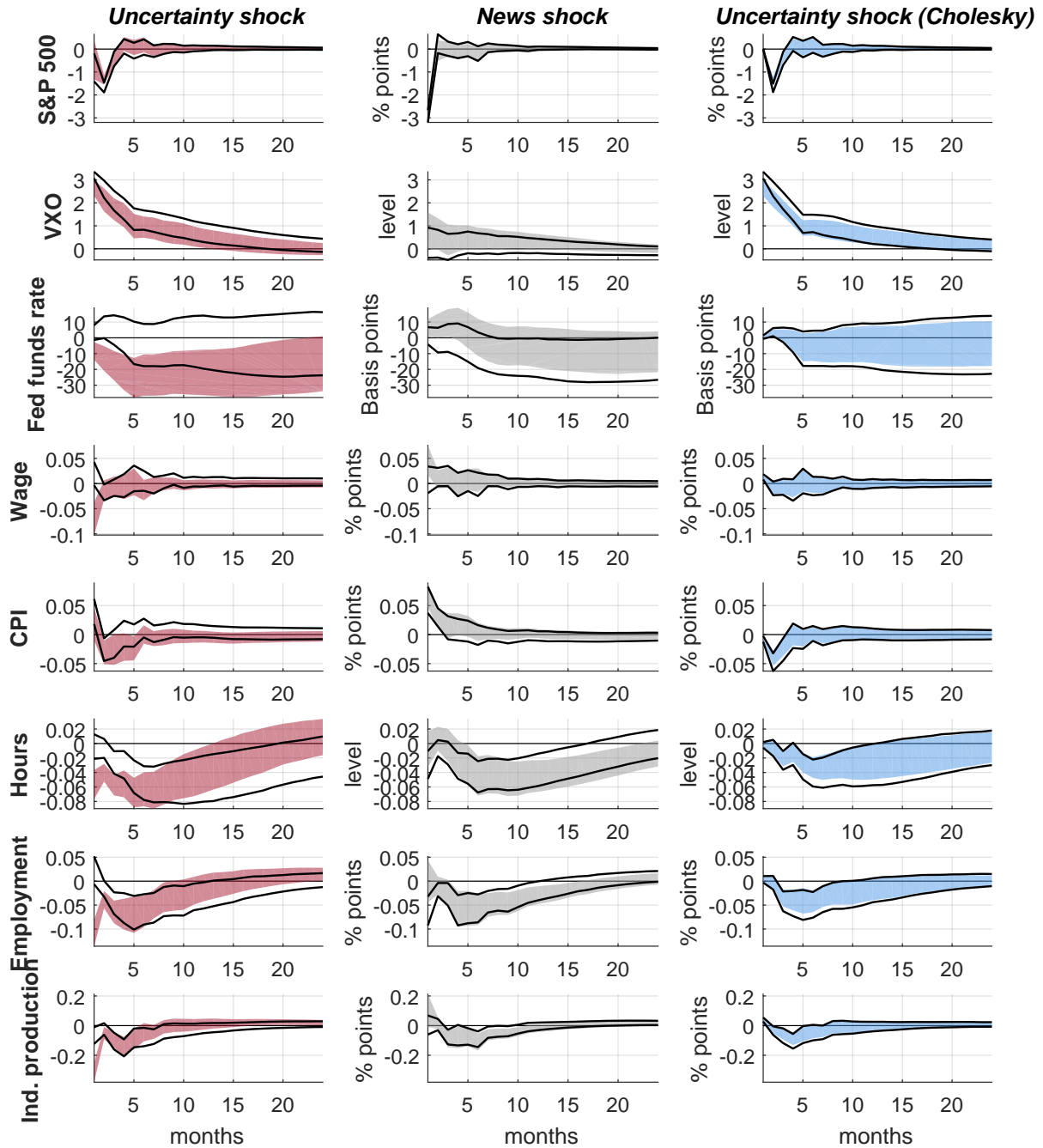
Note: Pointwise 95% bands computed on 1000 bootstrap replications, computing the proxy for the uncertainty shock from the price of gold (baseline specification, shaded area) or from the daily variations in the VXO around the baseline events (solid line).

Figure H26: Impulse responses, using as proxy for the uncertainty shock a dummy variable taking value 1 when a baseline event occurred



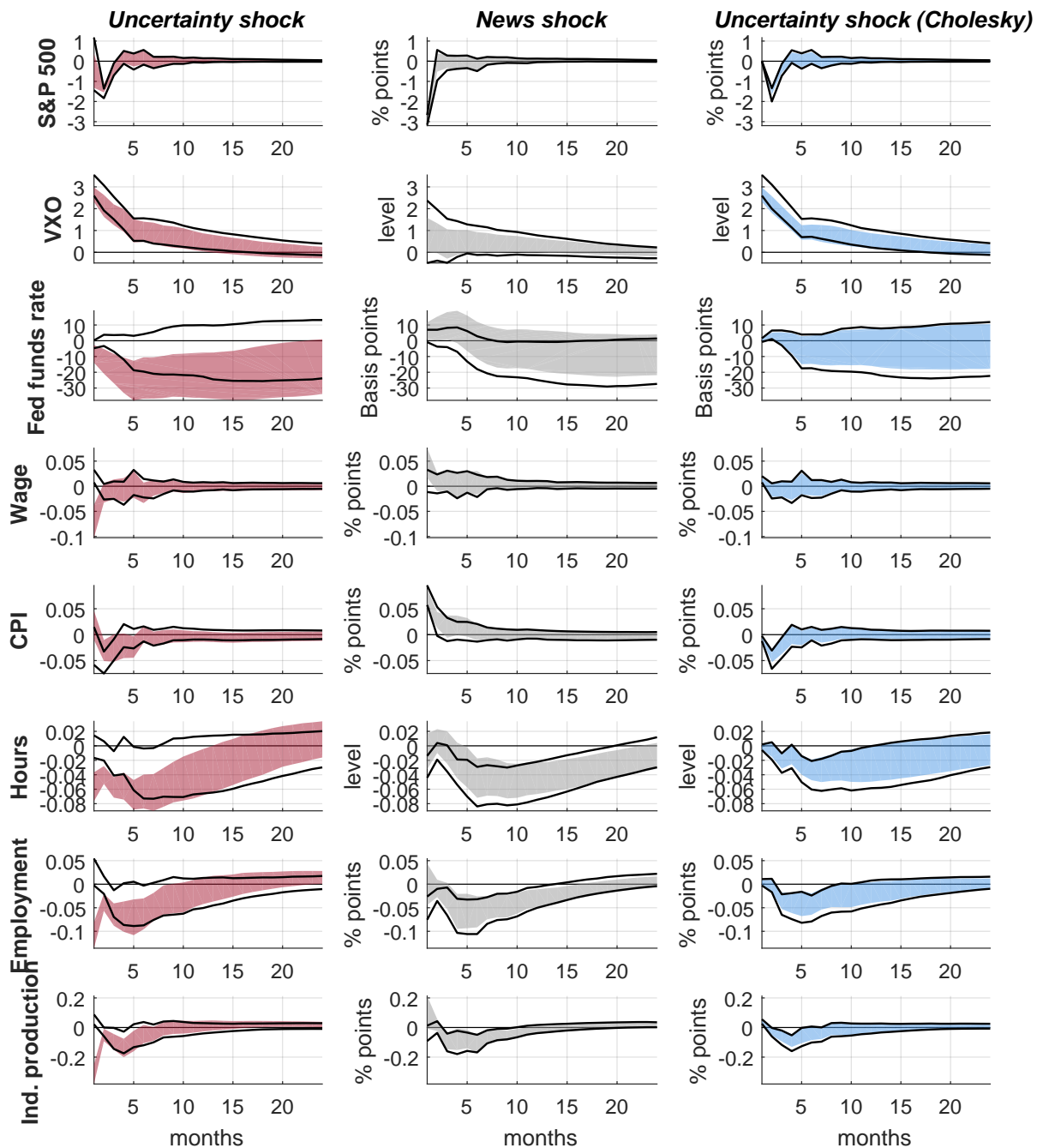
Note: Pointwise 95% bands computed on 1000 bootstrap replications, using as proxy for the uncertainty shock the proxy based on the price of gold (baseline specification, shaded area) or a dummy variable taking values 0/1 when a baseline event occurred (solid line).

Figure H27: Impulse responses, using as proxy for the uncertainty shock the dummy variable by Bloom (2009)



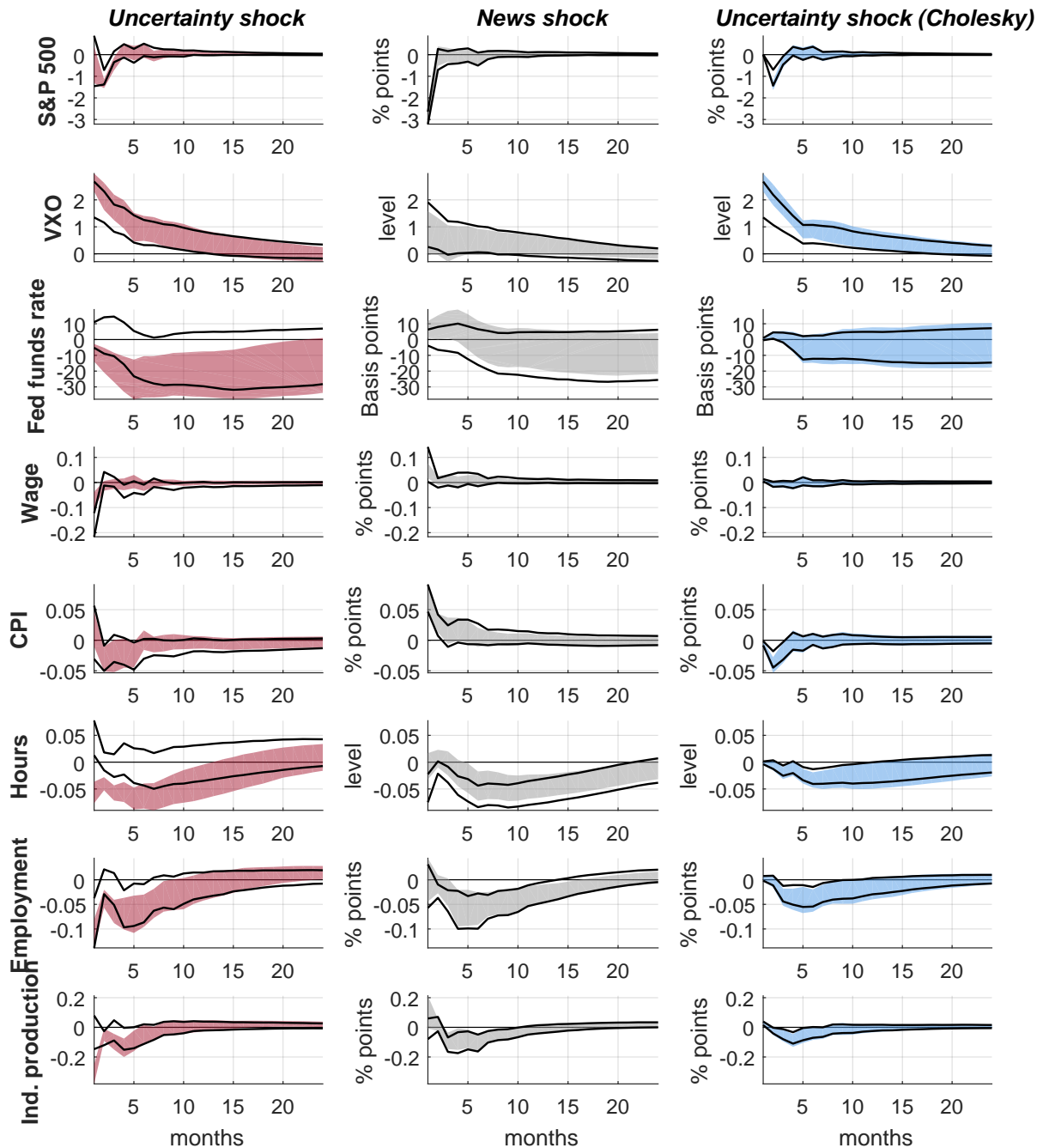
Note: Pointwise 95% bands computed on 1000 bootstrap replications, using as proxy for the uncertainty shock the proxy based on the price of gold (baseline specification, shaded area) or a dummy variable taking values 0/1 when the VXO reached the peaks used by Bloom (2009) (solid line).

Figure H28: Impulse responses, using as proxy for the uncertainty shock the first instrument for the uncertainty shock by Stock and Watson (2012)



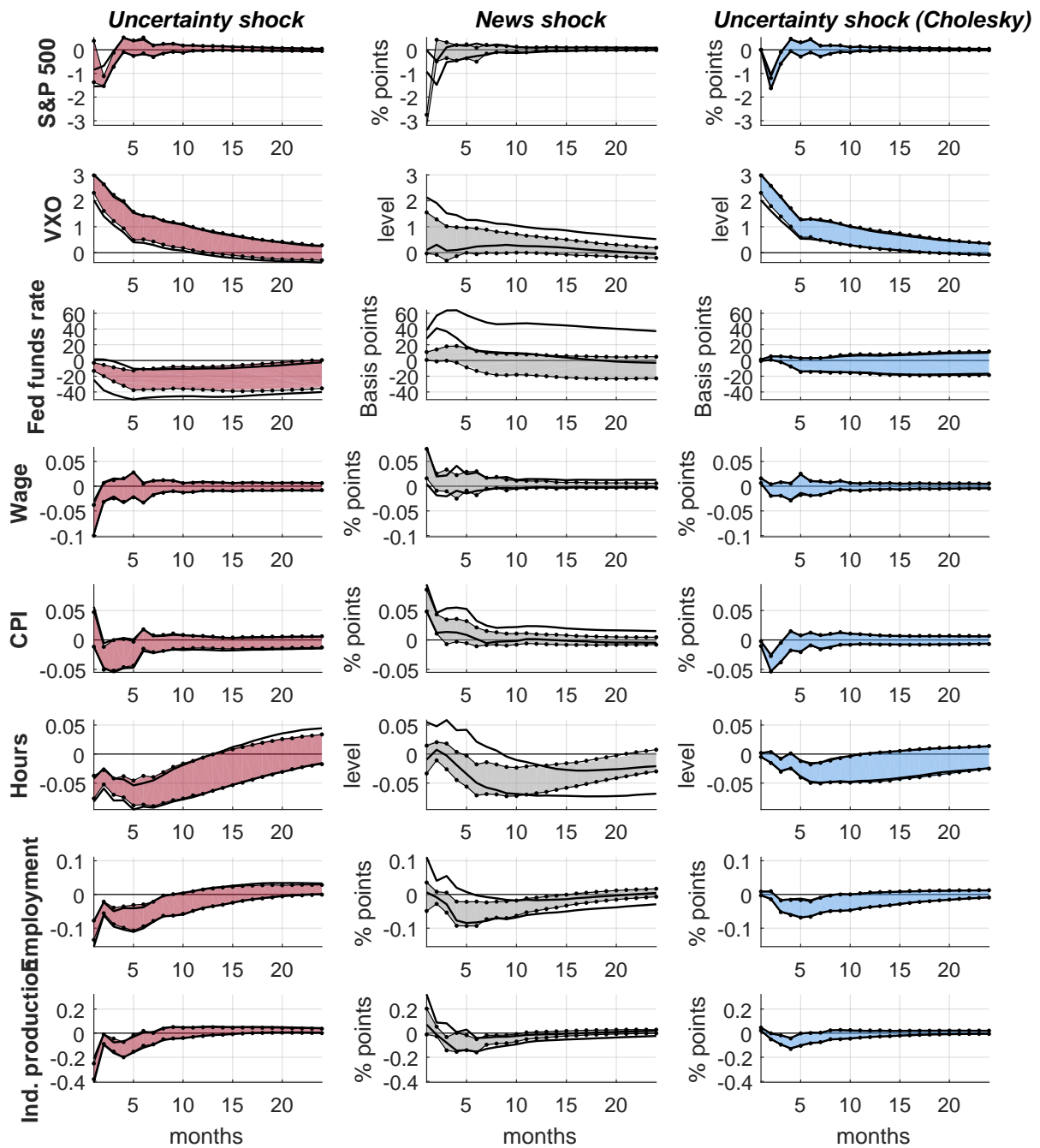
Note: Pointwise 95% bands computed on 1000 bootstrap replications, using as proxy for the uncertainty shock the proxy based on the price of gold (baseline specification, shaded area) or the residual from an AR(2) regression on the VIX (solid line).

Figure H29: Impulse responses, using as proxy for the uncertainty shock the second instrument for the uncertainty shock by Stock and Watson (2012)



Note: Pointwise 95% bands computed on 1000 bootstrap replications, using as proxy for the uncertainty shock the proxy based on the price of gold (baseline specification, shaded area) or the common component of the policy uncertainty index by Baker *et al.* (2016) (solid line).

Figure H30: Impulse responses, using alternative proxies for the news shock



Note: Pointwise 95% bands computed on 1000 bootstrap replications, using as proxy for the news shock the first principal component of all the estimated shocks listed in [footnote 8](#) (baseline specification, shaded area), of the shocks reflecting the identification strategies by [Barsky and Sims \(2011\)](#) and by [Kurmann and Otrok \(2013\)](#) (solid line) or of the shocks reflecting the identification strategy by [Beaudry and Portier \(2014\)](#) (dotted line).

References

- An, S. and Schorfheide, F. (2007). ‘Bayesian analysis of DSGE models’, *Econometric Reviews*, vol. 26(2-4), pp. 113–172.
- Arias, J., Rubio-Ramirez, J.F. and Waggoner, D.F. (2014). ‘Inference based on SVAR identified with sign and zero restrictions: Theory and applications’, Working Paper, Federal Reserve Bank of Atlanta.
- Bachmann, R., Elstner, S. and Sims, E.R. (2013). ‘Uncertainty and economic activity: Evidence from business survey data’, *American Economic Journal: Macroeconomics*, vol. 5(2), pp. 217–249.
- Baker, S.R., Bloom, N. and Davis, S.J. (2016). ‘Measuring economic policy uncertainty’, *Quarterly Journal of Economics*, vol. 131(4), pp. 1593–1636.
- Barsky, R.B. and Sims, E.R. (2011). ‘News shocks and business cycles’, *Journal of Monetary Economics*, vol. 58(3), pp. 273–289.
- Bassett, W.F., Chosak, M.B., Driscoll, J.C. and Zakrajšek, E. (2014). ‘Changes in bank lending standards and the macroeconomy’, *Journal of Monetary Economics*, vol. 62, pp. 23–40.
- Basu, S., Fernald, J. and Kimball, M. (2006). ‘Are technology improvements contractionary?’, *American Economic Review*, vol. 96(5), pp. 1418–1448.
- Baur, D.G. and Lucey, B.M. (2010). ‘Is gold a hedge or a safe haven? An analysis of stocks, bonds and gold’, *Financial Review*, vol. 45(2), pp. 217–229.
- Baur, D.G. and McDermott, T.K. (2010). ‘Is gold a safe haven? International evidence’, *Journal of Banking and Finance*, vol. 34(8), pp. 1886–1898.

- Beaudry, P. and Portier, F. (2014). ‘News-driven business cycles: Insights and challenges’, *Journal of Economic Literature*, vol. 52(4), pp. 993–1074.
- Binning, A. (2013). ‘Underidentified SVAR models: A framework for combining short and long-run restrictions with sign-restrictions’, Working Paper, Norges Bank.
- Bloom, N. (2009). ‘The impact of uncertainty shocks’, *Econometrica*, vol. 77(3), pp. 623–685.
- Christiano, L.J., Eichenbaum, M. and Evans, C.L. (2005). ‘Nominal rigidities and the dynamic effects of a shock to monetary policy’, *Journal of Political Economy*, vol. 113(1), pp. 1–45.
- De Wind, J. *et al.* (2014). ‘Time variation in the dynamic effects of unanticipated changes in tax policy’, CPB Netherlands Bureau for Economic Policy Analysis.
- Fisher, J.D. and Peters, R. (2010). ‘Using stock returns to identify government spending shocks’, *Economic Journal*, vol. 120(544), pp. 414–436.
- Galí, J. (1999). ‘Technology, employment, and the business cycle: Do technology shocks explain aggregate fluctuations’, *American Economic Review*, vol. 89(1), pp. 249–271.
- Gertler, M. and Karadi, P. (2014). ‘Monetary policy surprises, credit costs and economic activity’, *American Economic Journal: Macroeconomics*, vol. 7(1), pp. 44–76.
- Giacomini, R. (2013). ‘The relationship between DSGE and VAR models’, in (T. B. Fomby, L. Kilian and A. Murphy, eds.), *VAR Models in Macroeconomics—New Developments and Applications: Essays in Honor of Christopher A. Sims*, pp. 1–25, Emerald Group Publishing Limited.

- Gilchrist, S. and Zakrajšek, E. (2012). ‘Credit spreads and business cycle fluctuations’, *American Economic Review*, vol. 102(4), pp. 1692–1720.
- Gurkaynak, R.S., Sack, B.P. and Swanson, E.T. (2005). ‘Do actions speak louder than words? The response of asset prices to monetary policy actions and statements’, *International Journal of Central Banking*, vol. 1(1), pp. 55–93.
- Hamilton, J.D. (2003). ‘What is an oil shock?’, *Journal of Econometrics*, vol. 113(2), pp. 363–398.
- Jurado, K., Ludvigson, S.C. and Ng, S. (2015). ‘Measuring uncertainty’, *American Economic Review*, vol. 105(3), pp. 1177–1216.
- Kilian, L. (2008). ‘Exogenous oil supply shocks: how big are they and how much do they matter for the US economy?’, *Review of Economics and Statistics*, vol. 90(2), pp. 216–240.
- Komunjer, I. and Ng, S. (2011). ‘Dynamic identification of dynamic stochastic general equilibrium models’, *Econometrica*, vol. 79(6), pp. 1995–2032.
- Kurmann, A. and Otrok, C. (2013). ‘News shocks and the slope of the term structure of interest rates’, *American Economic Review*, vol. 103(6), pp. 2612–2632.
- Lucey, B., Larkin, C. and O’Connor, F.A. (2013). ‘London or New York: Where and when does the gold price originate?’, *Applied Economics Letters*, vol. 20.
- Mertens, K. and Ravn, M.O. (2013). ‘The dynamic effects of personal and corporate income tax changes in the United States’, *American Economic Review*, vol. 103(4), pp. 1212–1247.

- O'Connor, F.A., Lucey, B.M., Batten, J.A. and Baur, D.G. (2015). 'The financial economics of gold — A survey', *International Review of Financial Analysis*, vol. 41, pp. 186–205.
- Olea, J.L.M., Stock, J.H. and Watson, M.W. (2012). 'Inference in structural VARs with external instruments', Unpublished manuscript, Harvard University.
- Paustian, M. (2007). 'Assessing sign restrictions', *BE Journal of Macroeconomics*, vol. 7(1), pp. 1–33.
- Ramey, V.A. (2011). 'Identifying government spending shocks: it's all in the timing', *Quarterly Journal of Economics*, vol. 126(1), pp. 1–50.
- Ramey, V.A. and Vine, D.J. (2010). 'Oil, automobiles, and the US economy: How much have things really changed?', *NBER Macroeconomics Annual*, vol. 25, pp. 333–367.
- Romer, C.D. and Romer, D.H. (2004). 'A new measure of monetary shocks: Derivation and implications', *American Economic Review*, vol. 94(4), pp. 1055–1084.
- Romer, C.D. and Romer, D.H. (2010). 'The macroeconomic effects of tax changes: Estimates based on a new measure of fiscal shocks', *American Economic Review*, vol. 100, pp. 763–801.
- Rotemberg, J.J. and Woodford, M. (1997). 'An optimization-based econometric framework for the evaluation of monetary policy', *NBER Macroeconomics Annual*, vol. 12, pp. 297–346.
- Sims, C.A. and Zha, T. (2006). 'Were there regime switches in US monetary policy?', *American Economic Review*, vol. 96(1), pp. 54–81.

- Smets, F. and Wouters, R. (2007). ‘Shocks and frictions in US business cycles: A Bayesian DSGE approach’, *American Economic Review*, vol. 97(3), pp. 586–606.
- Stock, J.H. and Watson, M.W. (2012). ‘Disentangling the channels of the 2007–2009 recession’, *Brookings Papers on Economic Activity*, pp. 81–135.
- Stock, J.H. and Yogo, M. (2005). ‘Testing for weak instruments in linear IV regression’, in (D. W. Andrews, ed.), *Identification and Inference for Econometric Models*, pp. 80–108, New York: Cambridge University Press.